T-3556

ISOCHORIC PVT MEASUREMENTS FOR (0.99 CO_2 + 0.01 C_2H_6) AND MODELLING PVT BEHAVIOR OF CARBON DIOXIDE RICH MIXTURES

By

Gerald. J. Sherman

T-3556

A thesis submitted to the Faculty and Board of Trustees of the Colorado School of Mines in partial fulfillment of the requirements for the degree of Master of Science (Chemical and Petroleum-Refining Engineering).

Golden, Colorado

Date 2/23/88

Signed: Gerald J. Sherman

Gerald J. Sherman

Approved: James F. Ely

Dr. James F. Ely
Thesis Advisor

Golden, Colorado

Date 2/23/88

Dr. Arthur J. Kinday
Department Head and,
co-advisor Chemical
Engineering and
Petroleum Refining

ABSTRACT

Comprehensive isochoric PVT measurements have been obtained for (0.99 CO_2 + 0.01 C_2H_6) at densities for 2 - 24 mol/dm^3. These measurements cover a range of temperatures from 245 to 400 K, at pressures up to 35 MPa. The apparatus used in this investigation is capable of measuring mixture densities with an accuracy of 0.2 % for densities of 2 - 10 mol/dm^3 and 0.1 % for densities of 11 - 24 mol/dm^3. Comparisons have been made with a predictive model based on corresponding states, and the model was improved by implementing the Schmidt-Wagner equation of state.

TABLE OF CONTENTS

LIST OF FIGURES

Figure | Page

Figure | Page

Figure | Page

LIST OF TABLES

ACKNOWLEDGEMENTS

I would like to express my sincere gratitude to Dr. James F. Ely for his patience, counsel and support throughout the course of this study. I would also like to Dr. Joseph W. Magee for his assistance and support in the experimental aspect of this study.

INTRODUCTION

There has developed a great interest in the properties of pure carbon dioxide and carbon dioxide rich mixtures during the past ten years. This interest has evolved from several sources, most notably enhanced oil recovery using CO_2 and related CO_2 pipeline and CO_2 ruch gas processing technologies. There also exist many potential applications for using CO_2 as a solvent in supercritical fluid extractions. It has also been shown, with regard to enhanced oil recovery (Zudkevitch et al. 1985), that uncertainties in the pressure-volume-temperature (PVT) as well as phase behavior of CO_2 rich mixtures hinder our capability to model flow mobility, permeability and ultimate recovery. In addition, Elliot et al. (1984) have demonstrated that an improved database and predictive models founded upon accurate measurements are needed to avoid potential failures in design and process operation calculations for CO_2 rich systems.

CO_2 injection as an enhanced oil recovery technique is both in extensive field testing and commercial use in the United States. There are large volumes of oil that remain in U.S. oil reserviors which cannot be recovered by standard methods. Supercritical carbon dioxide can be used to

recover part of that remaining oil. If the CO_2 is dense enough, it can extract hydrocarbons from the oil to make a mixture miscible with crude oil. Such a mixture can recover 95 percent of the oil contacted in controlled laboratory flow settings (Orr & Taber 1984).

Transportation studies by several investigators have reached the conclusion that high-pressure supercritical CO_2 pipelines are the most economical transportation mode for these volumes of CO_2 (Farris 1983, Meissner 1980, Stripling 1980). It is currently necessary to determine mass flow rates of CO_2 rich mixtures at individual source and injection wells as a gas and as a dense fluid in CO_2 pipeline systems. The presence of small amounts of non-condensible gases has an abnormally large impact on the fluid's thermophysical properties in the near critical state. For example, small changes in the composition of the mixture will result in relatively large differences in expected densities. Temperature also has a marked effect on fluid properties. The problem which arises is that carbon dioxide has a critical point temperature which is close to atmospheric temperature and is produced and transported as a mixture, typically 94-98% pure. The critical properties of CO_2 are presented in Table 1 as well as the regions of interest in carbon dioxide pipelines. If the temperature is

Table 1. Conditions of Interest for CO_2 Custody Transfer

Property	Critical Value	Range of Interest
Temperature	304.13 K	260 - 325 K
Pressure	73.752 Bar	55 - 210 Bar
Density	10.63 mol/l	2 - 24 mol/l
Composition		
	CO_2	94 - 99.7 mol %
	CH_4	0 - 2
	C_2H_6	0 - 1
	C_3^+	0 - 2
	N_2	0 - 2

far enough away from the critical temperature of the mixture, small temperature changes are of little consequence. But, if the transportation temperature is near that of the mixture temperature, small changes in temperature may result in phase changes and thus changes in the system density.

Special problems exist because of the proximity of the region of interest to the critical point of CO_2. These problems must be considered in any measurement technique and associated thermodynamic model. It is well known that at the critical point of a pure fluid that the isothermal compressibility is infinite

$$\frac{1}{V}\left(\frac{\partial V}{\partial p}\right)_{T_c} = \infty$$

where V is the molar volume, p is the pressure and the subscript c denotes a critical point value. What is perhaps less well known is that other anomolies exist in the near critical region of a mixture. Chang et al. (1984) have shown that in a classical fluid

$$\left(\frac{\partial V}{\partial x}\right)_c \alpha \frac{1}{x^{2/3}}$$

and

$$\frac{1}{V}\left(\frac{\partial^2 V}{\partial x \partial p}\right) \alpha \frac{1}{x^{5/3}}$$

where x denotes the concentration of a solute and the

subscript c for the mixture derivatives indicates a path along the critical isotherm-isobar. These effects have serious implications for the metering of any fluid, pure or mixed, in the vicinity of its critical point. These implications include the density being strongly affected by small changes in the pressure and composition. Therefore, a highly accurate compositionally dependent model for pipeline and custody transfer calculations is needed.

As of yet, relatively few data exist for these systems; therefore, this investigation will provide some of the useful and required data. The primary objective of this work was to determine the experimental densities of (0.99 CO_2 + 0.01 C_2H_6) and use them to evaluate and further develop a predictive thermodynamic model for the properties of CO_2 rich mixtures. The PVTx relationship of a fluid constitutes one of the most important and fundamental properties of pure fluids and mixtures. An accurate and precise description of the PVTx surface can, in principle, be used to calculate all equilibrium properties. From a correlational point of view, one requires accurate PVTx data to obtain this relationship. In addition, comprehensive PVTx data are required for incorporation into databases for the development and testing of predictive models for thermodynamic properties of fluid mixtures.

The predictive model used in this study is based upon the extended corresponding states theory. The model, DDMIX, was developed by Dr. J.F. Ely, and incorporates a one-fluid concept originally due to van der Waals. It uses inputs of composition, temperature and pressure and returns the thermodynamic values of enthalpy, entropy, sound speed, Gibbs free energy, viscosity, thermal conductivity, vapor-liquid equilibria and mixture densities. This study is primarily concerned with the calculation of densities and the comparsion of these densities with experimental measurements which were performed in the course of this investigation.

The preliminary results show that the predictive model was not "flat" enough in the near critical region (Fig.17). Models of this class use a reference fluid for calculation of the mixture thermodynamic properties. DDMIX uses pure propane as its reference fluid, and it is believed that this is where the problem lies. Thus, a new approach was sought. This approach consists of implementing the Schmidt-Wagner (Schmidt & Wagner 1986) equation of state into DDMIX. Since the Schmidt-Wagner equation of state gives much flatter isotherms in the near critical region, it should take care of this problem.

DENSITY MEASUREMENT TECHNIQUES

There are several basic techniques used in the acquisition of PVT data for the determination of fluid densities. Some methods measure both the mass and volume of a sample and others measure the mass of a fixed volume of sample. There are still other methods available which do not require a measurement of mass or volume, but rather determine the density through other physical properties. There are five major methods by which density measurements can be made. These methods are described below with advantages and disavantages listed for each.

Burnett Method

The classical Burnett (Burnett 1936) method consists of successive gas expansions to establish the density behavior for the fluid along an isotherm. The Burnett system (Figure 1) usually consists of two spherical cells of different volumes and an accurate pressure transducer. The cells usually have nominal volume ratios of 1.5:1 but different volume ratios may be selected. The spheres, transducer, valves, and tubing are immersed in a stirred

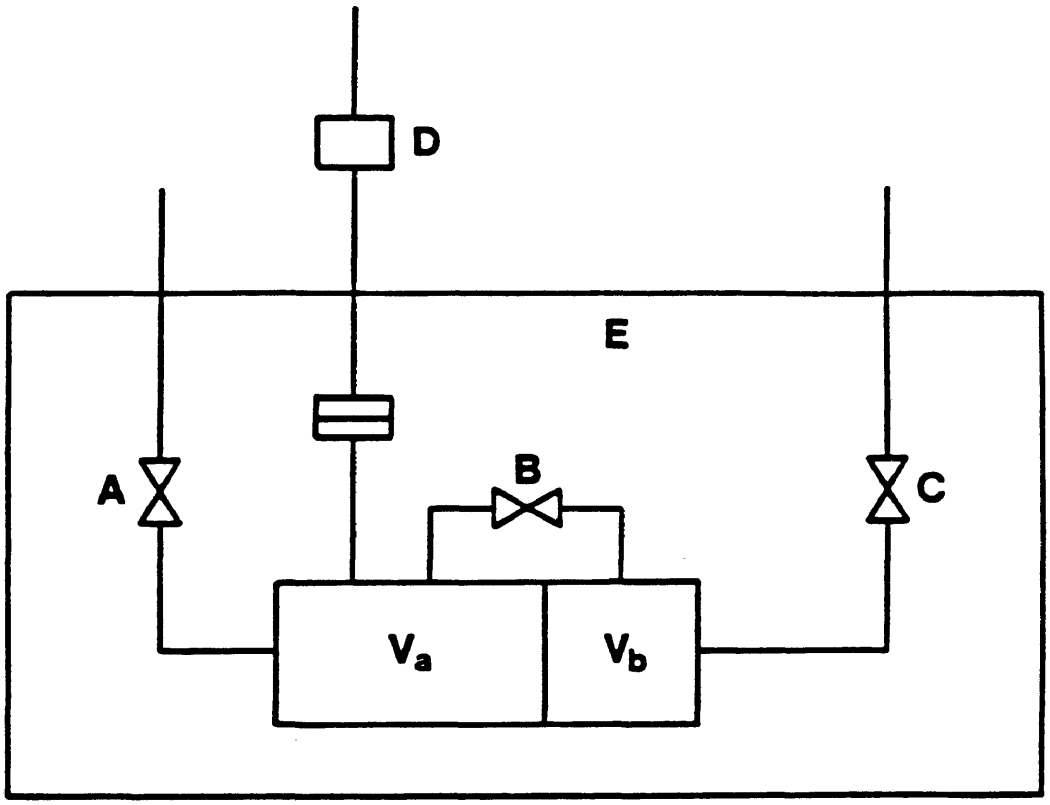

Figure 1. Sketch of Burnett apparatus V_a larger volume, V_b smaller volume, A charging line, B expansion valve C vent and vacuum line D differential pressure indicator, E thermostat.

liquid bath or an oven with vigorous circulation in order to maintain a constant temperature.

The major advantage of this method is that it requires no absolute volume calibrations nor any measurements of mass. The sample densities are obtained through a data-reduction technique of pressure ratios. For any particular expansion,

$$\frac{P_i}{P_{i+1}} = \frac{Z_i}{Z_{i+1}} N_i$$

where p is the pressure, $Z = p/(\rho RT)$,ρ is the density and $N_i = (V_1 + V_2)/V_1$. The temperature is assumed to be constant and identical for both V_1 and V_2. Also, the volume ratio N_i is slightly pressure dependent. There are a number of ways to analyze such data (Hall and Canfield 1970, Wieloplski and Warowny 1978), but a common way is to express the compressibility factor Z as some function of pressure

$$Z = F(p)$$

The parameters N_0 and Z are non-linear and require an iterative regression. A non-linear least squares analysis can be applied to the experimental data using the above equation to determine the volume ratio N_0 at zero pressure and the parameters of F(p). The Burnett apparatus is however, unsuitable for operation in the liquid phase, and large errors in derived quantities can result at low temperature.

Isochorically Coupled Burnett Method

The isochorically coupled Burnett method (Pope 1971, Hall 1972) was developed to reduce the errors associated with derived quantities, such as the compressibility factor, from the classical Burnett method. It does this by providing additional experimental data in the form of isochores connecting the isotherms. This eliminates the necessity of determining the compressibility factor for each run by extrapolation or regression. To do this, a series of Burnett expansions are conducted at the highest allowable temperature for a given gas in a given apparatus. To reach the next lower temperature, the system is charged at the higher temperature to exactly the same pressure as one of the expansions. The system is then cooled to the lower temperature where the pressure is measured. This is the isochoric part of the experiment. After that measurement another set of isothermal Burnett measurements are performed. The system at the end of the high temperature expansion series can also be cooled by "jumping" two or three temperatures to a run at a much lower temperature. Thus, all isotherms are connected isochorically. The major advantage of this method, like the Burnett method, is that no volume calibrations are needed. This method is

considered one of the best PVT methods for gases but it is not appropiate for high density fluids.

Piezometers

A piezometer (Tekc et al. 1984) is a basic part of an apparatus used for the direct measurement of PVT properties of liquids and liquid mixtures. It usually denotes a vessel filled with a fluid and equipped with a device by means of which the compression can be measured. The word piezometer is used to describe instruments by which the compression can be determined directly, i.e., by measuring temperature, pressure, and volume of the fluid. A piezometer consists of two basic parts (Figure 2) a contaniner A, whose volume determines the magnitude of observed volume changes of the liquid under investigation and a volumometer B, a device that makes it possible to measure the volume changes. The piezometer is usually a thin walled vessel placed inside a thick walled pressure vessel D (or separately D and E). Thus the maximum difference in pressures inside and outside the piezometer is given by the difference in hydrostatic pressures. The volumometer usually serves as a pressure-transmitting device separating the experimental fluid from a

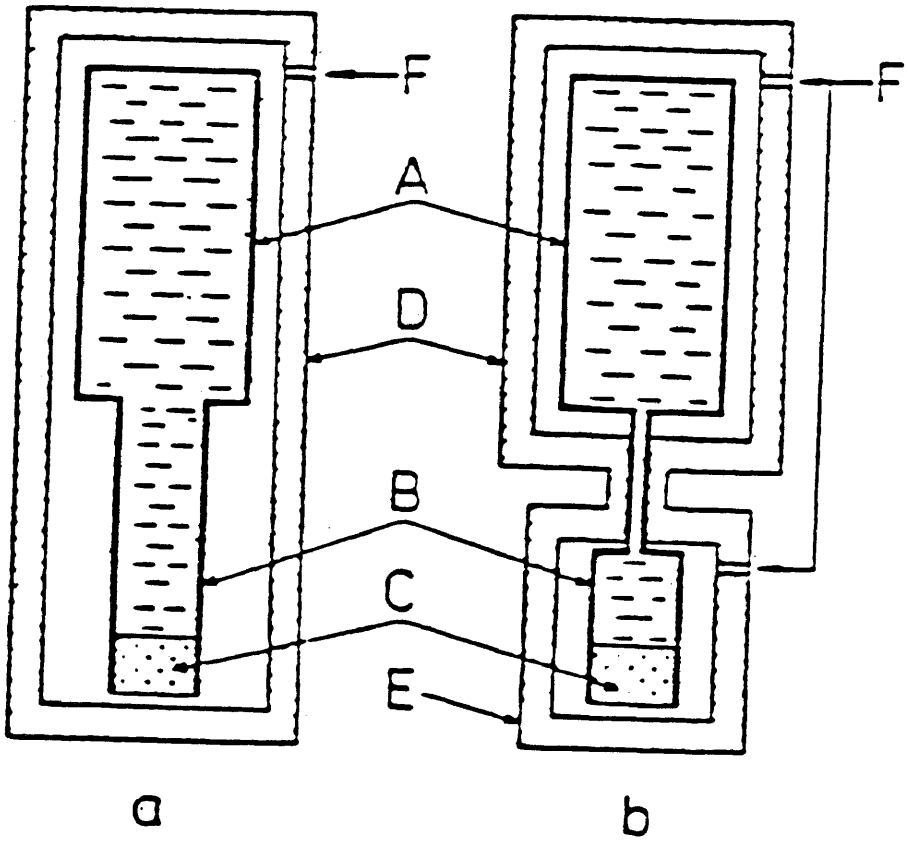

Figure 2. Schematic Diagrams of piexometers: a) variable-volume: b) constant-volume. A. container: B. volumometer: C. volume sensor: D. pressure vellel at temperature of measurement: E. pressure vessel at constant temperature: and F. pressure transmitting (hydraulic) fluid. (Ref. Tekac *et al.* 1984).

hydraulic fluid.

There are two basic types of piezometers: variable-volume piezometers (Figure 2a) and constant-volume piezometers (Figure 2b). The container and the volumometer of the variable-volume piezometer are both placed in the same pressure vessel. The temperature of these two parts is the experimental one. The volume of the experimental liquid being studied changes due to changes in both the temperature and pressure. These volume changes are measured by the volumometer.

The container of the constant-volume piezometer is at the experimental temperature, while the temperature of the volumometer is kept at some constant temperature. The container and the volumometer are connected to one another via a thick-walled capillary. The volume of the experimental liquid at the measurement temperature and pressure remains constant. The experimental liquid is injected to or ejected from the container as the temperature and pressure are changed. The amount of liquid injected or ejected is measured by the volumometer. The data obtained by means of constant-volume piezometers are usually more precise than those obtained by variable-volume piezometers, especially while measuring a wide range of temperatures. This is due to the volumometer temperature being constant,

thus eliminating the need for corrections for changes of volumometer properties caused by temperature changes. A disavantage of this method is that one must know exactly how the volume varies with pressure and temerature. This is a problem because volumetric calibrations are usually the most difficult and poorest type of measurements.

Mechanical Oscillator

A vibrating densimeter (Picker et al. 1973) makes relative measurements on fluid densities by measuring resonant frequencies. Figure 3 illustrates the essential features of the flow densimenter presented by Picker. The resonant frequencies are sustained and monitored by appropriate electronic devices. A vibrating densimeter consists of V-shaped tubing which is thermostated to achieve constant temperature, and a magnetic pickup which is used to activate and sustain the resonant vibrations. This magnetic pickup is an integrated part of a electrical detector-drive circuit. The period of oscillation of the tube is measured using a digital frequency meter. The liquid being studied is circulated at a constant flow rate through the vibrating tube during the frequency measurement. The natural

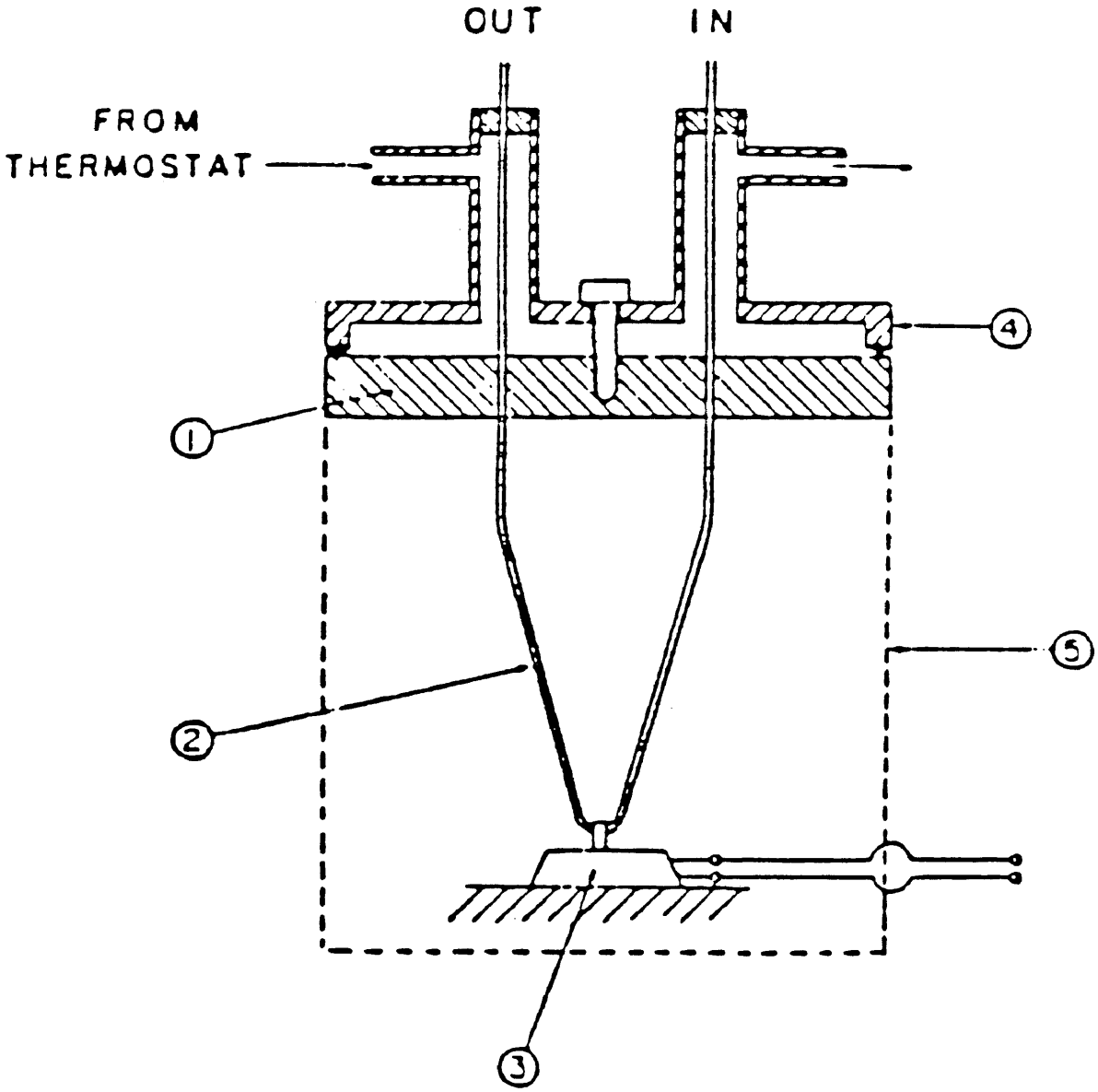

Figure 3. Mechanical design of flow densimeter. 1. Brass anchoring plate: 2. stainless steel vibrating tube: 3. magnetic pickup: 4. thermoregulated jacket for anchoring plate and liquid intake : thermoregulated vessel. (Ref. Picker *et al.* 1973).

vibration period of the tube is related to the density of the liquid as shown by Kratky et al. (1969)

$$d = A + B\tau^2$$

where d is the liquid density, τ the oscillation period, and A and B are constants for a given mechanical system. These parameters can be determined from calibration measurements on two fluids of accurately known densities such as water and air.

This method is very good when making dynamic measurements on fluid densities close to that of the calibration fluid. Other advantages are the ease of application at higher temperatures and measurements on fluids with suspended particles such as blood in the human body. A disadvantage of this method is that when densities deviate from that of the calibration fluid, a second reference fluid with accurately known densities is needed, but is not always available.

Isochoric Method

The isochoric or constant volume method confines a sample of fixed mass in a cell of nearly fixed volume. The volume of the cell (Figure 4) is accurately known as a

function of pressure and temperature. The noxious volumes of all tubing must also be accurately known. The isochoric method usually consists of charging the system to a nominal density, setting the temperature and measuring the corresponding pressure. Several of the temperature-pressure measurements are made on each pseudo-isochore. The are refered to as pseudo-isochores since the cell volume changes with temperature and pressure. The sample is then removed to a weighing cylinder where the exact mass of the sample is obtained by differential weighings. The density of the sample fluid is then determined from a knowledge of the sample mass and the volume of the cell at each temperature and pressure. Although the volume is only approximately constant, common practice refers to each set of temperature-pressure measurements as isochoric.

This method is better for liquid samples. The major difficulty with this method is in the accurate calculation of all the volumes associated with the system: the PVT cell and all noxious volumes.

An alternative approach to determine the density of the sample is by expanding it into a gasometer consisting of accuarately calibrated volumes where the moles of the sample is obtained. The gasometer consists of four glass bulbs of accurately known volumes. A disavantage of using a

gasometer is the difficulties in accurately determining the volume of the expanded sample and in maintaining the glass bulbs at constant temperature. These difficulties can result in large uncertainties in the measured values.

LITERATURE SURVEY

During the past twenty years there have been extensive experimental measurements of the properties of pure carbon dioxide as well as pure ethane . These measurements are summarized in the reviews Ely et al. (1987) and Tekac et al. (1985). But, there has been very little density data available for CO_2-rich hydrocarbon mixtures, and even less for carbon dioxide-ethane mixtures. Table 2 lists CO_2-hydrocarbon vapor-liquid equilibra (VLE) and density mixture data available in the literature.

Vapor-liquid equilibra measurements usually consist of charging an equilibrium cell with an amount of the mixture desired. The cell is placed in some type of controlled temperature environment so as to maintain a constant temperature. Once the sample is confined in the cell, vapor is removed from the top half of the cell and the system pressure is measured. The vapor is then recirculated into the bottom half of the cell where it bubbles through the liquid sample. When the system reaches equilibrium, i.e. when the pressure is sufficiently stabilized, the vapor is sent to a gas chromatograph where the mixture composition corresponding to the system temperature and pressure is obtained. The density of the mixture may be obtained by

using a mechanical oscillator attached to the equilibrium cell.

Kuenen was perhaps the first to investigate the behavior of binary mixture of CO_2 and light hydrocarbons (Kuenen 1897, Kuenen and Robson 1902). These measurements indicated minimum boiling azeotropic characteristics for the CO_2-C_2H_6 system. Reamer and co-workers investigated several CO_2-rich systems including CO_2-CH_4 (Reamer et al. 1944), CO_2-C_2H_6 (Reamer et al. 1945), CO_2-C_3H_8 (Reamer et al. 1951) and CO_2-nC_4H_{10} (Olds et al. 1949). They have claimed a volumetric uncertainity of not greater than 0.2 % throughout the entire range of conditions reported. Gugnoni et al. (1974) were the other investigators which have made density measurements on the carbon dioxide-ethane system, and they have claimed reproducibility and uncertainity in the liquid density measurements of 0.2 % also. Lau (1986) reported density measurements for the CO_2-C_2H_6 systems at three different compositions and claims an accuracy of better than 0.1 %. Further examination of Table 2 shows that there is no data available for the entire range of the 0.99 CO_2 + 0.01 C_2H_6 system studied in this investigation, and there are also very little density data available for carbon dioxide-hydrocarbon mixtures.

As was stated above, highly accurate density measurements are needed in order to model the fluid behavior in CO_2 pipelines. Therefore, an improved and expanded database of these systems are needed to insure reliable predictive models.

Table 2. Summary of Experimental Density Data for Mixtures Containing Carbon Dioxide

Carbon Dioxide	T-range (K)	P-range (bar)	x_{CO_2}-range (mol %)	Ref
+ Methane	310-511	13-690	15-80	Reamer et al. (1944)
	253-288	20-152	1-99	Arai et al. (1971)
	225-400	20-350	98	Magee and Ely (1988)
+ Ethane	310-511	13-690	17-82	Reamer et al. (1945)
	240-350	16-350	25-90	Lau (1987)
	241-283	10-50	8-94	Gugnoni et al. (1974)
+ Propane	277-511	13-690	20-80	Reamer et al. (1951)
+ n-Butane	310-511	13-690	18-84	Olds et al. (1949)
	255-284	1-42	1-99	Kalra et al. (1976)
+ i-Butane	310-395	7-72	3-91	Besserer et al. (1973)
+ Nitrogen	313-354	59-589	23-68	Kosov et al. (1975)
	250-330	22-331	0-98	Haynes et al. (1988)
+ Methane (0.1)[a]				
+ Nitrogen (0.1)	245-400	35-330	98	Magee and Ely (1988)

[a] (mole %)

EXPERIMENTAL

The apparatus (Figure 4) used in this work has a long history of studies of pure fluids and mixtures. It was initially designed by Robert D. Goodwin (Goodwin 1961) in 1961 to obtain PVT data for parahydrogen from 16 to 100 K and from 2 to 350 atm. It has also been used to obtain PVT data for pure ethene (Straty 1980), compressed fluid nitrogen (Straty & Diller 1980), a compressed and liquefied mixture of nitrogen and methane (Straty & Diller 1980, Haynes & McCarty 1983), and was altered to be compatable with fluorine (Straty & Prydz 1970). The apparatus was extensively modified (Magee 1986) to allow automated data aquisition and control and to raise the upper limit of temperature to 450 K. The experimental method used in these studies was the isochoric method.

Preparation of mixture

Table 3 gives a brief summary of the preparation apparatus and purity of the gases. The (0.99 CO_2 + 0.01 C_2H_6) mixture was gravimetrically prepared by the following procedure. A 660 cubic inch gas cylinder was

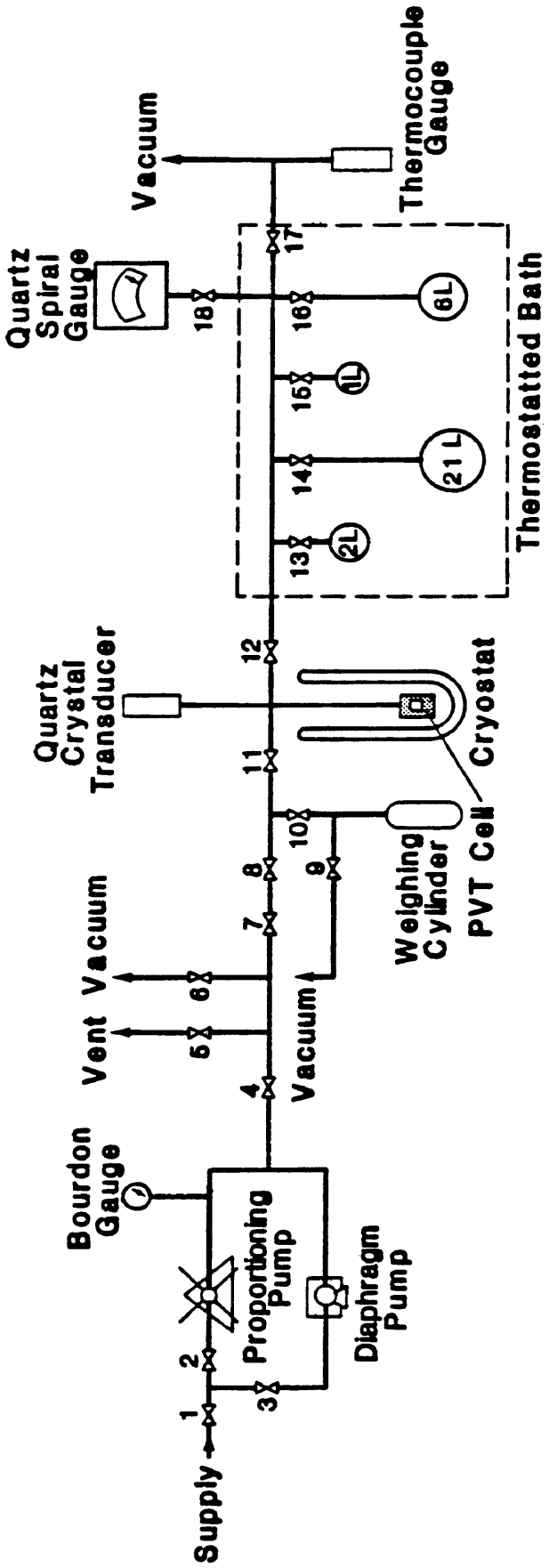

Figure 4. Schematic of isochoric PVT apparatus.

Table 3. Gravametric Mixture Preperation Apparatus

Key Equipment: Commercial load cell 24 kg capacity with 0.1 g resolution in the 2000 g tare range

Two pan balance 25 kg capacity with 0.001 g resolution and 0.01 g accuracy

Ultrahigh vacuum system capable of less than 0.0001 torr

Pure gases available : CO_2 0.999946 % pure

C_2H_6 0.99989 % pure

Mixture preperation:

nominal composition 0.99 CO_2 + 0.01 C_2H_6

realized composition 0.9900010 CO_2 + 0.0099990 C_2H_6

composed of 1774.703 g CO_2 + 12.247 g C_2H_6

accuracy of gravimetric composition

1 part in 100,000 for CO_2

2 parts in 100,000 for C_2H_6

evacuated with an ultrahigh vacuum system capable of less than 1.0×10^{-5} torr for 10 days. The vacuum system has a cold trap available, which was filled with liquid nitrogen and used to remove all remaining condensables from the cylinder. The evacuated cylinder is weighed on a 24 kg commercial load cell with 0.1 g resolution in the 2 kg tare range to obtain an estimate of the nul reading. It was then weighed on a 25 kg two pan balance with 0.001 g resolution and 0.01 g accuracy against a balast weight to obtain an accurate nul reading. The cylinder was then placed on the load cell and 12.247 g of 99.999 % pure ethane was added. The cylinder was then weighed using the two pan balance, and the exact mass of ethane was obtained by the difference of the above weighing and the null weighing. Stoichiometry was used to calculate the amount of CO_2 which should be added to the cylinder to account for the 99:1 mixture. The mixture cylinder was again placed on the load cell and 1774.703 g of 99.9946 % pure CO_2 were added. The exact mass of CO_2 was obtained by weighing the cylinder on the two pan balance and subtracting the weight from the prior reading. The exact composition of the mixture was 99.00010 % CO_2 + 0.99990 % C_2H_6 with an accuracy of 10 ppm for CO_2 and 20 ppm for C_2H_6. The final mixture pressure at ambient temperature was approximately 5 MPa, which is less than the

vapor pressure of pure CO_2 (6 MPa) at ambient temperature. The mixture cylinder is stored at a pressure which is less than the dew point pressure of the mixture, thus the mixture is stored as a single phase vapor at ambient temperature.

Isochoric Method

The isochoric or constant volume method confines a sample of fixed mass in a cell of nearly fixed volume. The volume of the cell (Figure 5) is accurately known as a function of pressure and temperature. The noxious volumes (tubing and valves) are also accurately known. The temperature is changed in increments and the corresponding pressures are measured until the upper limit of temperature (400 K) or pressure (35 MPa) is achieved. The sample is cryopumped into a weighing cylinder which is immersed in boiling liquid nitrogen after the final data point is obtained. The sample mass is obtained from the difference of precise weighings before and after the sample is placed in the weighing cylinder. The density of the sample is determined from the sample mass and the volume of the cell at each pressure and temperature.

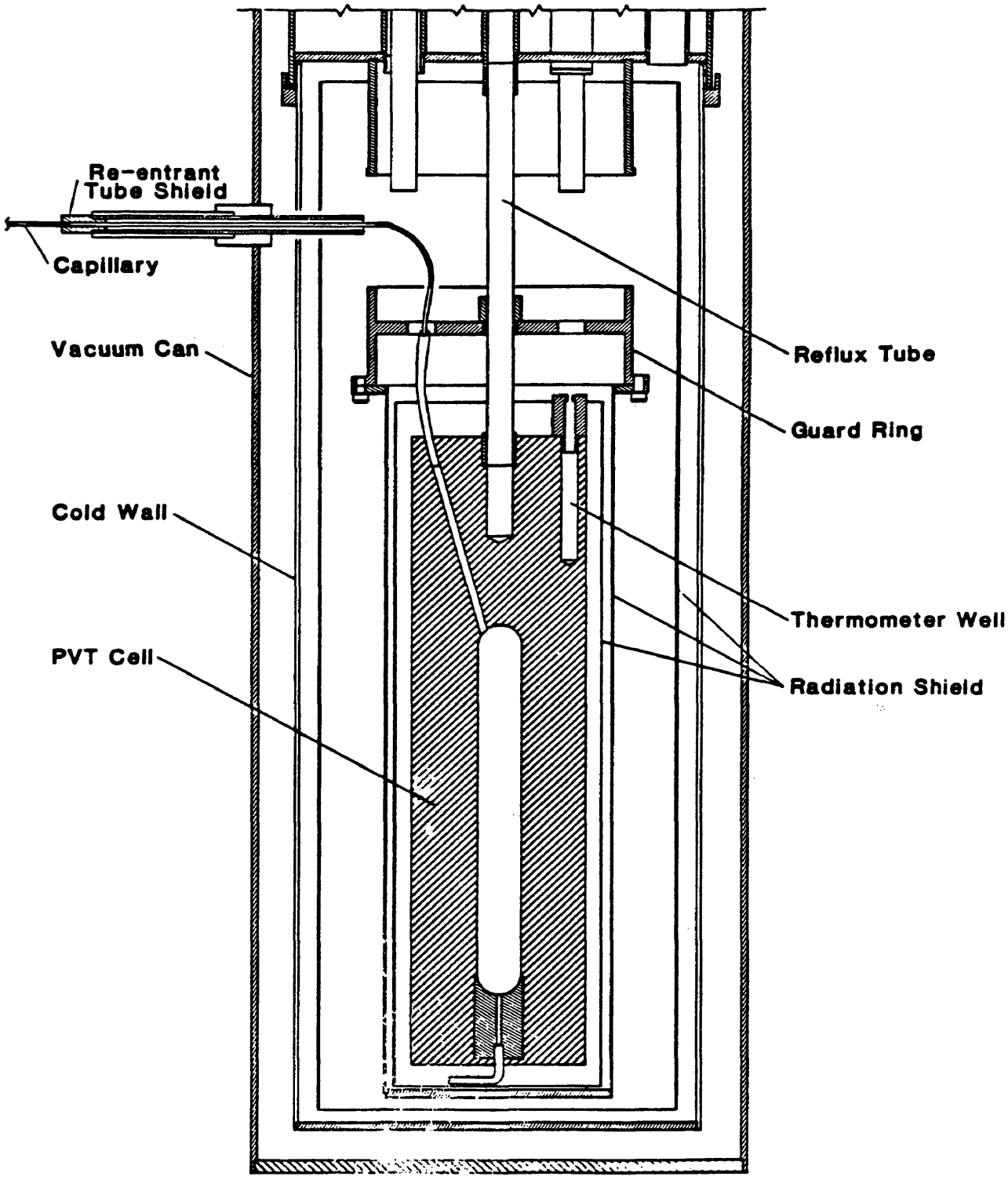

Figure 5. Details of PVT cell and cryostat.

Temperature Measurement

The temperatures are measured with a platinum resistance thermometer (PRT) circuit. This circuit consists of a 25 ohm PRT calibrated on the IPTS-68 by the National Bureau of Standards (NBS) Temperature Section, a precision 2 mA current source stable to 2 ppm, a 10 ohm standard resistor calibrated by the NBS Electricity Division, low thermal emf solder connections, ultralow thermal emf relays, and a 6 ½ nanovoltmeter. The current source powers the thermometry circuit with two milliamperes and is equipped with relays capable of reversing the direction of current in the circuit, which enables an average foward and reverse potential readings, eliminating errors associated with any spurious emf's.

Temperature measurements are made as follows. The relays switch the current to the foward direction and the standard resistor potential, V_{std} is read. The current in the measurement loop is calculated by $I = V_{std}/R_{std}$. The relays switch the nanovoltmeter to the platinum resistance thermometer and the corresponding potential, V_{prt} is read. The PRT resistance is calculated by $R_{prt} = V_{prt}/I$. The relays then switch the current to the reverse direction and the above procedure is repeated. The average PRT resistance

is calculated by $R_{avg} = (R_{fwd} + R_{rev})/2$ and the corresponding IPTS-68 temperature $T(R_{avg})$ is obtained by refering to the PRT calibration.

Pressure Measurement

The pressures are measured by reading the average period of vibration of an oscillating quartz crystal pressure transducer via a frequency counter over an averaging time of 10 seconds, yielding a resolution of 1 part in 100,000 The pressure transducer is connected to the sample cell by a fine diameter, 0.02 cm ID, capillary (Figure 5). It is thermostatted at 335.15 ± 0.05 K and has been calibrated versus an oil lubricated piston gauge, accurate to 0.01 %. The calibration was made in an ascending and descending pressure series to determine the maximum hysteresis. The maximum hysteresis occured at 150 bar and was less than 0.01 %. The transducer was originally calibrated by Dr. J.W. Magee in May 1986 and was recalibrated for this study in July 1987. Figure 6 shows that the transducer is extremely stable over the 14 month span. It exibits deviations of less than 0.003 % between the two calibrations. The pressure is obtained through a

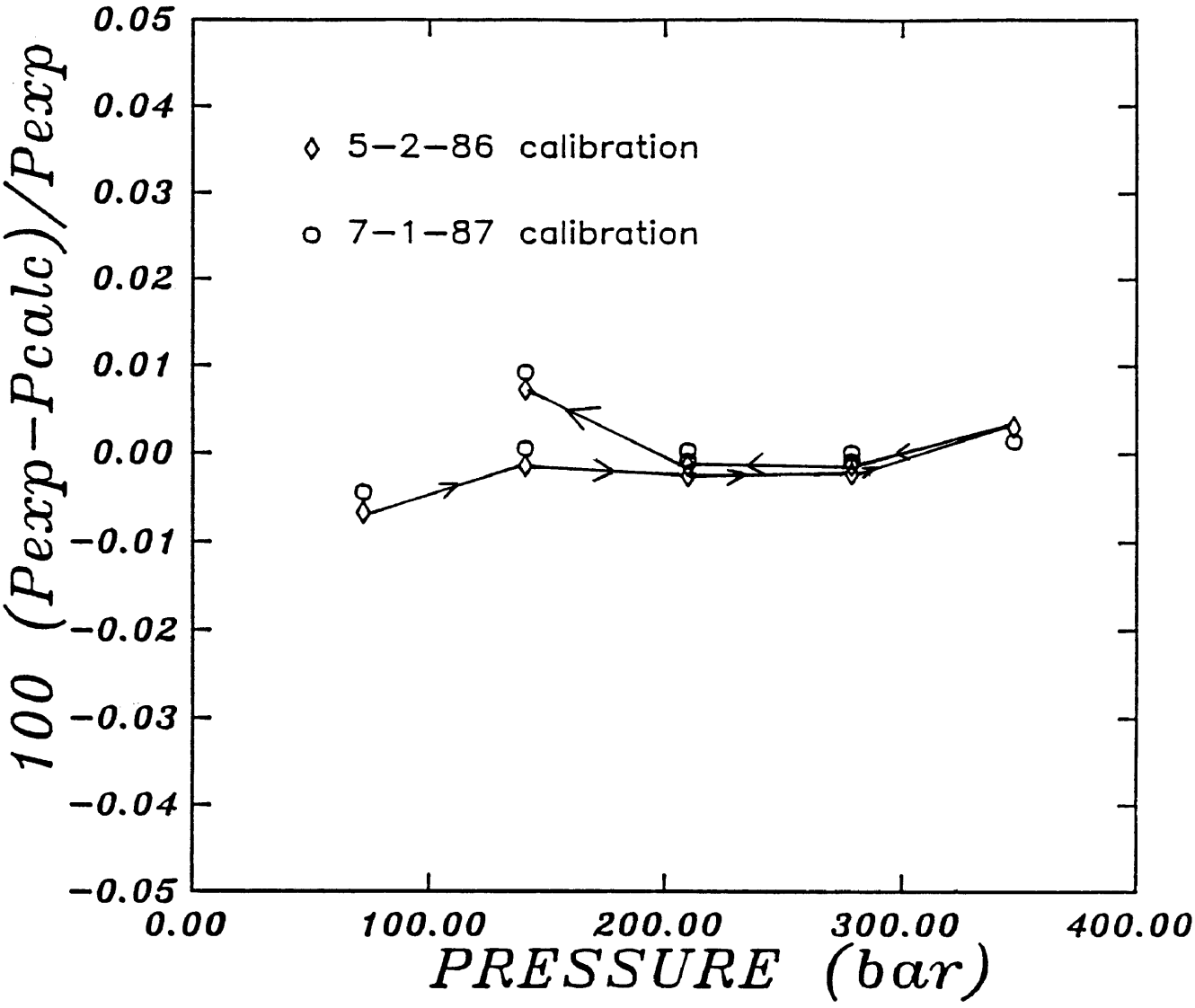

Figure 6 . Deviations of two sets of calibration data for quartz pressure transducer from pistion gauge pressures.

regression routine used to fit the pressure(p) - period(Tau) data by,

$$p = C\,[(1 - Tau_0/Tau) - D\,(1 - Tau_0/Tau)^2]$$

where,

Tao_0 = average period at zero pressure

C,D = coefficients of the model.

The root mean square deviation of the pressures was found to be 0.0053 % for the calibration.

Computer Control

A detailed FORTRAN program is responsible for automated data aquisition, temperature control, and data processing. The program controls when relays are to close, the direction of thermometry currents, instrument readings, and the power sent to the heaters. The heaters are controlled with a proportional plus integral approach. The program can scan a range of target temperatures, recording data when equilibrium conditions are met.

The aquisition of data is as follows. After the system has been charged to the selected nominal density, the temperature is changed and the corresponding pressure is measured. The data point can be recorded if the temperature

is within 0.005 K of the target temperature, the change in temperature with respect to time is less than 0.5×10^{-3} K per minute and the change in pressure with respect to time is less than 0.5×10^{-4} bar per minute. When the data point has been recorded, the temperature is raised and the proceedure repeated until the upper limit of temperature or pressure is achieved.

The pressure transducer period of oscillation and thermometry circuit potentials are communicated to the host computer via an IEEE-488 standard interface. Digital and analog signals are used to control relays and power supplies. The program also allows for monitoring and control from remote locations equipped with a modem and microcomputer.

As stated above, the temperature is measured with a PRT circuit, and is controlled by giving the computer a target temperature. The temperature measured by the PRT is read by the computer. The computer calculates the difference between the measured temperature and the target temperature and sends the appropriate signal to power the heaters. The apparatus is equipped with a cell heater and a guard ring heater (Figure 5). A differential type thermocouple senses the difference in temperature between the gaurd ring and cell. A proportional plus integral algorithm drives the

guard ring heater so that the guard ring temperature tracks that of the cell, thus eleminating any temperature gradients between the top and bottom of the cell.

Charging the System

The entire system, sample cell, all tubing and valves, and the weighing cylinder are evacuated to an ultrahigh vacuum for 2-3 hours. The mixture cylinder was heated to near 340 K on a hot plate while heat lamps where used to warm all other volumes in the charging system (Figure 4). The system was heated to avoid phase separation of the sample, which has a critical temperature of about ambient, during the charging. The entire system is then repeatedly purged with hot sample gas.

The system is charged using the following procedure. The predictive model, DDMIX, was used to obtain a table of pressures and densities at a temperature of 320 K for the mixture in this study. A density is chosen and the calculated pressure is input into a FORTRAN program to obtain the correspomning transducer frequency. A diaphragm compressor is used to boost the gas pressure in the cell to the target pressure. The cell is charged with the mixture

gas to a transducer reading above that which was calculated. Gas is then released until the target frequency is obtained and the system charging valve is closed.

Density Measurement

The densities in this study were obtained using the gravimetric method. A 300 cc cylinder was evacuated to an ultrahigh vacuum for approximately 3 hrs. The weighing cylinder was then purged repeatedly with hot mixture gas. It was vented to approximately atmospheric pressure after the final purge was completed. The cylinder was weighed on a 25 kg two pan balance to obtain an initial weight w_1. All capillary tubing leading from the PVT cell to the weighing cylinder was evacuated. When the upper limit of the run was reached, the weighing cylinder was immersed in liquid nitrogen. Refering to Figure 4, the system charging valve (11) and the weighing cylinder valve (10) were opened, thus freezing the gas sample in the weighing cylinder. This is continued until a high vacuum reading is observed by the cell pressure transducer at which time the cylinder valve is closed. After the cylinder has warmed to ambient temperature, it is weighed on the two pan balance to obtain a final weight w_2. The isometric mass is given by

$$m = w_2 - w_1.$$

The density is calculated using a FORTRAN program with inputs of isometric mass, temperature and pressure. All volumes must be acurately known in order to obtain the densities.

The volume of the PVT cell was originally calculated by hydrogen gasometry. The volume of a glass bulb was calibrated by differential weighings using water. The volume was determined to be

$$V_{bulb} = 128.591\ [1.0 + 2.5 \times 10^{-5}\ (T - 21.85)].$$

The volume of the PVT cell was determined by various hydrogen expansions in the glass bulb with the system pressure measured by a quartz spiral gauge and was found to be:

$$V_{cell} = a\ V(T)$$

where

$$a = 1.0 + \{\ 2.3 \times 10^{-6}\ [1.0 + 4.35 \times 10^{-4}\ T]\ P\ \}$$

$$V(T) = 28.505\ [1.0 + 3.0 \times 10^{-5}\ (A + BT + CT^2)]$$

$$A = -33.43516480$$

$$B = 0.608228022$$

and

$$C = 0.002160275.$$

EXPERIMENTAL RESULTS AND DISCUSSION

A total of thirteen isochores were studied at densities ranging from 2 to 24 mol/dm^3. Each isochore consists of five to ten data points with temperatures ranging from 245 K to 400 K and pressures ranging form 28 to 353 bar. The accuracy of the experimental measurements were 0.20 % for densities of 2 - 10 mol/dm^3 and 0.10 % for densities of 11 - 24 mol/dm^3. The 0.1% accuracy for the higher density range is the result of errors associated with volume calibrations, temperature and pressure measurements, compositional accuracy and mass measurements. The accuracy is lower for the low density range because of the larger error associated with the mass measurement. Table 4 gives a summary of the accuracies and precisions claimed in this investigation. This study was primarily concerned with the determination of experimental densities of (0.99 CO_2 + 0.01 C_2H_6) and the use of these measurements to evaluate and further develop a predictive thermodynamic model for the properties of CO_2 rich mixtures. One of the ultimate goals of this study was to improve the predictive model.

Table 4. (0.99 CO_2 + 0.01) C_2H_6 Densities

Range of state conditions

temperature	245 - 400 K
pressure	20 - 350 Bar
density	2 - 24 mol/l

Estimated accuracy and precision of measurements

	Accuracy	Precision
composition		
CO_2	0.006	0.0002 %
C_2O_6	0.003	0.0004 %
temperature	0.005 K	0.001 K
pressure	0.01 %	0.001 %
density		
2-10 mol/l	0.20 %	0.10 %
11-24 mol/l	0.10 %	0.01 %

Predictive Model

The predictive model used in this study was based upon the extended corresponding states theory. The model, DDMIX, was developed by Dr. J.F. Ely, and incorporates a one-fluid concept originally due to van der Waals. It uses inputs of composition, temperature and pressure and returns the thermodynamic values of enthalpy, entropy, sound speed, Gibbs free energy, viscosity, thermal conductivity, liquid-vapor equilibria and mixture densities.

Corresponding States for Conformal Molecules

The corresponding states principle has been known for many years for simple pure molecules and is well summarized in advanced statistical mechanical texts (Reed and Gubbins 1973, McQuarrie 1976). The basic result derived from statistical mechanics is that if two pure fluids are conformal, i.e. they obey the same reduced intermolecular force law, simple scaling arguments lead one to the conclusion that

$$a_j^r(\rho_j, T_j) = a_0^r(\rho_0, T_0) \qquad (1)$$

In this equation

$$a^r \equiv [A(\rho,T) - A^*(\rho,T)]/RT \qquad (2)$$

where A is the Helmholtz free energy, the asterisk indicates an ideal gas value, R is the gas constant and T is the absolute temperature. The subscript j indicates the fluid of interest and the subscript o indicates a reference fluid whose thermodynamic properties are known, in principle, with great accuracy. A relationship between the density and temperature of the fluid j and the corresponding values for the reference fluid o can be arrived at by the scaling arguments which lead to eq. (1) :

$$T_o = T_j/f_j \quad \text{and} \quad \rho_o = \rho_j h_j \qquad (3)$$

The scale factors f_j and h_j are called the equivalent substance reducing ratios. They are related to ratios of the intermolecular potential parameters by

$$f_j = \varepsilon_j/\varepsilon_o \quad \text{and} \quad h_j = (\sigma_j/\sigma_j)^3 \qquad (4)$$

where the conformal potential has been assumed to be of the form

$$u_{jj}(r) = \varepsilon_j F(r/\sigma_j) \qquad (5)$$

The Lennard-Jones 12-6 potential is an example of a conformal intermolecular potential

$$u(r) = 4\varepsilon\{(\sigma/r)^{12} - (\sigma/r)^6\} \qquad (6)$$

For pure fluid corresponding states, it can be shown from the mechanical stability criteria that

$$f_j = (T_j^c/T_o^c) \quad \text{and} \quad h_j = (V_j^c/V_o^c) \qquad (7)$$

where the subscript j denotes a pure fluid other than the reference fluid and the superscript c denotes a critical point value.

Corresponding States for Nonconformal Molecules

Extended Corresponding States

In order to apply the corresponding states theory to a nonconformal fluid, the extended corresponding states model was originally proposed by Leland and co-workers (Leland and Mueller 1959, Reid and Leland 1965, Leach 1967, Leland, Rowlinson and Sather 1968) in the late 1960's and early 1970's. This extension is accomplished by the use of molecular shape factors. These shape factors are introduced into the equivalent substance reducing ratios for pure fluids and are allowed to be functions of density and temperature. This in effect assumes that the intermolecular parameters are density and temperature dependent but the potential itself is conformal to the potential of some reference fluid, i.e.

$$\varepsilon_j = \varepsilon_j(\rho,T) = k_1(\rho,T)T_j^c \qquad (8a)$$

and

$$\sigma_j^3 = \sigma_j^3(\rho,T) = k_2(\rho,T)V_j^c \qquad (8b)$$

where k_1 and k_2 are universal functions. Dividing by the reference fluid potential parameters

$$h_j = (V_j^c/V_o^c)\Phi_j(\rho,T) \tag{9a}$$

and

$$f_j = (T_j^c/T_o^c)\Theta_j(\rho,T) \tag{9b}$$

The parameters Θ_j and Φ_j are called shape factors. It can be theoretically shown that the apparent temperature and density dependence in the shape factors may be attributed to differences in the long range electrostatic and short range repulsive electronic structures of nonspherical molecules.

Generalized formulas (Leach 1967) were used for the shape factors appearing in Eqs. (9a) and (9b) during the early applications of the extended corresponding states model. Highly accurate equations of state and a broad base of accurate experimental data were not available when these formulas were developed. One can, however, use recent highly accurate pure fluid experimental data and correlate these data to predict exact shape factors which could be used in mixture calculations. This leads to a mixture model which will have essentially no uncertainties in the pure component limit. A discussion on the calculation of shape factors appears in a later section.

Corresponding States for mixtures

In order to extend corresponding states to mixtures, approximations must be made concerning the microscopic interactions and resulting structure of the mixture. The problem which arises in this extension is that the configurational energy in the mixture is a function of the position of the molecules and the species of the molecule assigned to a particular position. This can be compared to the pure fluid case where the molecules are indistinguishable and the configurational energy of the system is only a function of molecular positions. Therefore, the scaling arguments which led to eq. (1) for pure fluids do not apply to a mixture, even if the intermolecular potentials for all mixture components are conformal.

Several theoretically based arguments were arrived at in order to deal with this problem, the earliest of which was the concept of random mixing. This concept averages the configurational energy of a mixture over all possible random assignments of species to a given position. It leads to an effective, hypothetical pure fluid or equivalent substance potential which can be used in the formalism developed for pure fluids. Mixing rules for the equivalent substance reducing ratios of the hypothetical pure fluid can be

obtained by considering the explicit form of the conformal potential i.e. Lennard-Jones potential. An example would be

$$f_x = (\{x_i\},\{f_{ij}\},\{h_{ij}\}) \tag{10a}$$

$$h_x = (\{x_i\},\{f_{ij}\},\{h_{ij}\}) \tag{10b}$$

where the subscript x denotes the hypothetical pure fluid and

$$f_{ij} = \varepsilon_{ij}/\varepsilon_o \tag{10c}$$

$$h_{ij} = (\sigma_{ij}/\sigma_o)^3 \tag{10d}$$

where the subscript ij denotes the interaction of an ij pair in the mixture.

The concept of random mixing played an important role in the development of mixture theories, but its predictions are not reliable because the random assignment of molecules is an unrealistic physical basis. The idea that the properties of a mixture can be equated to those of a hypothetical pure fluid whose properties can be evaluated from corresponding states has persisted. This idea is known as the one-fluid concept and forms the basis for what are currently the most accurate corresponding states models for mixtures.

The van der Waals one-fluid theory, developed by Leland and co-workers, is the most successful corresponding states theory for mixtures. It is formed from an expansion of the properties of a system about a hard sphere system. A hard

sphere system is one whose molecules only have repulsive intermolecular potentials with no attractive contributions ($\varepsilon_{ij} = 0$). The theory is based on a rigorous statistical mechanical result for the equation of state of a mixture of pairwise additive spherically symmetric molecules. It uses a radial distribution function, g_{ij}, which gives the probability of finding a molecule of type i at a distance r from the central molecule of type j, and an intermolecular potential which is assumed to be composed of a hard sphere term plus a long range attraction term.

An assumption concerning the radial distribution functions of mixture pairs must be made in order to use the model. The one used in model DDMIX is the mean density approximation. It states that the distribution function of the ij pair is identical to that of a pure fluid evaluated at the reduced conditions of the pair and a mean number density. An expansion of the radial distribution function about that of a hard sphere (Kirkwood et al. 1952) is carried out on the approximation to obtain the distribution function of a real fluid in terms of that of a hard sphere. These approximations are substituted into the statistical mechanical equation for the compressibility factor and are the basis for forming the mixing rules

$$\sigma_x^3 = \sum \sum x_i x_j \sigma_{ij}^3 \qquad (11a)$$

and

$$\varepsilon_x \sigma_x^3 = \sum \sum x_i x_j \varepsilon_{ij} \sigma_{ij}^3 \tag{11b}$$

Dividing through by the reference fluid parameters

$$h_x = \sum \sum x_i x_j h_{ij} \tag{12a}$$

and

$$f_x h_x = \sum \sum x_i x_j f_{ij} h_{ij} \tag{12b}$$

These are exactly the relations that van der Waals assumed in the generalization of his equation of state to mixtures.

In order to use these mixing rules one must adopt combining rules which relate the unlike pair parameters to those of the pure components. In this work we have assumed that

$$f_{ij} = (f_i f_j)^{\frac{1}{2}}(1 - k_{ij}) \tag{12c}$$

and

$$h_{ij} = \left[(h_i^{1/3} + h_j^{1/3})/2\right]^3 (1 - l_{ij}) \tag{12d}$$

In these equations k_{ij} and l_{ij} are binary interaction parameters which can be adjusted to optimize the performance of the corresponding states model.

Implementation of Model

Thus far, only the theory of the model has been presented. The next logical step is to show how the theory

can be inplemented so as to arrive at a working form of the model. There are three major questions which must be asked in this implementation:

1) What is a reference fluid ?

2) How does one calculate shape factors ?

and

3) What type of mixing rules are being used ?

Reference Fluid Equation of State

The reference fluid is a fluid whose thermodynamic properties are known, in principle, with great accuracy. In order to perform the shape factor calculations, high accuracy representations of the PVT surfaces for the components of the mixture and the reference fluid are required. Since a large number of fluid PVT surfaces had previously been represented with the 32 term BWR type equation proposed by Stewart and Jacobsen (1973), this functional form was retained in the shape factor investigations, and shall be refered to as the MBWR-32. The mathematical form of the equation is essentially a polynomial in density and temperature

$$p = \sum_{n=0}^{9} a_n(T)\rho^n + e^{-\gamma\rho^2} \sum_{n=10}^{15} a_n(T)\rho^{2n-17} \qquad (13)$$

The temperature dependence of the a_n is given in Table 5. The equation contains one nonlinear parameter, , which was always set to $1/\rho_c^2$. The fitting procedure of this equation consists of: 1) collecting and evaluating experimental data for PVT, second virial coefficients, saturation, heat capacities and sound velocities, 2) the independent correlation of the vapor pressure and orthobaric densities and 3) a multiproperty regression analysis of the thermodynamic surface im posing constraints on the critical point and saturation boundary as determined in step 2. The data were weighted using a statistical error propagation formula proposed by McCarty (1975). The formula states that for a dependent variable, f, which is a function of several independent variables x_j, the weight for a given experimental point becomes

$$w_i^{-1} = \sigma_f^2 + \sum_{j=1}^{N} \sigma_{x_j} \left(\frac{\partial f}{\partial x_j}\right)^2 \qquad (14)$$

where σ is a variance which is estimated from the experimental reports, w_i is the weight and the derivatives are obtained from an unweighted or previous fit of the surface.

Ely et al. (1985) determined the coefficients for this equation of state for eight fluids: methane, ethane, propane, i-butane, n-butane, carbon dioxide, carbon monoxide and hydrogen sulfide. In addition, previous work has

Table 5. Temperature Dependence of the 32 term BWR Coefficients

$a_1 = RT$

$a_2 = b_1 + b_2T^{1/2} + b_3 + b_4/T + b_5/T^2$

$a_3 = b_6T + b_7 + b_8/T + b_9/T^2$

$a_4 = b_{10}T + b_{11} + b_{12}/T$

$a_5 = b_{13}$

$a_6 = b_{14}/T + b_{15}/T^2$

$a_7 = b_{16}/T$

$a_8 = b_{17}/T + b_{18}/T^2$

$a_9 = b_{19}/T^2$

$a_{10} = b_{20}/T^2 + b_{21}/T^3$

$a_{11} = b_{22}/T^2 + b_{23}/T^4$

$a_{12} = b_{24}/T^2 + b_{25}/T^3$

$a_{13} = b_{26}/T^2 + b_{27}/T^4$

$a_{14} = b_{28}/T^2 + b_{29}/T^3$

$a_{15} = b_{30}/T^2 + b_{31}/T^3 + b_{32}/T^4$

R is the gas constant an T is the absolute temperature in Kelvin

provided equation of state coefficients for nitrogen (Stewart 1981), oxygen (Stewart 1981), argon (Stewart 1981) and ethylene (McCarty and Jacobsen 1981). Thus, at the time of this study there have been reported high accuracy equations of state by which shape factors can be calcluated for twelve fluids. The equations reproduce the density to within 0.3 percent and pressures to 2 percent, except in the near critical region.

Shape Factor Calculations

The ideal situation for determining molecular shape factors for each mixture component would be a generalized expression for the shape factors so that they could be used in a predictive model. In the past, several attempts to generalize shape factors have been made, the most successful being that of Leach, *et al.* who found that

$$\theta_j = 1 + (\omega_j + \omega_o)F(T_r,V_r) \tag{15}$$

and

$$\Phi_j = \{1 + (\omega_j - \omega_o)G(T_r,V_r)\}(Z_o^c/Z_j^c) \tag{16}$$

where

$$F(T_r,V_r) = a + bT_r' + (c + \frac{d}{T_r'})(V_r - 0.5) \tag{17}$$

and

$$G(T_r, V_r) = \alpha(V_r' + \beta) + \gamma(V_r' + \delta)(V_r' - 0.5)\ell n T_r' \quad (18)$$

where ω is Pitzer's acentric factor defined by

$$\omega = \log_{10}(p^{sat}/p_c)_{T_R = 0.7} - 1.0 \quad (19)$$

and a-d and α-β are universal constants. The subscript r denotes a quantity reduced by the corresponding critical point value. Leach's formulas have restricted the values of V_r and T_r, to lie between 0.5 and 2.0, i.e.

$$V_r' = [\max 0.5, \min (2.0, V_r)]$$

$$T_r' = \max [0.5, \min (2.0, V_r)]$$

This formalism was developed before high accuracy equations of state and broad base experimental data for homologous series were available. Ely (1985) decided that these data should be correlated and exact shape factors could be calculated. These calculations would then be used to test the validity of existing shape factor correlations and to extend their useful range.

From thermodynamics we know that for the compressibility factor

$$\left(\frac{\partial a^r}{\partial \rho}\right)_T = \frac{Z^r}{\rho} \quad (20)$$

Differentiating eq. (1) with respect to d we find

$$\frac{Z_j^r}{\rho_j} = \left(\frac{\partial a_o^r}{\partial T_o}\right)_{\rho_o}\left(\frac{\partial T_o}{\partial \rho_j}\right)_{T_j} + \left(\frac{\partial a_o^r}{\partial \rho_o}\right)\left(\frac{\partial \rho_o}{\partial \rho_j}\right)_{T_j} \quad (21)$$

or

$$Z_j = u_o^r \frac{\rho_j}{f_j}\left(\frac{\partial f_j}{\partial \rho_j}\right)_{T_j} + Z_o^r\left[1 + \frac{\rho_j}{h_j}\left(\frac{\partial h_j}{\partial \rho_j}\right)_{T_j}\right] \tag{22}$$

where $u_0 = (U_0 - U_0^*)/RT_0$. Defining $f_\rho = (\partial f_j/\partial \rho_j)(\rho_j/f_j)$ and $h_\rho = (\partial h_j/\partial \rho_j)(\rho/h)$ we then have

$$Z_j^r = Z_o(1 + h_\rho) + u_o^r f_\rho \tag{23}$$

Similar expressions may be derived for other properties and are summarized in Table 6.

The equations in Table 6 show that it is not possibe to unabiguously calculate shape factors (or equivalently the f_j and h_j) from experimental thermodynamic data. There are two shape factors which need to be calculated, Θ_j and Φ_j , or equivalently f_j and h_j. Therefore, two equations are needed to solve for this system. If the equations for the Helmholtz energy and the compressibility factor are choosen

$$a_j^r = (\rho_j, T_j) = a_o^r(\rho_o, T_o) \tag{1}$$

and

$$Z_j^r = (1 + h_\rho)Z_o^r + u_o^r f_\rho \tag{24}$$

the derivatives of f and h enter into the calculation. This leads to thermodynamic relationships which provide an undetermined system of equations. Therefore, a particular set must be choosen in order to perform the calculations of f_j and h_j.

The most convenient set computationally is the set of

Table 6. Dimensionless Residual Thermodynamic Properties in the Extended Corresponding States Model with Density and Temperature Dependent Shape Factors

Property	Relation
Helmholtz Energy	$a_j^r = a_o^r$
Compressibility Factor	$Z_j^r = (1 + h_\rho)Z_o^r + f_\rho u_o^r$
Internal Energy	$u_j^r = (1 - f_T)u_o^r - h_T Z_o^r$
Entropy	$s_j^r = s_o^r - f_T u_o^r - h_T Z_o^r$
Enthalpy	$h_j^r = h_o^r + (f_\rho + f_T)u_o^r + (h_\rho - h_T)Z_o^r$
Gibbs Energy	$g_j^r = g_o^r + h_\rho Z_o^r + f_\rho u_o^r$

All energies are $x - (X - X^*)/RT$, entropy is $s = (S - S^*)/RT$ All ideal gas (*) properties are at the same density and temperature as the system. $f_T = (\partial f/\partial T)(T/f)$, etc.

solutions for the case where the density derivatives of f and n satisfy the relation

$$Z_o^r h_\rho = -u_o^r f_\rho \tag{25}$$

This is achieved when we require $Z_o^r = Z_j^r$. In order to find the shape factors or equivalently f_j and h_j, from high accuracy equations of state, one simultaneously solves the corresponding states relations for the Helmholtz free energy and the compressibility factor for each component

$$a_j^r(\rho_j, T_j) = a_o^r(\rho_o, T_o) \tag{1}$$

and

$$Z_j^r(\rho_j, T_j) = Z_o^r(\rho_o, T_o) \tag{26}$$

for ρ_o and T_0 given ρ_j, T_j and accurate equations of state for the PVT behavior of fluids j and o. This solution may be easily accomplished numerically using a two-dimensional Newton-Raphson iteration.

A problem does occur in the solution for shape factors when the density becomes so low that the fluid behavior can be represented by a virial equation of state. If, for example, $Z = 1 + B\rho$ it can be shown that $a_j^r = B\rho$ and both the equations given above reduce to $B_j(T_j)\rho_j = B_0(T_0)\rho_o$. When this occurs, the iteration method must be switched to one which maps virial coefficients rather than thermodynamic properties. This will be satisfied if one assumes that

$$Z^r = B\rho + C\rho^2 \tag{27}$$

and

$$a^r = B\rho + \tfrac{1}{2}C\rho^2 \tag{28}$$

These equations will be satisfied if one finds a T_0 such that

$$\frac{B_j(T_j)}{B_o(T_o)} = \left[\frac{C_j(T_j)}{C_o(T_o)}\right]^2 \tag{29}$$

This leads to $h_j = B_j/B_0$ and the criteria of equal Helmholtz energy and compressibility factors are satisified.

A third method may be necessary if the two methods mentioned above fail to converge. This method consists of a generalized functional form for the shape factors such as those presented by Leach et al..

Mixing Rules

As decribed previously, the application of the extended corresponding states model becomes even more complex for mixtures because it is not clear how one introduces composition dependence into the one-fluid model.

In this implementation we have used the van der Waals one-fluid theory. It assumes the relation $a_{mix} = a_x$ as the starting point for mixture calculations. This statement

contains two assumptions: 1) one must assume that a_{mix} is equivalent to some hypothetical pure fluid a_x and 2) that the properties of this pure fluid can be calculated using pure fluid corresponding states. Table 5 then states the relations between the reference fluid properties and mixture properties. The only new equation which must be introduced is

$$\ell n(f_i/x_i p) = g_o^r + u_o^r f_{n_i} + Z_o^r h_{n_i} \tag{30}$$

where $f_{n_i} = \frac{n_i}{f_x}\left(\frac{\partial f_x}{\partial n_i}\right)_{n_j}$ and f_i is the fugacity of a component in solution. The van der Waals one-fluid mixing rules were used in this investigation but a modification of these mixing rules was explored.

There has been a great deal of interest in improving equation of state mixing rules for fluid modeling during the past few years. This has been driven by result that modified cubic equations of state using van der Waals mixing rules typically give as good if not better phase equilibrium results than the conformal solution models using the same mixing rules (Mentzer et al. 1981). This result becomes much more pronounced as the size differences in the mixture become large, much more so than for systems which display large energy differences. These observations are based on

data for real fluid mixtures and recent computer simulation studies (Hoheisel et al. 1983, Shing and Gubbins 1982, and Gupta 1984) on model Lennard-Jones mixtures. The computer simulations have shown the failures of the various conformal solution models as a function of size differences.

Ely (1986) has proposed a new set of mixing rules for use in conformal solution mixture calculations which are derived by making a new "mean density" approximation. As in the van der Waals one-fluid model the radial distribution function of a binary pair is expanded about that of a hard sphere. These new mixing rules reduce to the van der Waals one-fluid model in the limit of low density and are exact for the compressibility factor of hard sphere mixtures.

The improvement in the model occurs in the approximation of the radial distribution functions for the mixture. The van der Waals one-fluid approximation assumes that

$$g_{ij}(r;\{\rho_\alpha\},T;\{\varepsilon_{\alpha\beta}\}\{\sigma_{\alpha\beta}\}) = g_o(\frac{r}{\sigma_{ij}};\frac{kT}{\bar{\varepsilon}};\rho\bar{\sigma}^3) \qquad (31)$$

while the mean density approximation (MDA) introduced by Mansoori and Leland (1972) assumes that

$$g_{ij}(r;\{\rho_\alpha\},T;\{\varepsilon_{\alpha\beta}\}\{\sigma_{\alpha\beta}\}) = g_o(\frac{r}{\sigma_{ij}};\frac{kT}{\varepsilon_{ij}};\rho\bar{\sigma}^3) \qquad (32)$$

Ely made a simple modification to the MDA which leads to

$$g_{ij}(r;\{\rho_\alpha\},T;\{\varepsilon_{\alpha\beta}\}\{\sigma_{\alpha\beta}\}) = g_o(\frac{r}{\sigma_{ij}};\frac{kT}{\varepsilon_{ij}};\rho\bar{\sigma}^3)R_{ij} \quad (33)$$

where

$$R_{ij} = g_{ij}^{HS}(\sigma_{ij};\{\rho_\alpha\};\{\sigma_{\alpha\beta}\})/g_o^{HS}(\bar{\sigma};\rho\bar{\sigma}^3) \quad (34)$$

and refered to this as the "modified" mean density approximation (MMDA).

The new approximation results in the new desired mixing rules

$$\bar{\sigma}^3 = \sum\sum x_i x_j \sigma_{ij}^3 R_{ij} \quad (35a)$$

and

$$\varepsilon_x \bar{\sigma}_x^3 = \sum\sum x_i x_j \varepsilon_{ij} \bar{\sigma}_{ij}^3 R_{ij} \quad (35b)$$

where R_{ij} is difined in eq. (34). Dividing through by the reference fluid parameters

$$h_x = \sum\sum x_i x_j h_{ij} R_{ij} \quad (36a)$$

and

$$f_x h_x = \sum\sum x_i x_j f_{ij} h_{ij} R_{ij} \quad (36b)$$

Since

$$\lim_{\rho\to o} g_{ij}^{HS} = \lim_{\rho\to o} g_o^{HS} = 1 \quad (37)$$

the mixing rules reduce to the common van der Waals one-fluid rules from eqs. (12a) and (12b) in the limit of low density and equal size ratios.

In order to use these mixing rules for VLE calculations, one must evaluate the derivative terms appearing in Eq. (30).

The results obtained in this study are

$$\frac{n}{\eta_x}\left(\frac{\partial \eta_x}{\partial n_k}\right) = \frac{-2 + A + B + D}{(1 - C)} \tag{38}$$

and

$$\frac{n}{\varepsilon_x \eta_x}\left(\frac{\partial(\varepsilon_x \eta_x)}{\partial n_k}\right) = -2 + E + F \tag{39}$$

where the composition and density dependence of the terms A - F is given in appendix A.

As was stated above, these new mixing rules are an improvement over past rules because they help to account for size differences amoung molecules. This is not of great concern for the system being studied here. The size difference between CO_2 and C_2H_6 are small, and one can safely assume that these new mixing rules will not improve the results obtained with the model, which uses the van der Waals one-fluid mixing rules. They have been included because the work was finished before a decision on which system should be studied was arrived at.

Evaluation of Model and Comparision with Experimental Data

The deviations of the calculated densities from experimental densities using the MBWR-32 and the another equation of state discussed later are presented as a function of pressure p and temperature T (IPTS-68) for the mixture in Table 7. The model, in it's original state, consisted of using the MBWR-32 equation of state with propane as the reference fluid. Propane was selected because of it's low reduced triple point, which enables it to be used over a wide range of temperatures. These single phase densities are calculated by the model as follows. The user inputs the mixture composition, temperature and pressure. The program takes the MBWR-32 equation of state for each mixture component and the reference fluid and attempts to map the mixture properties to the reference properties. It does this by calculating exact shape factors for the mixture using the desired mixing rules. When the shape factors are exactly mapped to the reference state, all thermodynamic mixture properties are calculated.

A total of 13 isochores were studied at densities ranging from 2 to 24 mol/dm^3. Each isochore consists of five to ten data points with temperatures ranging from 245 K to 400 K and pressures ranging form 28 bar to 353 bar.

Table 7 . Measured Densities for CO_2 + C_2H_6

Temp (K)	Press (bar)	Density (expt)	Density (BWR)	Density (SW)	$\frac{D_{expt}-D_{BWR}}{D_{expt}}$	$\frac{D_{expt}-D_{SW}}{D_{SW}}$
270.000	31.8505	2.008	1.986	1.990	-1.056	-0.872
280.000	34.2851	2.006	1.998	1.999	-0.400	-0.343
300.000	38.8026	2.002	2.002	2.002	-0.011	-0.017
310.000	40.9315	2.001	2.000	2.000	-0.032	-0.050
320.000	43.0236	1.999	1.998	1.997	-0.035	-0.067
340.000	47.1226	1.995	1.995	1.994	0.001	-0.061
360.000	51.1260	1.991	1.992	1.990	0.055	-0.037
380.000	55.0432	1.987	1.989	1.987	0.093	-0.026
400.000	58.9091	1.983	1.986	1.983	0.156	0.019
290.000	53.4178	4.002	3.924	3.949	-1.941	-1.332
300.000	59.0459	3.998	3.976	3.985	-0.545	-0.326
310.000	64.2368	3.990	3.975	3.981	-0.368	-0.214
320.000	69.2641	3.986	3.973	3.979	-0.317	-0.161
330.000	74.1233	3.981	3.967	3.973	-0.352	-0.205
340.000	78.8923	3.976	3.963	3.968	-0.333	-0.205
360.000	88.2001	3.967	3.958	3.960	-0.226	-0.162
380.000	97.2607	3.956	3.953	3.952	-0.075	-0.087
400.000	106.1029	3.943	3.946	3.943	0.074	-0.003

Table 7. (Continued)

Temp (K)	Press (bar)	Density (expt)	Density (BWR)	Density (SW)	$\frac{D_{expt}-D_{BWR}}{D_{expt}}$	$\frac{D_{expt}-D_{SW}}{D_{SW}}$
290.000	53.3101	3.962	3.903	3.927	-1.478	-0.878
300.000	58.7790	3.957	3.936	3.945	-0.533	-0.315
310.000	63.8917	3.950	3.935	3.941	-0.385	-0.233
320.000	68.8640	3.945	3.934	3.939	-0.303	-0.152
330.000	73.6767	3.941	3.929	3.935	-0.302	-0.160
340.000	78.3798	3.936	3.925	3.930	-0.297	-0.175
360.000	87.5893	3.927	3.920	3.923	-0.165	-0.106
380.000	96.5452	3.916	3.916	3.915	-0.012	-0.026
400.000	105.2686	3.904	3.909	3.906	0.117	0.038
300.000	67.1093	6.034	5.966	5.989	-1.130	-0.755
310.000	76.1210	6.027	6.007	5.999	-0.328	-0.454
320.000	84.7085	6.019	5.992	5.995	-0.445	-0.399
330.000	93.0368	6.010	5.979	5.989	-0.526	-0.348
340.000	101.1698	6.001	5.969	5.983	-0.537	-0.298
360.000	116.9801	5.980	5.954	5.968	-0.431	-0.194
380.000	132.3569	5.959	5.944	5.954	-0.251	-0.080
400.000	147.3964	5.941	5.934	5.940	-0.118	-0.017

Table 7. (Continued)

Temp (K)	Press (bar)	Density (expt)	Density (BWR)	Density (SW)	$\frac{D_{expt}-D_{BWR}}{D_{expt}}$	$\frac{D_{expt}-D_{SW}}{D_{SW}}$
310.000	81.3952	8.136	8.161	8.080	0.311	-0.688
320.000	93.8620	8.123	8.088	8.067	-0.437	-0.699
330.000	106.1495	8.109	8.071	8.074	-0.471	-0.437
340.000	118.1997	8.093	8.054	8.065	-0.484	-0.345
360.000	141.8090	8.065	8.030	8.044	-0.426	-0.262
380.000	164.9964	8.044	8.018	8.029	-0.318	-0.186
400.000	187.8528	8.026	8.009	8.017	-0.213	-0.108
310.000	82.7162	9.096	9.108	9.034	0.131	-0.683
320.000	97.0897	9.081	9.068	9.061	-0.150	-0.230
330.000	111.2485	9.064	9.041	9.051	-0.253	-0.145
340.000	125.2578	9.046	9.025	9.037	-0.233	-0.101
360.000	152.8811	9.017	9.000	9.008	-0.185	-0.099
380.000	180.1640	8.995	8.986	8.991	-0.102	-0.050
400.000	207.0775	8.977	8.972	8.976	-0.058	-0.013

Table 7. (Continued)

Temp (K)	Press (bar)	Density (expt)	Density (BWR)	Density (SW)	$\frac{D_{expt}-D_{BWR}}{D_{expt}}$	$\frac{D_{expt}-D_{SW}}{D_{SW}}$
310.000	82.6133	9.029	9.027	8.950	-0.027	-0.883
320.000	96.8421	9.015	8.990	8.980	-0.283	-0.386
330.000	110.8935	8.998	8.973	8.982	-0.286	-0.187
340.000	124.7209	8.980	8.950	8.962	-0.330	-0.198
360.000	152.0720	8.951	8.930	8.928	-0.237	-0.145
380.000	179.0691	8.930	8.917	8.922	-0.136	-0.079
400.000	205.7652	8.911	8.907	8.912	-0.042	0.007
310.000	83.8271	10.131	10.019	10.018	-1.105	-1.116
320.000	100.2054	10.114	10.059	10.090	-0.552	-0.238
330.000	116.5462	10.094	10.062	10.086	-0.318	-0.076
340.000	132.7845	10.074	10.052	10.065	-0.220	-0.084
360.000	165.0670	10.044	10.032	10.032	-0.121	-0.123
380.000	197.0760	10.022	10.014	10.010	-0.081	-0.121
400.000	228.8223	10.002	9.998	9.995	-0.046	-0.073

Table 7. (Continued)

Temp (K)	Press (bar)	Density (expt)	Density (BWR)	Density (SW)	$\frac{D_{expt}-D_{BWR}}{D_{expt}}$	$\frac{D_{expt}-D_{SW}}{D_{SW}}$
310.000	84.9831	11.202	10.957	11.062	-2.189	-1.252
320.000	103.6498	11.182	11.097	11.164	-0.761	-0.170
330.000	122.4691	11.159	11.127	11.156	-0.279	-0.019
340.000	141.2976	11.137	11.127	11.133	-0.094	-0.035
360.000	178.9349	11.108	11.108	11.097	0.004	-0.103
380.000	216.4741	11.085	11.088	11.074	0.027	-0.098
310.000	86.1920	12.142	11.813	11.971	-2.708	-1.406
320.000	107.1404	12.120	12.012	12.076	-0.892	-0.366
330.000	128.3996	12.093	12.056	12.069	-0.308	-0.202
340.000	149.8055	12.072	12.065	12.053	-0.061	-0.153
360.000	192.8045	12.042	12.051	12.027	0.076	-0.127
380.000	235.7553	12.018	12.026	12.005	0.069	-0.108
300.000	72.4922	16.089	16.070	16.058	-0.118	-0.194
310.000	107.5350	16.057	16.053	16.039	-0.027	-0.116
320.000	143.3268	16.018	16.029	15.999	0.069	-0.118
330.000	179.6938	15.993	16.007	15.974	0.087	-0.123
340.000	216.3729	15.975	15.985	15.955	0.063	-0.122

Table 7. (Continued)

Temp (K)	Press (bar)	Density (expt)	Density (BWR)	Density (SW)	$\frac{D_{expt}-D_{BWR}}{D_{expt}}$	$\frac{D_{expt}-D_{SW}}{D_{SW}}$
280.000	57.73034	20.294	20.295	20.293	0.007	-0.005
285.000	89.74609	20.269	20.268	20.266	-0.004	-0.013
290.000	121.56040	20.236	20.237	20.236	0.005	0.000
295.000	153.30370	20.208	20.207	20.207	-0.008	-0.007
300.000	185.54630	20.191	20.187	20.188	-0.022	-0.013
305.000	217.94900	20.177	20.169	20.173	-0.039	-0.020
310.000	250.45110	20.165	20.154	20.161	-0.054	-0.022
315.000	283.03170	20.154	20.141	20.150	-0.062	-0.019
320.000	315.46280	20.143	20.127	20.139	-0.080	-0.024
325.000	347.93060	20.133	20.115	20.129	-0.092	-0.022
245.000	27.93378	24.165	24.145	24.153	-0.083	-0.051
250.000	82.66400	24.133	24.114	24.115	-0.078	-0.073
255.000	135.00800	24.083	24.070	24.066	-0.056	-0.073
260.000	188.56730	24.053	24.040	24.033	-0.055	-0.087
265.000	243.43720	24.034	24.023	24.013	-0.047	-0.089
270.000	298.51410	24.019	24.010	23.999	-0.037	-0.084
275.000	353.45670	24.005	23.997	23.986	-0.030	-0.076

Figure 7 illustrates the range of the errors associated with the MBWR-32 equation of state. The accuracy of the experimental measurements were 0.20 % for densities of 2 - 10 mol/dm^3 and 0.10 % for densities of 11 - 24 mol/dm^3. A summary of the accuracies and precisions estimated in this investigation were presented in Table 4.

The most interesting way to evaluate the data is in terms of plotting isotherms on a differential density vs. density plot. Figure 8 represents the 310, 320 and 330 K isotherms. The 310 K isotherm shows the greatest deviation from the predictive model DDMIX. This occurs at a temperature of 310 K and a density of 12.1426 mol/dm^3. The errors decrease by more than 50 % when the temperature is increased to 320 K and the maximum error at 330 K is about 0.5 %. Figure 9 represents the 320, 330, 340, 360 and 380 K isotherms, and shows a steady decrease in error as the temerature is raised. Figure 10 shows that the 360, 380 and 400 K isotherms follow the same type of pattern as above. These figures also show an S-shaped configuration which is associated with the configuration of critical isotherms and a tendency tward zero error at low density.

Figures 11 - 16 represent plots of several isochores on a differential density vs. temperature graph. These figures show where the tendencies of the model change from negative

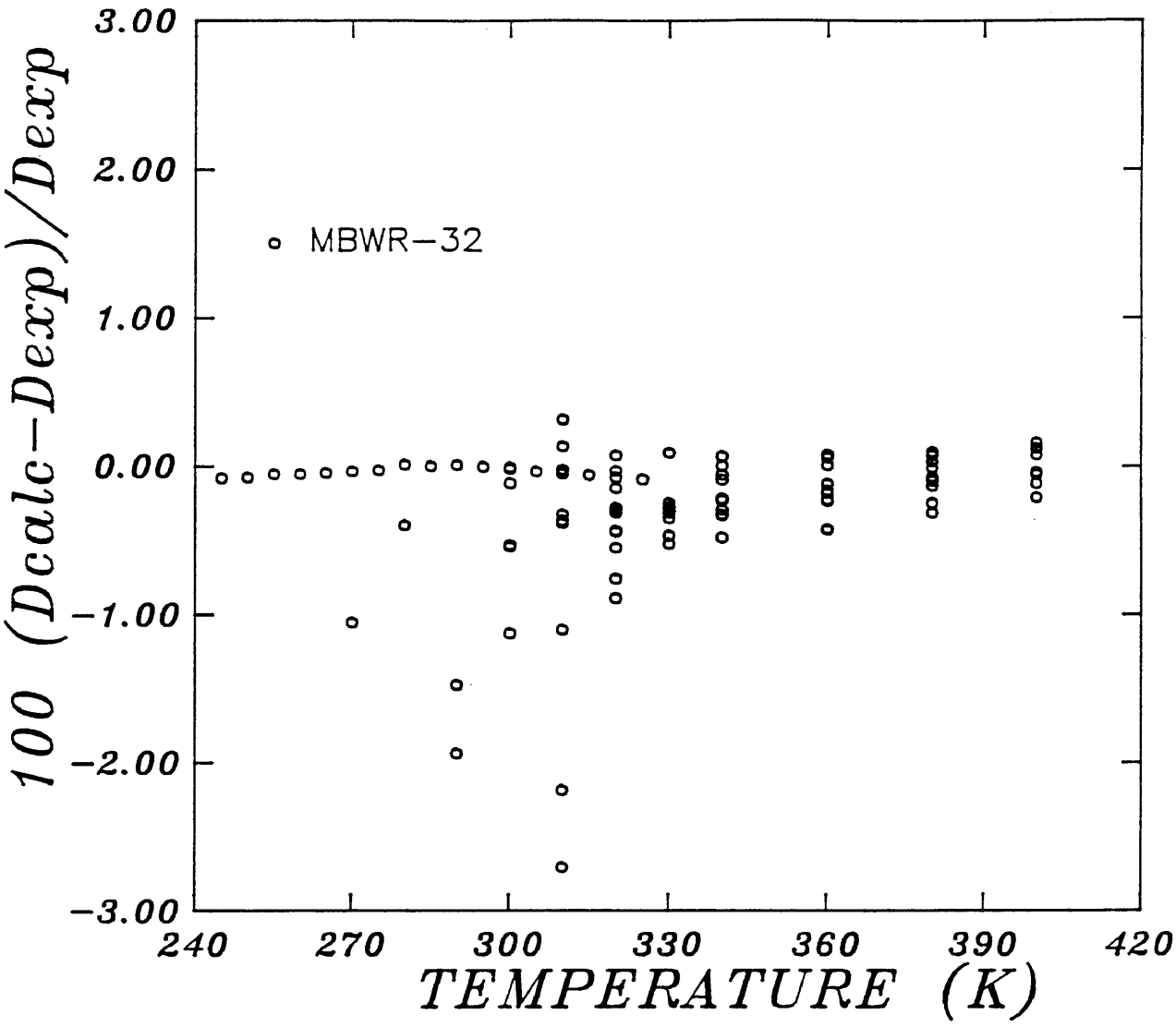

Figure 7 . Density deviation range for 0.99 CO_2 + 0.01 C_2H_6 using the MBWR-32 EOS.

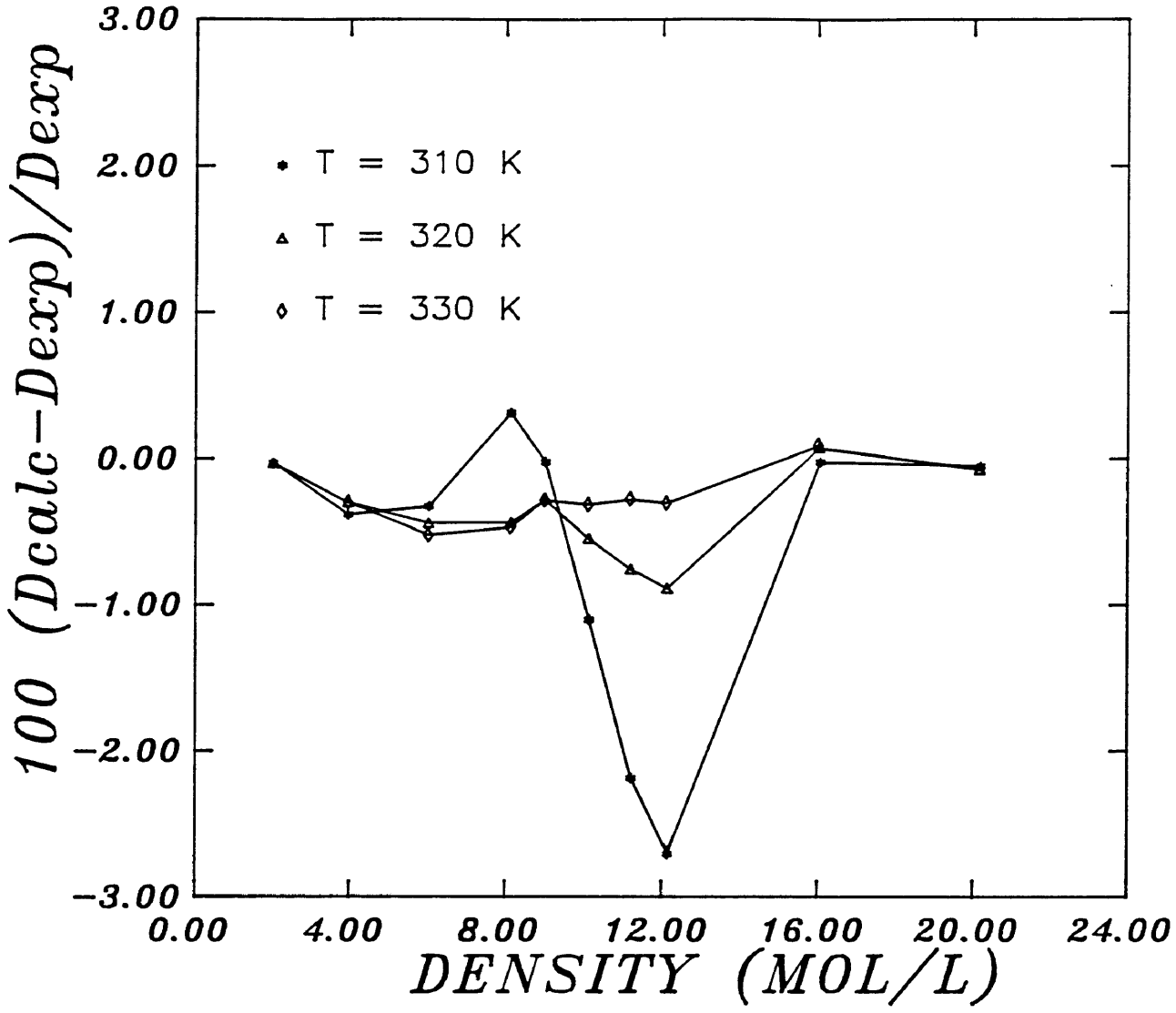

Figure 8. Density Deviation for 0.99 CO_2 + 0.01 C_2H_6 using the MBWR-32 EOS for isotherms of 310, 320 and 330 K.

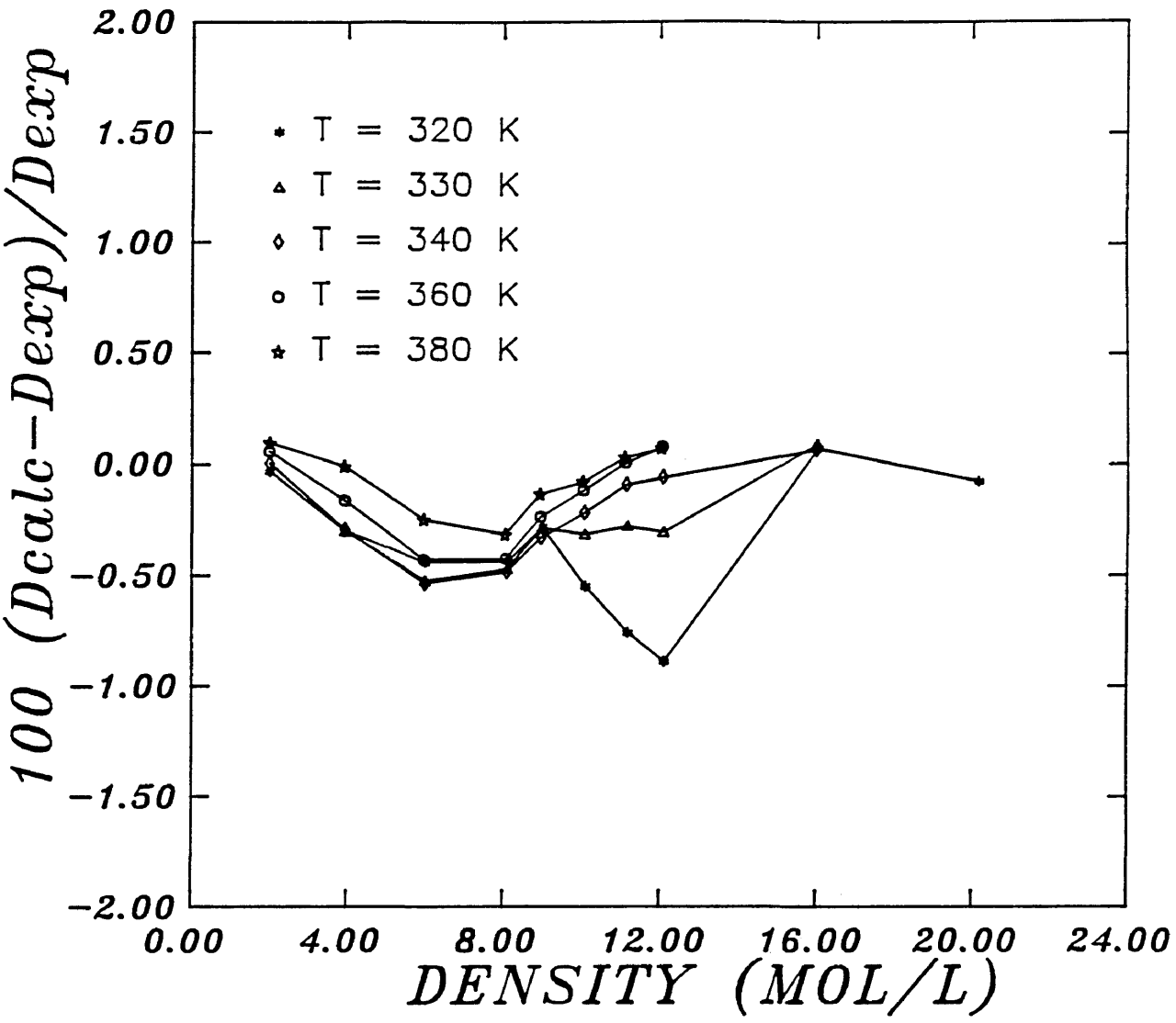

Figure 9. Density Deviation for 0.99 CO_2 + 0.01 C_2H_6 using the MBWR-32 EOS for isotherms of 320, 330, 340, 360 and 380 K.

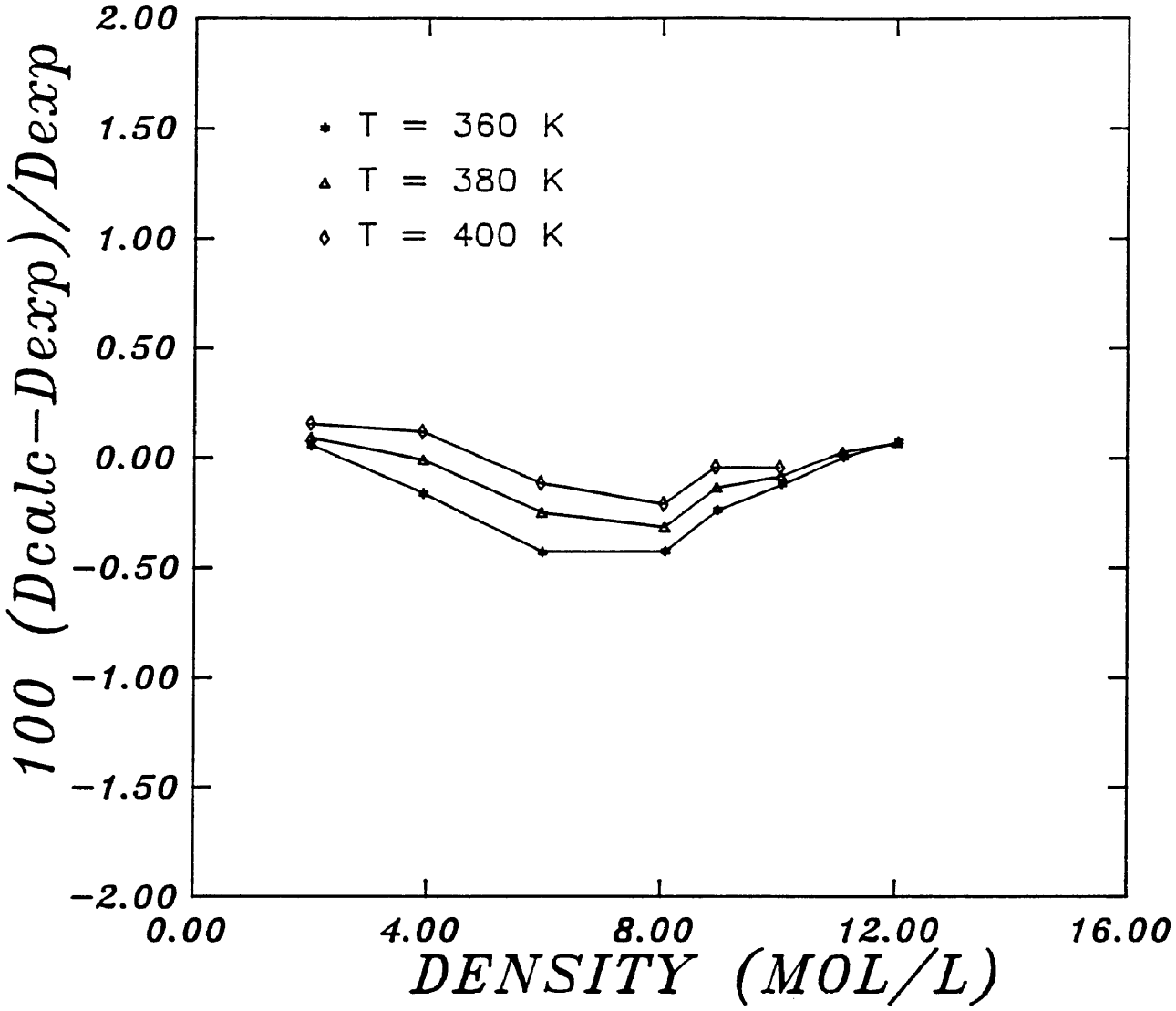

Figure 10. Density Deviation for 0.99 CO_2 + 0.01 C_2H_6 using the MBWR-32 EOS for isotherms of 360, 380 and 400 K.

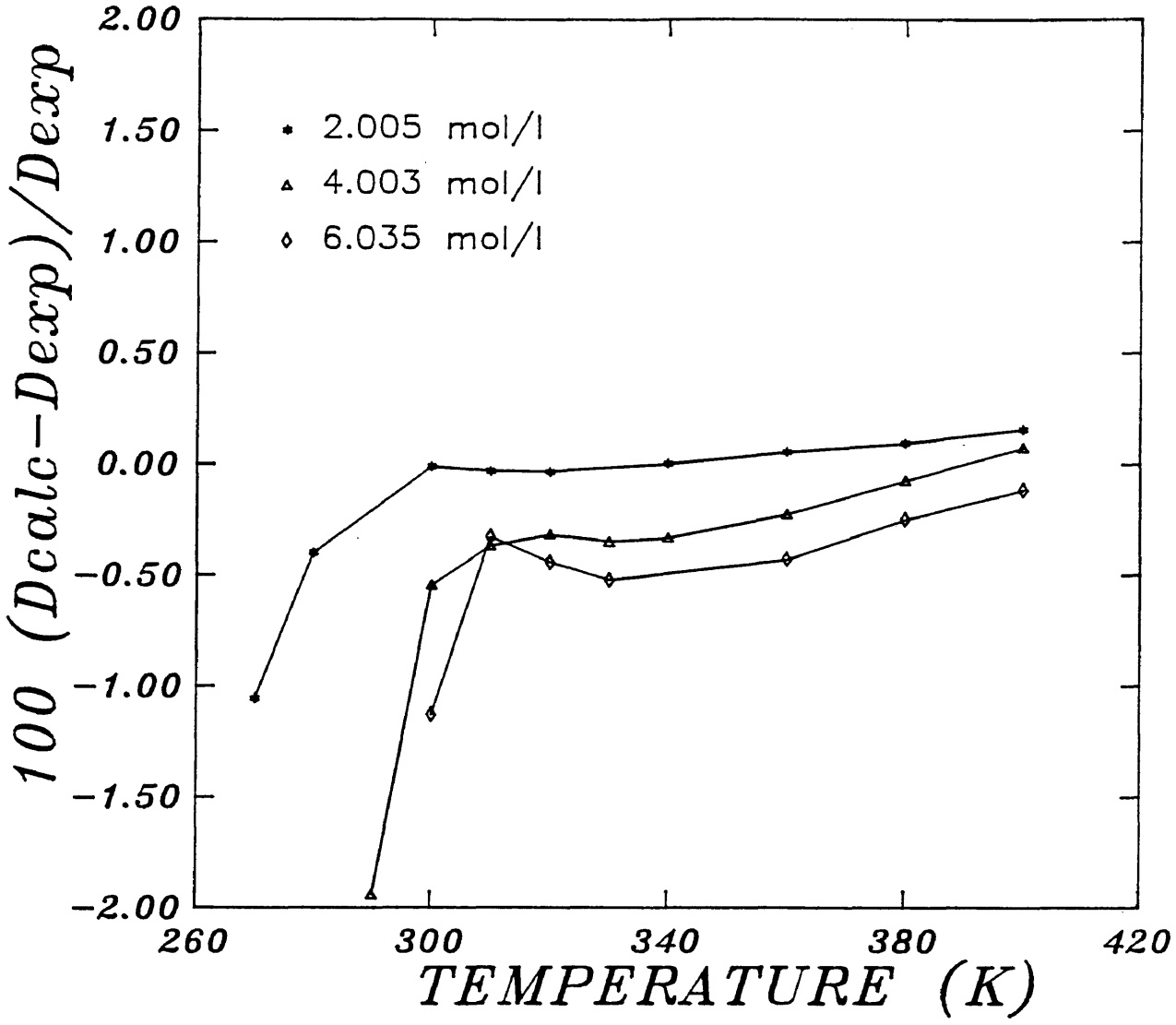

Figure 11. Density Deviation for 0.99 CO_2 + 0.01 C_2H_6 using the MBWR-32 EOS for isochores of 2.005, 4.003 and 6.035 mol/l.

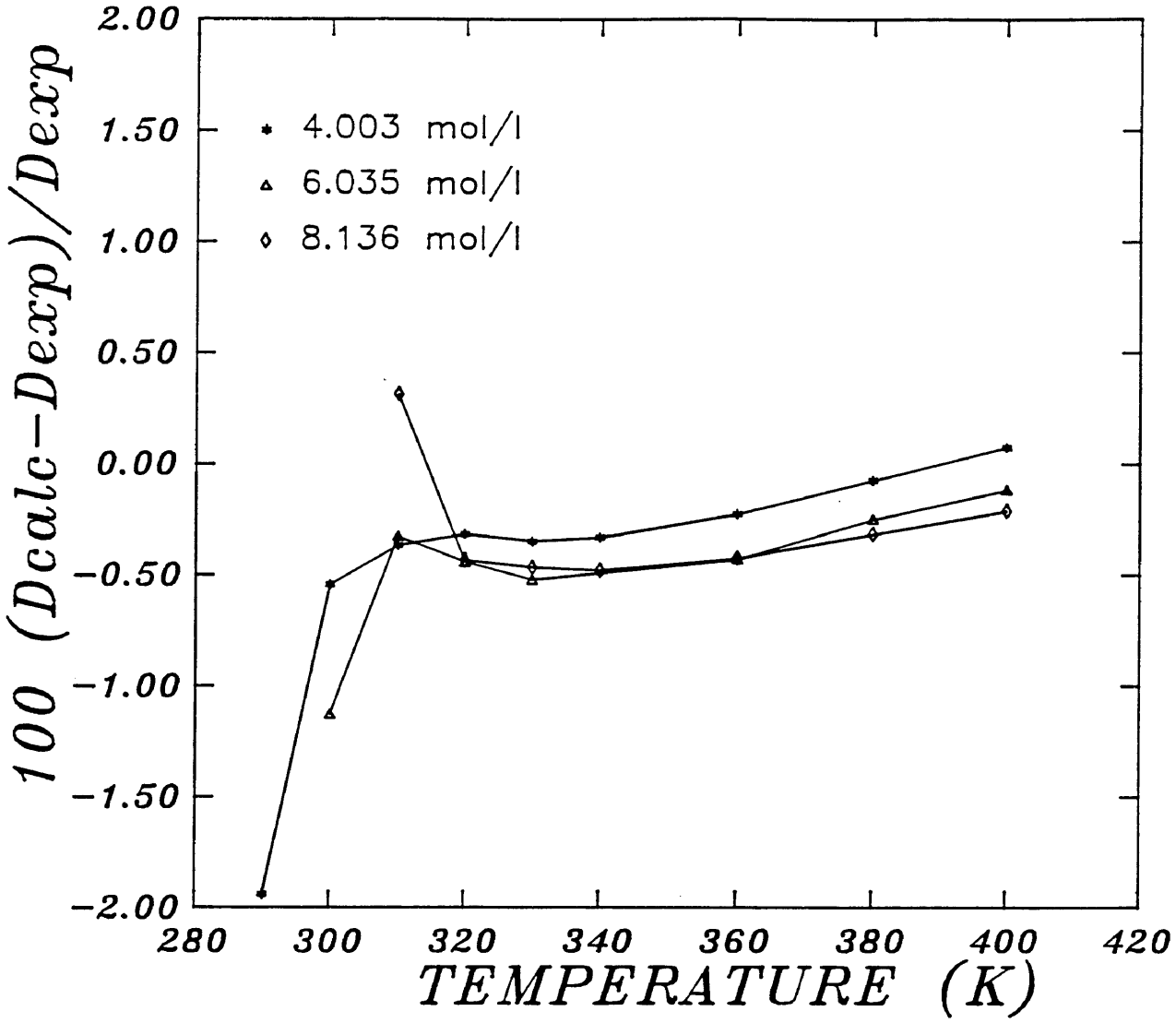

Figure 12. Density Deviation for 0.99 CO_2 + 0.01 C_2H_6 using the MBWR-32 EOS for isochores of 4.003, 6.035 and 8.136 mol/l.

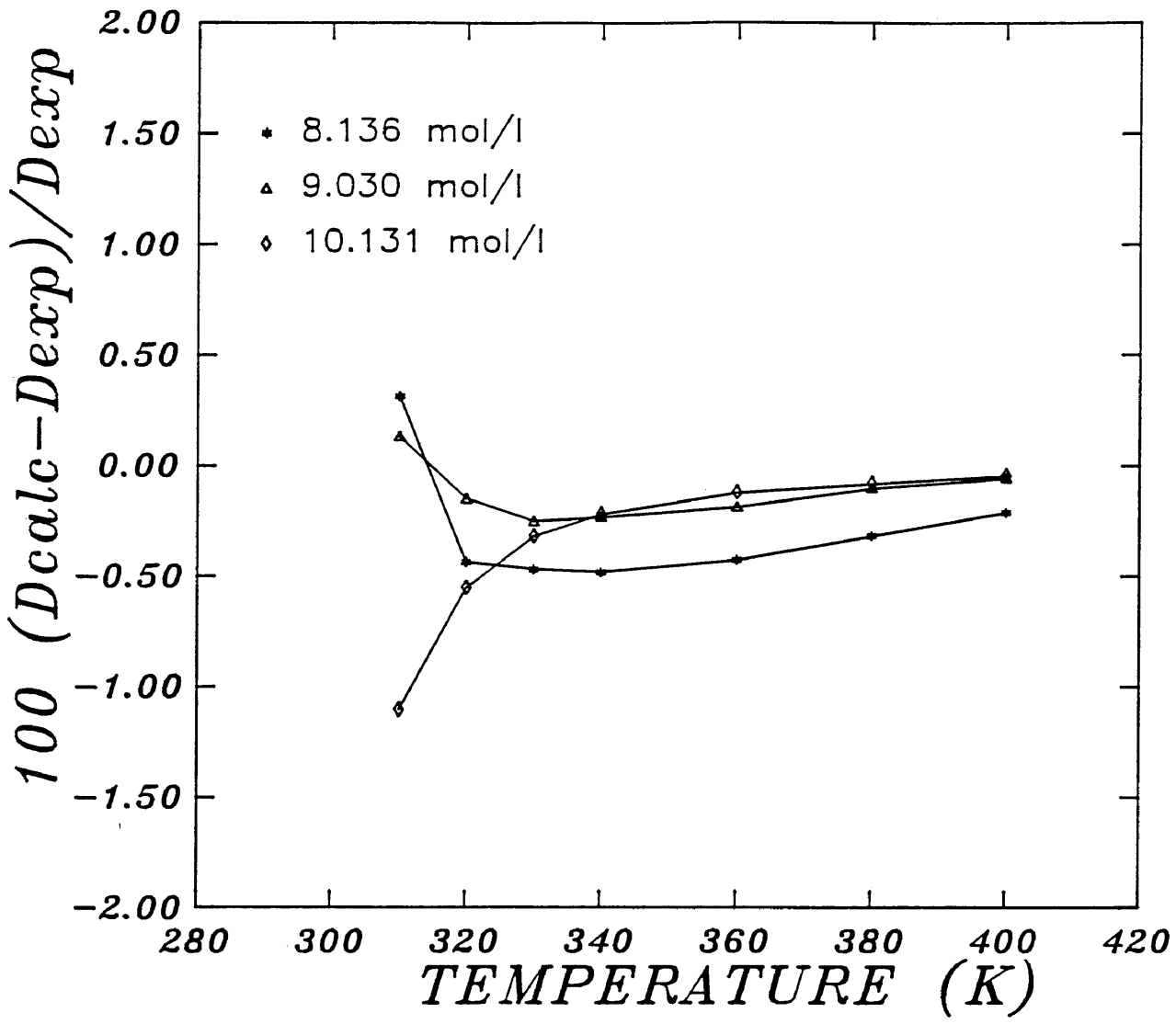

Figure 13. Density Deviation for 0.99 CO_2 + 0.01 C_2H_6 using the MBWR-32 EOS for isochores of 8.136, 9.030 and 10.131 mol/l.

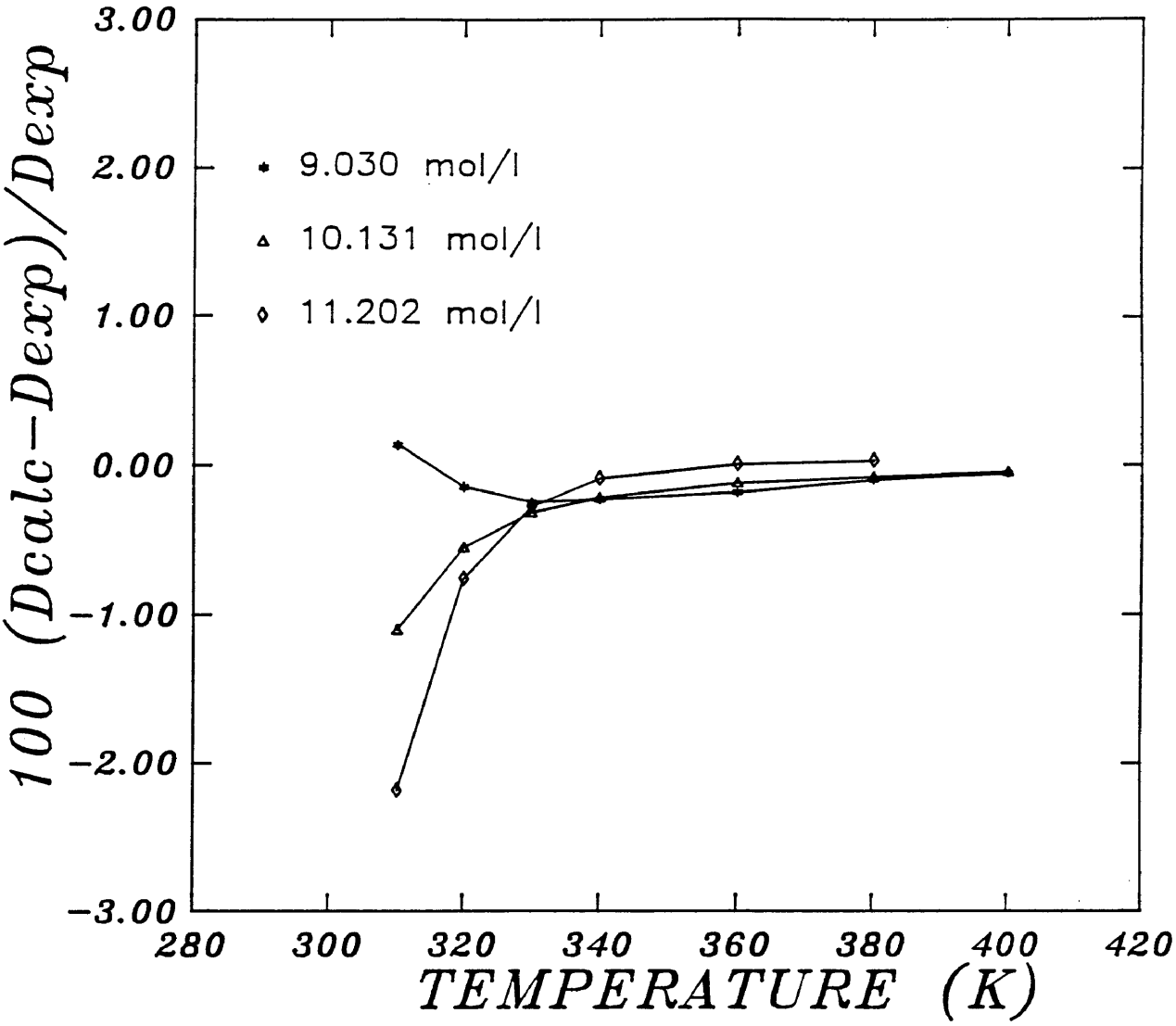

Figure 14. Density Deviation for 0.99 CO_2 + 0.01 C_2H_6 using the MBWR-32 EOS for isochores of 9.030, 10.131 and 11.202 mol/l.

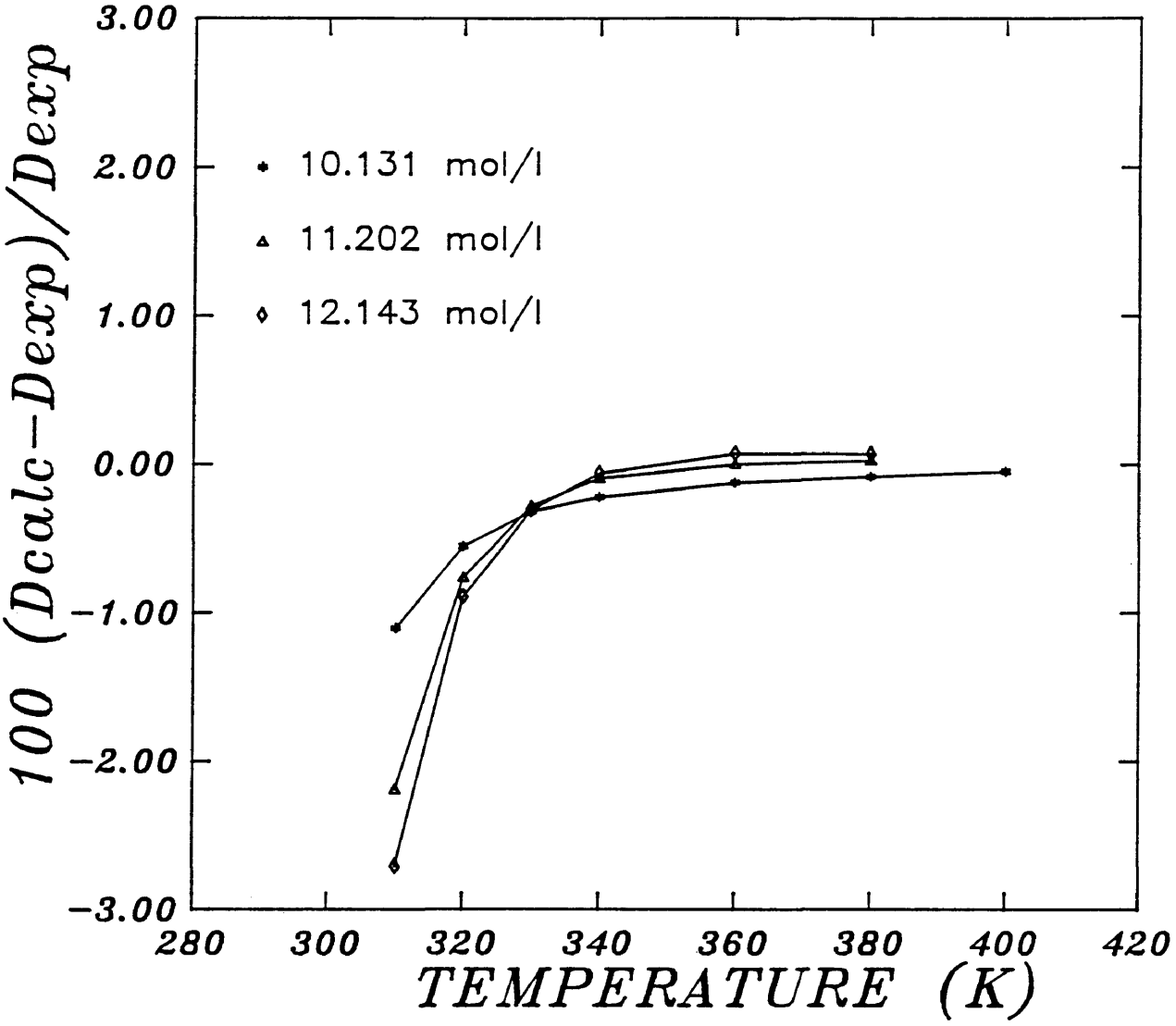

Figure 15. Density Deviation for 0.99 CO_2 + 0.01 C_2H_6 using the MBWR-32 EOS for isochores of 10.131, 11.202 and 12.143 mol/l.

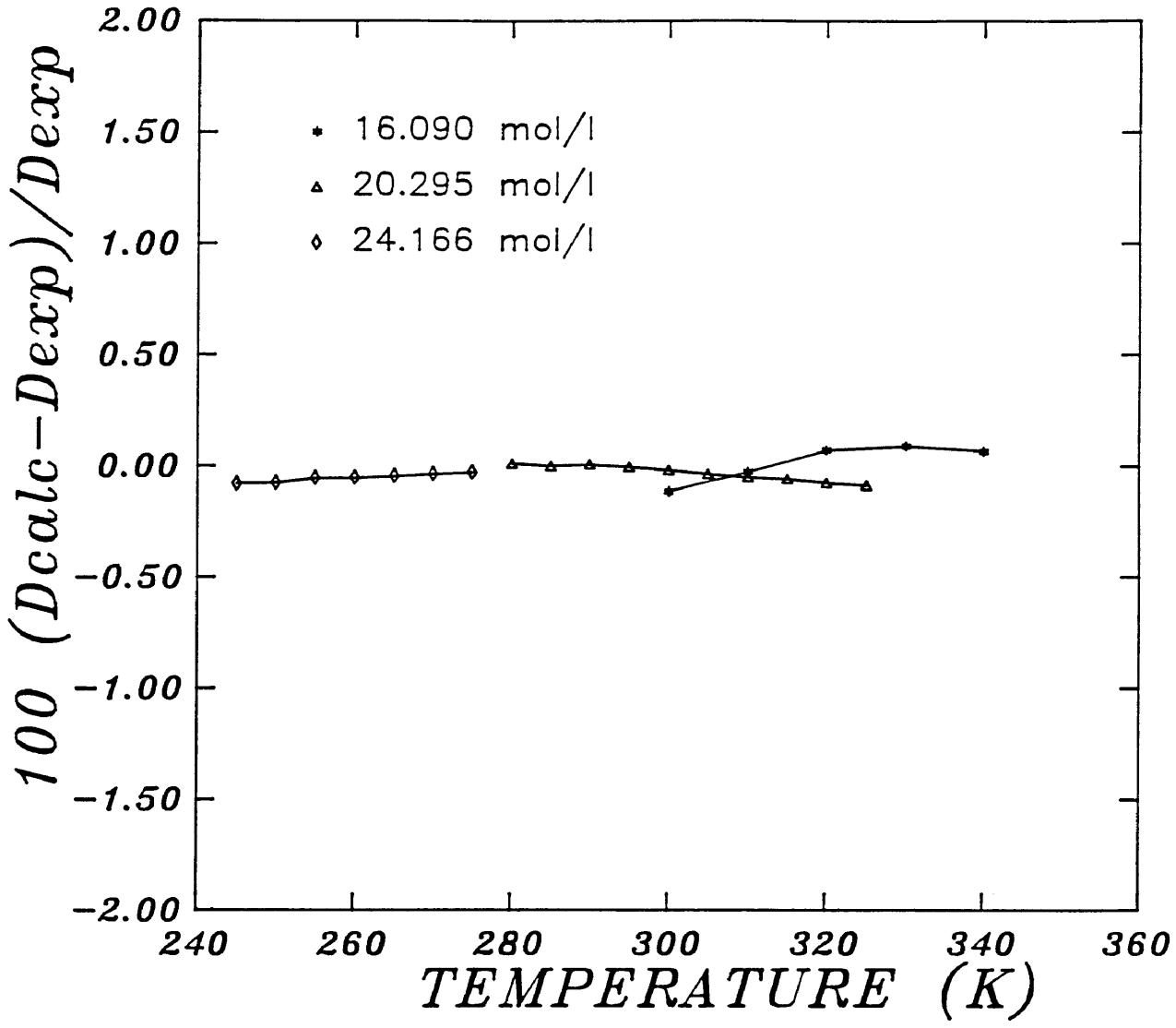

Figure 16. Density Deviation for 0.99 CO_2 + 0.01 C_2H_6 using the MBWR-32 EOS for isochores of 16.090, 20.295 and 24.166 mol/l.

to positive errors. This positive-negative swing is what causes the S-shaped configuration in the isotherms. The figures also show that the errors associtated with the model are the largest at the lowest temperature for each individual isochore. It is at this temperature where the model is forced to evaluate close to the phase boundary.

The original model performed quite well except in the near critical region. In order to improve the model, three areas must be looked at: 1) will the improved mixing rules mentioned above help in lowering the errors of the model: 2) how are the shape factors being calculated and 3) where is the reference fluid being evaluated.

The improved mixing rules will not help to improve the model because the size ratio of the mixture is close to one which causes the R_{ij} term to approach one. When the R_{ij} term is equal to one, the mixing rules reduce to the van der Waals one-fluid mixing rules which are currently used in the model. The size ratio of carbon dioxide and ethane is approximately $(10/6)^{1/3}$ or 1.185.

The next step was to determine how the shape factors were being calculated. As was mentioned above, three methods are available for shape factor calculations. The model was tested with the data obtained from this study, and it was found that for every situation, the shape factors

were exactly maped to the reference state by using the pure fluid equations of state and a two-dimensional Newton-Raphson type iteration. This is the most accurate method of the three and is therefore, the desired result. Since the two-dimensional Newton-Raphson iteration method was used to calculate the shape factors, and the improved mixing rules are not useful in this investigation, the error must be in the reference fluid equation of state.

The largest errors associated with the model occured in the near critical region. In this region the MBWR-32 equation is not "flat" enough. Figure 17 illustrates this structure for pure CO_2 by plotting the experimental data of Michels et al. (1937) at 0.005 K above the critical temperature and the isotherm calculated by the MBWR-32. It should be noted that the difference between the calculated and experimental isotherm is greatly enlarged by the scale used in Figure 17 and is in effect imperceptible to the eye on a normal PVT diagram. The net effect of this lack of flatness is that calculated densities are too high at subcritical pressures and too low at supercritical pressures. It should also be noted that since the isothermal compressibility is very large in this region, small pressure errors of 0.01 % can give rise to density errors of 1 % or more.

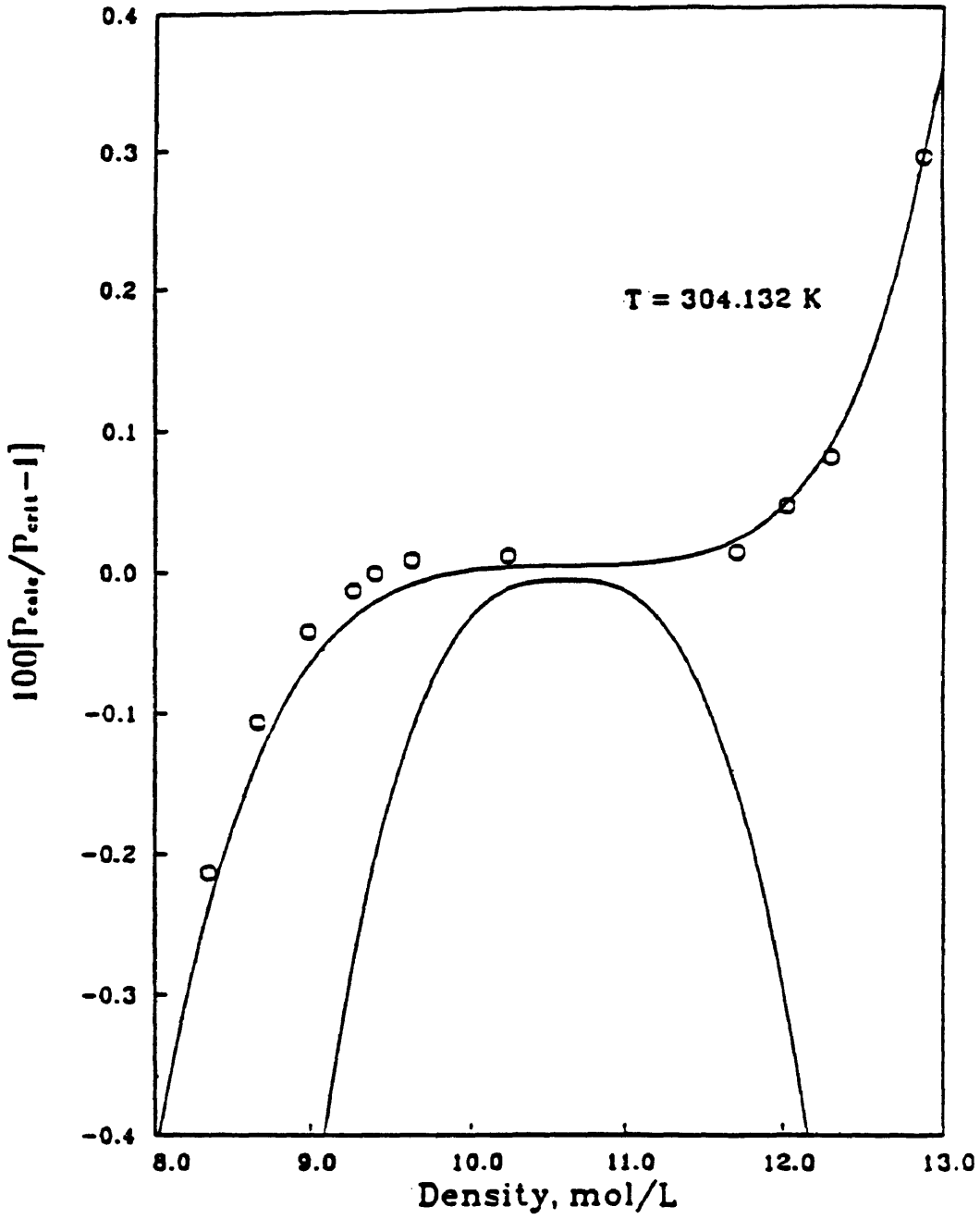

Figure 17 · Illustration of classical equation of state not being flat enough in the near critical region

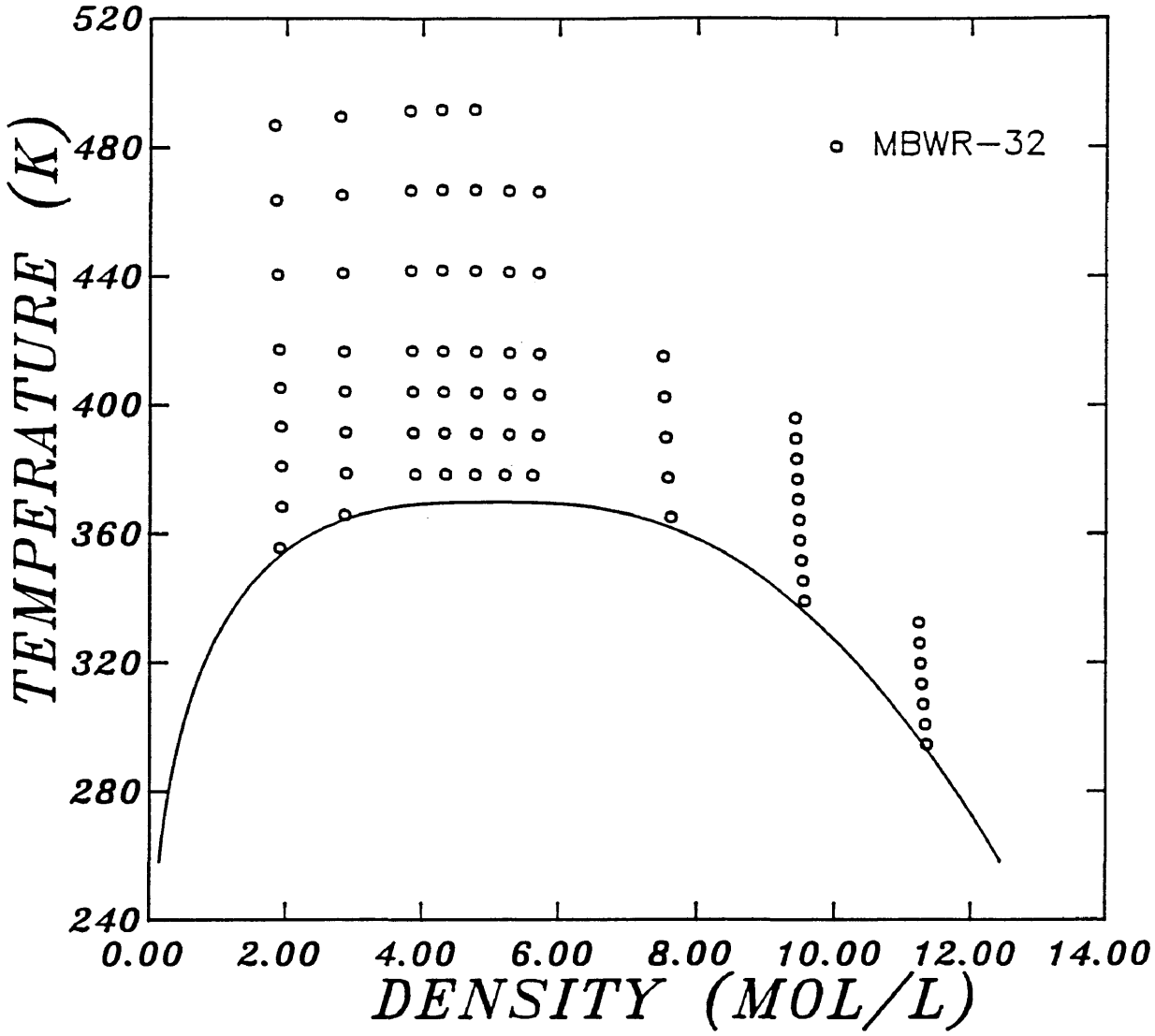

Figure 18 . Temperature vs. density for the propane reference fluid using the MBWR-32 EOS.

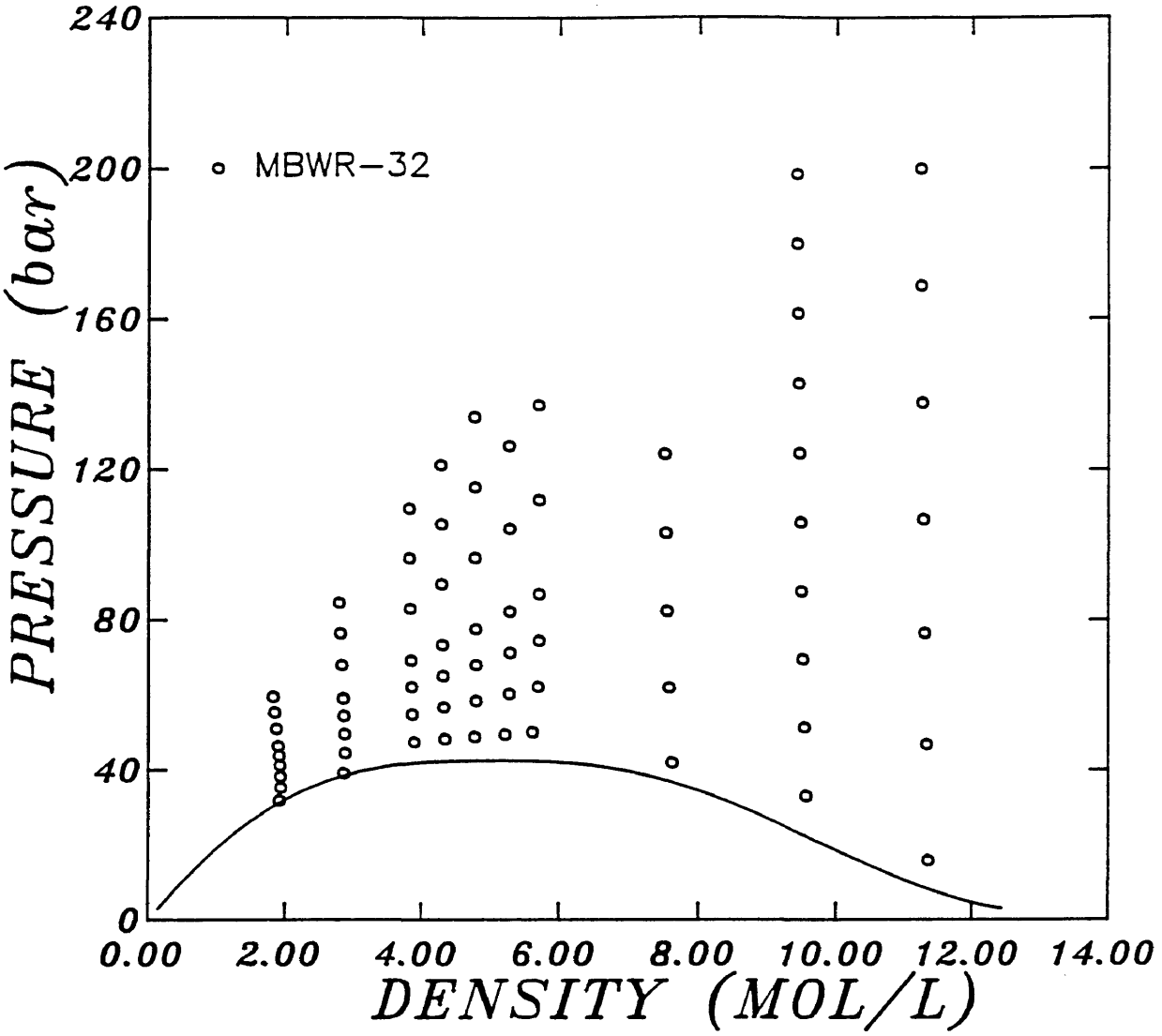

Figure 19. Pressure vs. density for the propane reference fluid using the MBWR-32 EOS.

Figures 18 and 19 show plots of temperature vs. density and pressure vs. density for the propane reference fluid. These are the reference fluid points which correspond to the actual experimental data. As one can see, there are many points evaluated in the near critical region and the saturation boundary area. Thus, a new equation of state was sought which would be more accurate in the near critical region.

Schmidt and Wagner (1985) have recently proposed a new BWR type equation of state which is designed to correct the problem shown in Figure 17. They noted in their work on oxygen that the near critical region isotherms could be made flatter by using an equation which has two exponential functions, in contrast with the MBWR-32 which uses only one. The functional form of the Schmidt-Wagner formulation is in terms of residual Helmholtz free energy and is given by

$$a^r = \frac{A(\delta,\tau)-A^*(\delta,\tau)}{RT} = F_1(\delta,\tau)+F_2(\delta,\tau)e^{-\delta^2}+F_3(\delta,\tau)e^{-\delta^4} \qquad (40)$$

where the F_n are polynomials, A is the Helmholtz free energy, the asterisk indicates an ideal gas value, $\delta = \rho/\rho_c$ and $\tau = T/T_c$. The deviations of the calculated densities from experimental densities using the Schmidt-Wagner equation are presented in Table 7 and Figure 20.

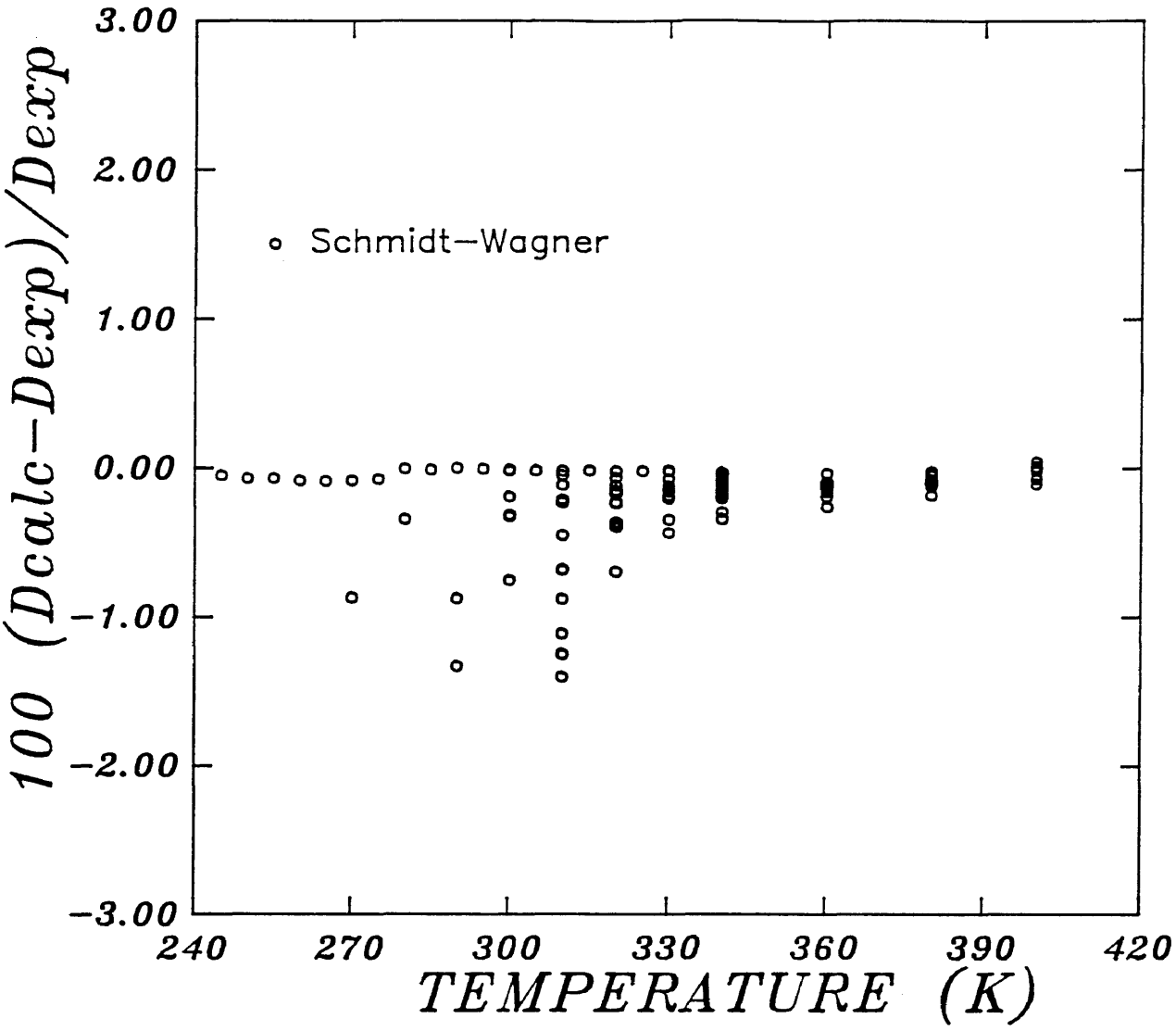

Figure 20. Density deviation range for 0.99 CO_2 + 0.01 C_2H_6 using the Schmidt-Wagner EOS.

Figure 21 represents the 310 K isotherm plotted on a differential density vs. density graph. In this figure, the density deviations calculated by using the Schmidt-Wagner EOS are compared with those calculated by using the MBWR-32 equation. As can be seen, the errors associated with predicted densities are greatly decreased when the Schmidt-Wagner equation of state is used. Figures 22 - 27 show how the remaining isotherms react when the Schmidt-Wagner equation is compared to the MBWR-32 equation for density predictions.

Figure 28 represents the 12.136 mol/dm^3 isochore plotted on a differential density vs. temerature graph. This figure shows how the density deviations calculated by using the Schmidt-Wagner equation of state are compared to those calculated by using the MBWR-32 equation. Again, the Schmidt-Wagner equation decreases the errors associated with predicted densities. The feature to note about this figure is how steeply the isochore rises and then flattens out. Figures 29 and 30 in appendix A show the same features. But, an examination of Figure 31 shows that the Schmidt-Wagner equation is only slightly better at predicting densities for the 2.009 mol/dm^3 isochore than the MBWR-32 equation. The same is also true for the 24.166 mol/dm^3 isochore represented in Figure 32. Figures 33 - 40 show how

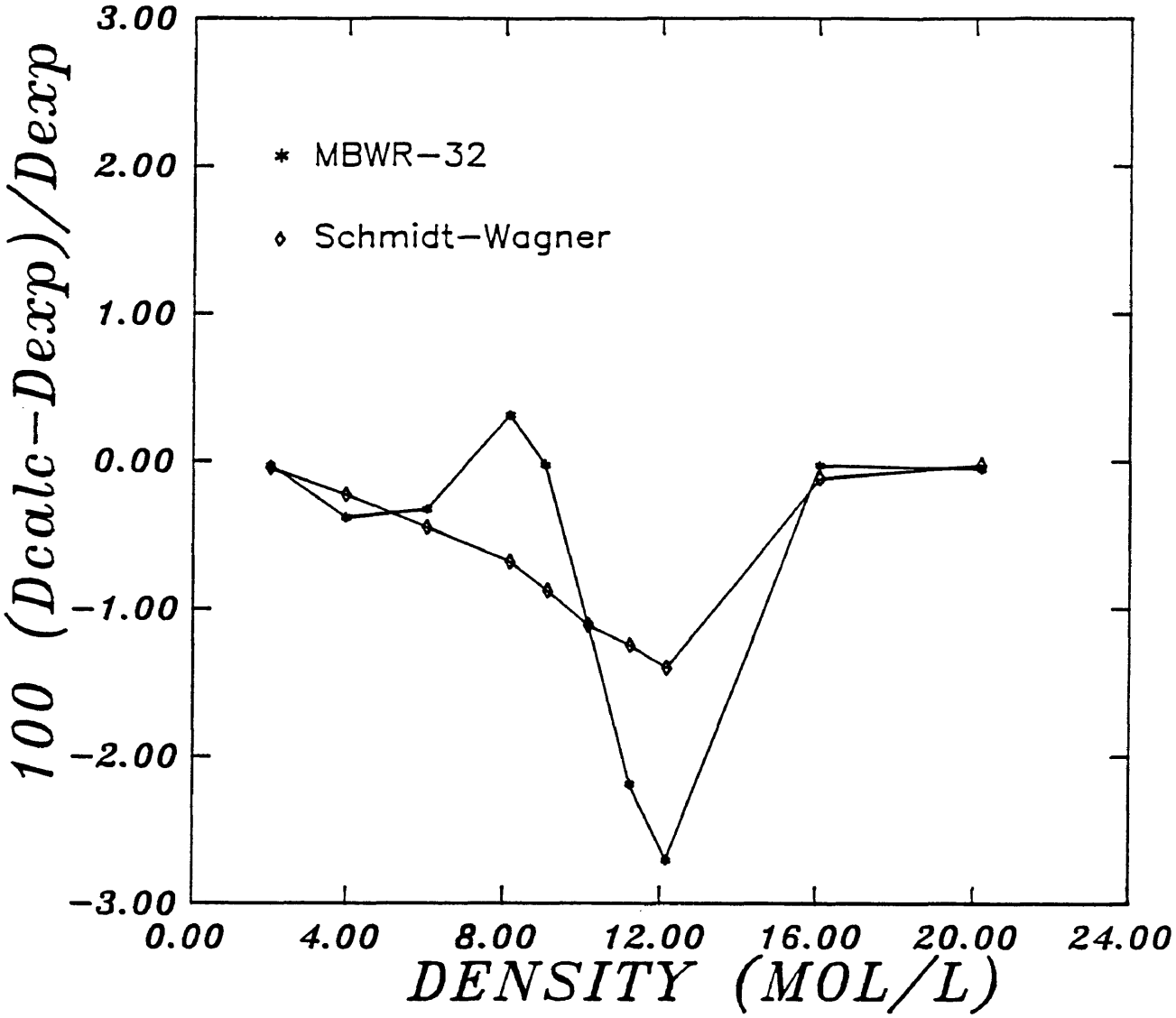

Figure 21. Deviations of calculated densities for 0.99 CO_2 + 0.01 C_2H_6 using the MBWR-32 and Schmidt-Wagner equations of state for the 310 K isotherm.

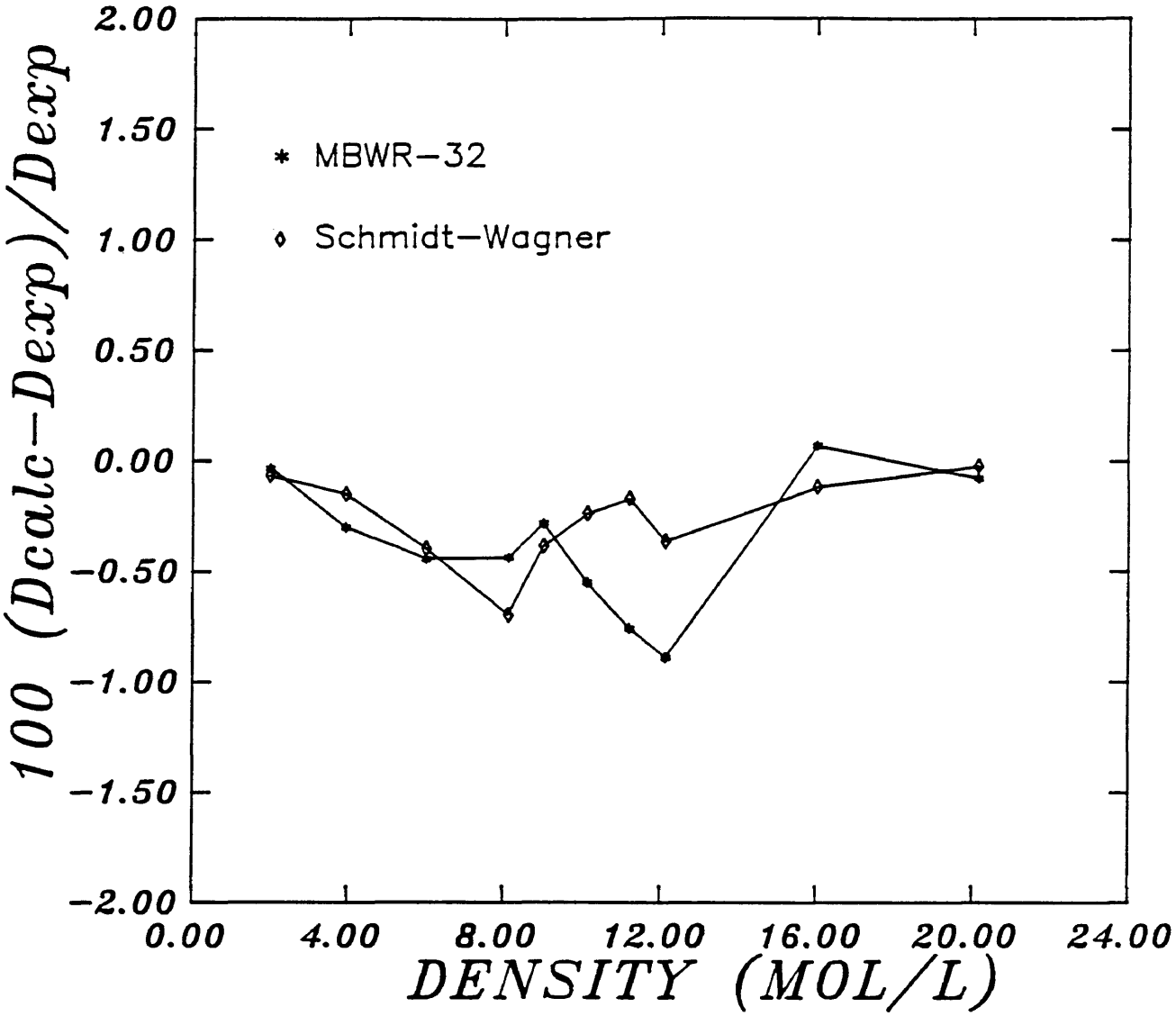

Figure 22. Deviations of calculated densities for 0.99 CO_2 + 0.01 C_2H_6 using the MBWR-32 and Schmidt-Wagner equations of state for the 320 K isotherm.

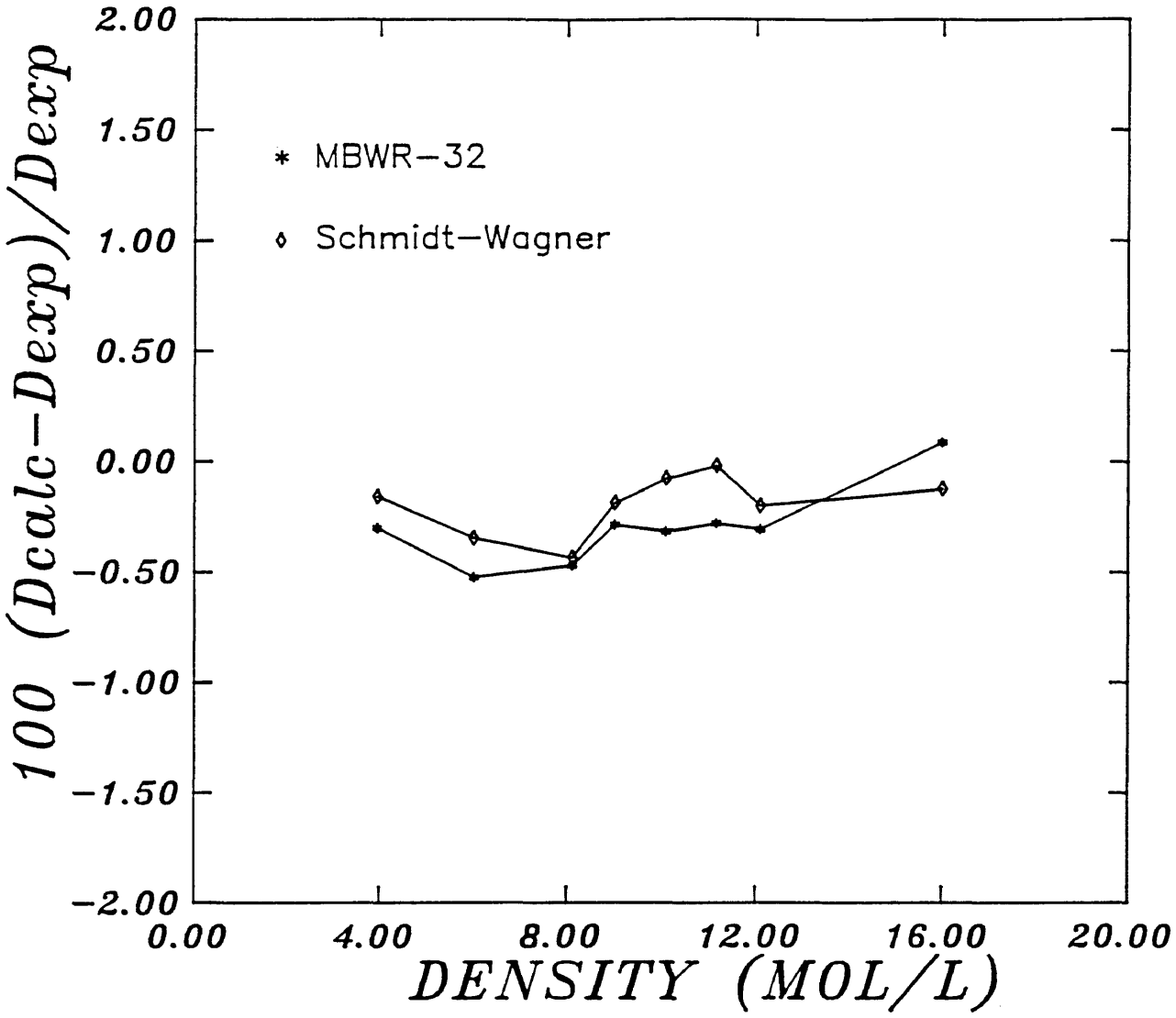

Figure 23. Deviations of calculated densities for 0.99 CO_2 + 0.01 C_2H_6 using the MBWR-32 and Schmidt-Wagner equations of state for the 330 K isotherm.

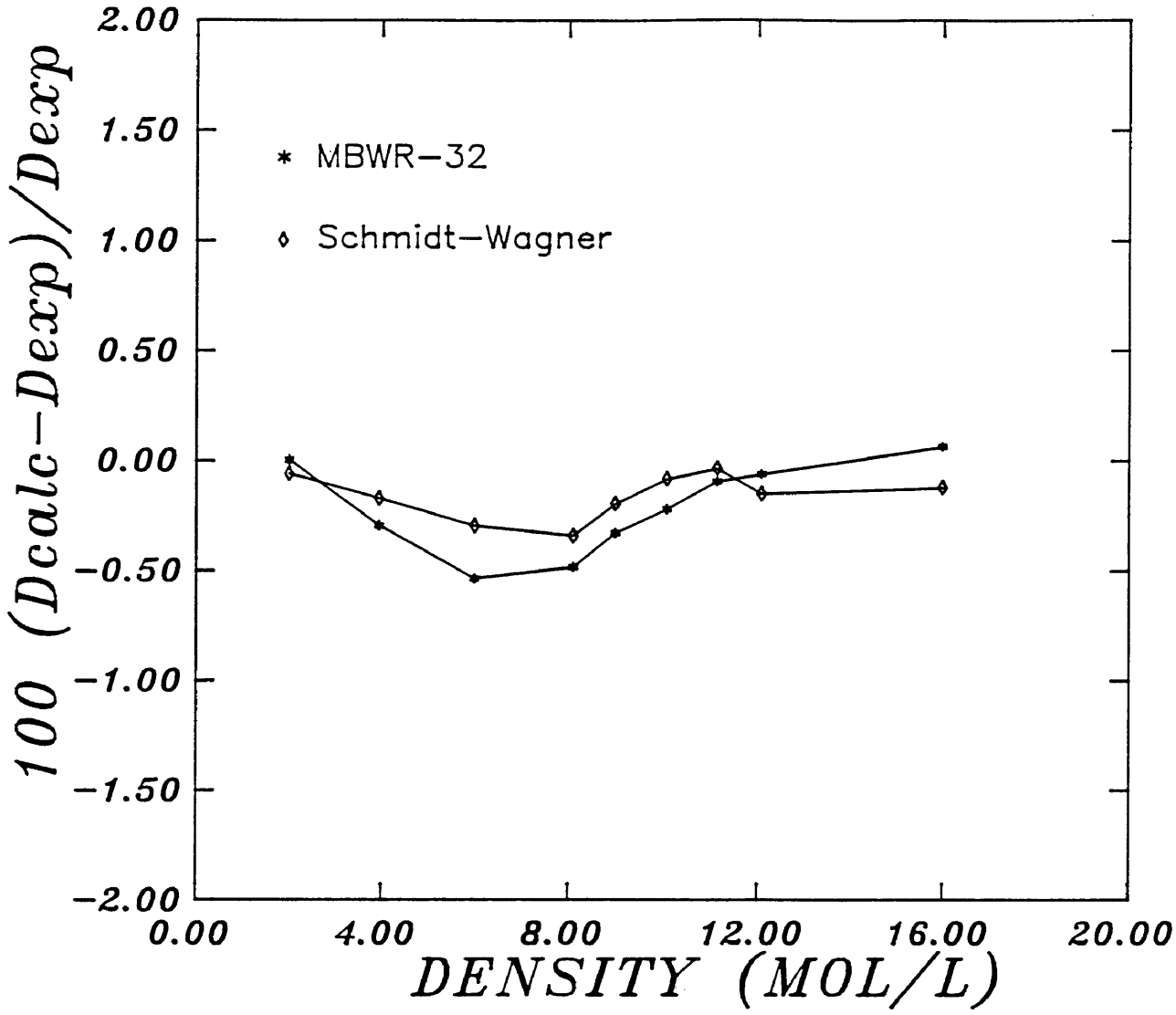

Figure 24. Deviations of calculated densities for 0.99 CO_2 + 0.01 C_2H_6 using the MBWR-32 and Schmidt-Wagner equations of state for the 340 K isotherm.

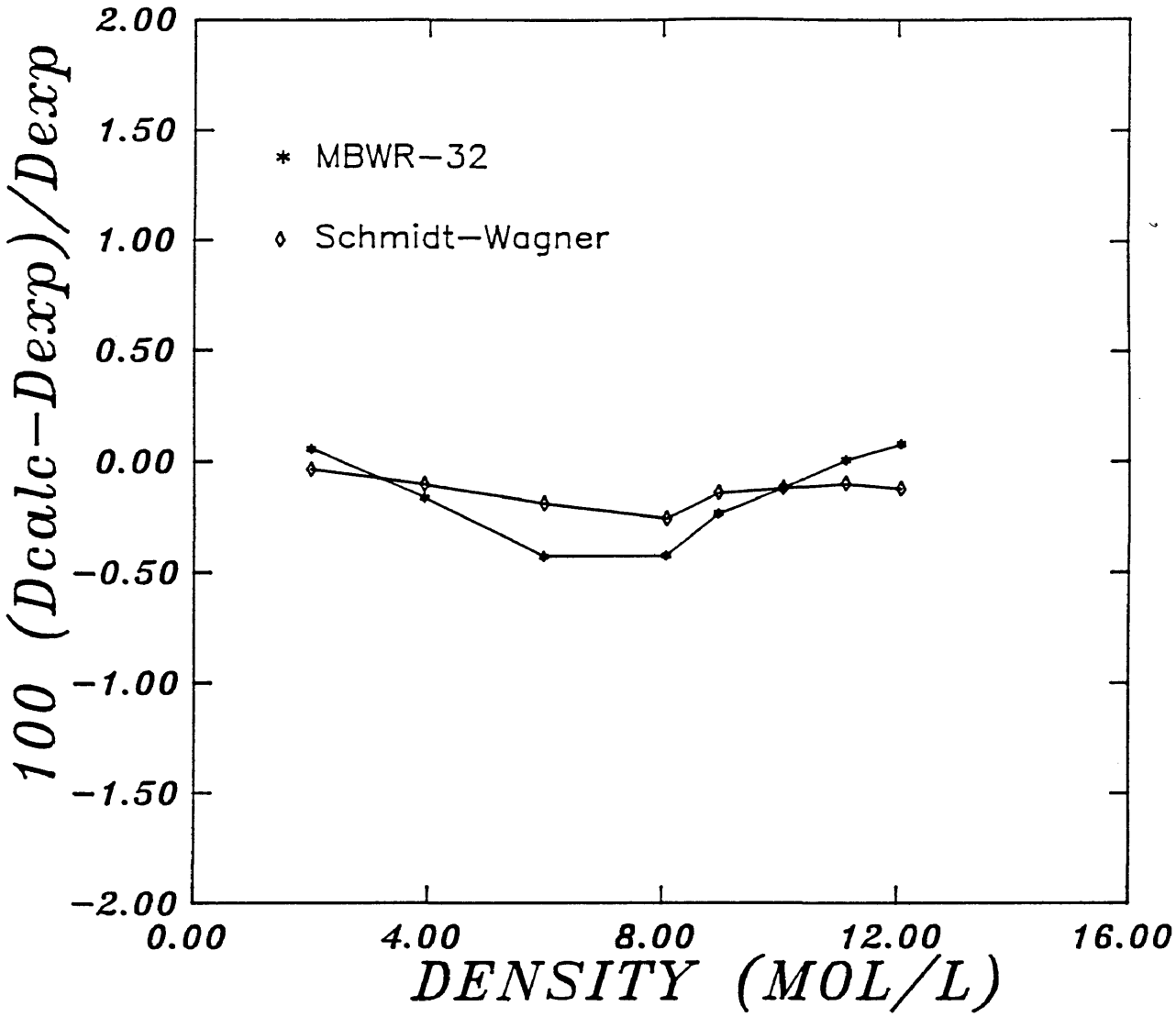

Figure 25. Deviations of calculated densities for 0.99 CO_2 + 0.01 C_2H_6 using the MBWR-32 and Schmidt-Wagner equations of state for the 360 K isotherm.

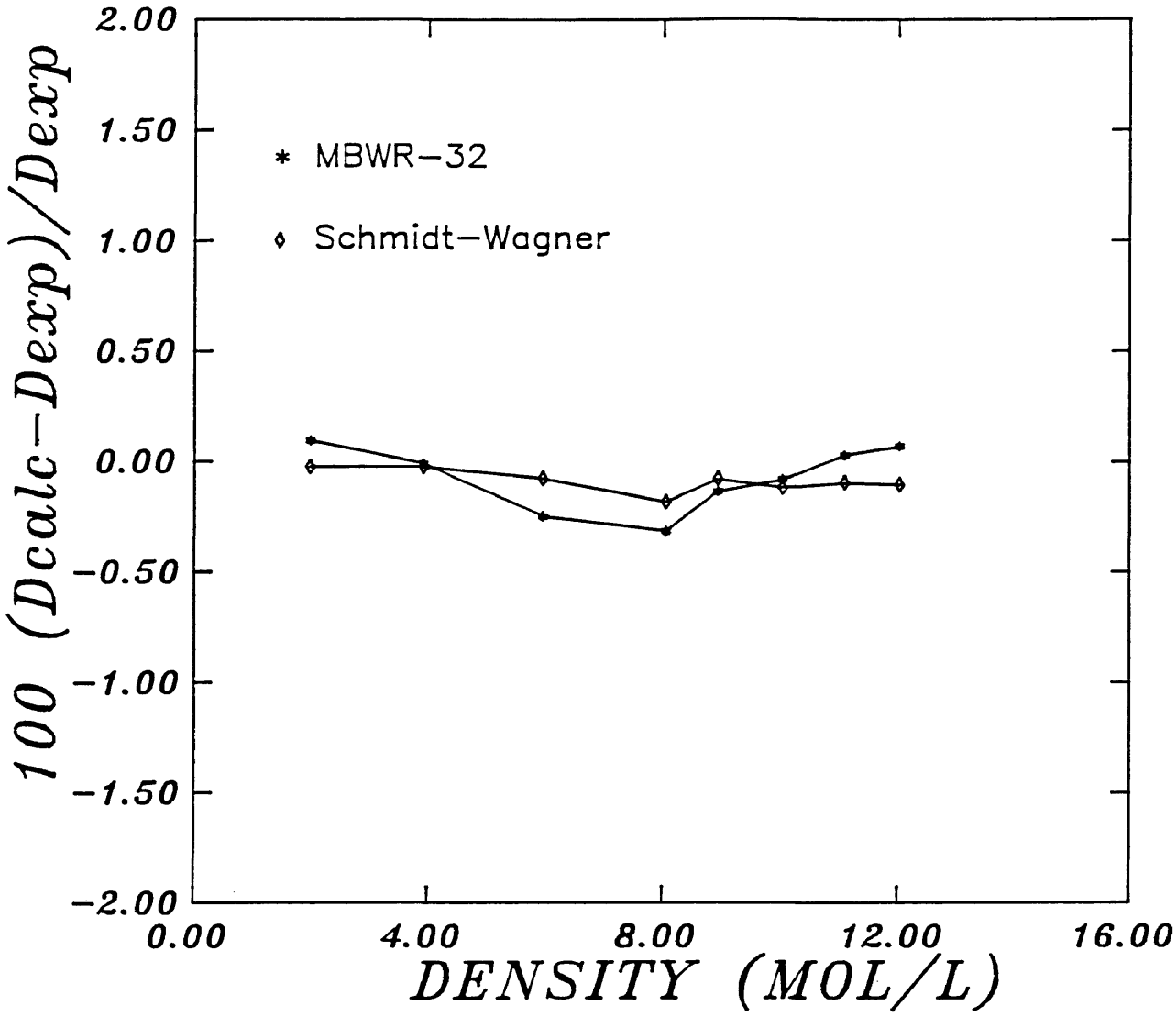

Figure 26. Deviations of calculated densities for 0.99 CO_2 + 0.01 C_2H_6 using the MBWR-32 and Schmidt-Wagner equations of state for the 380 K isotherm.

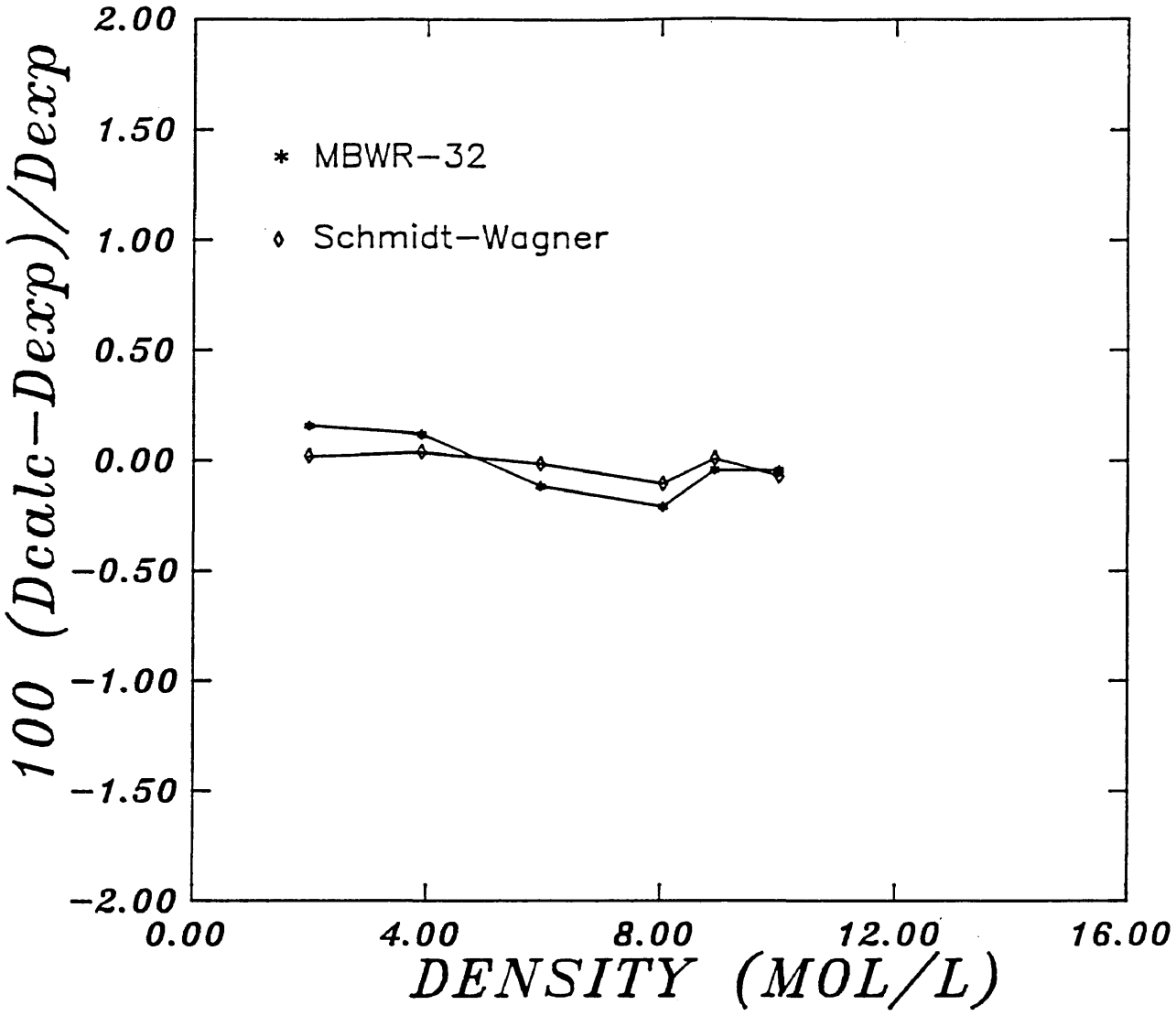

Figure 27 . Deviations of calculated densities for 0.99 CO_2 + 0.01 C_2H_6 using the MBWR-32 and Schmidt-Wagner equations of state for the 400 K isotherm.

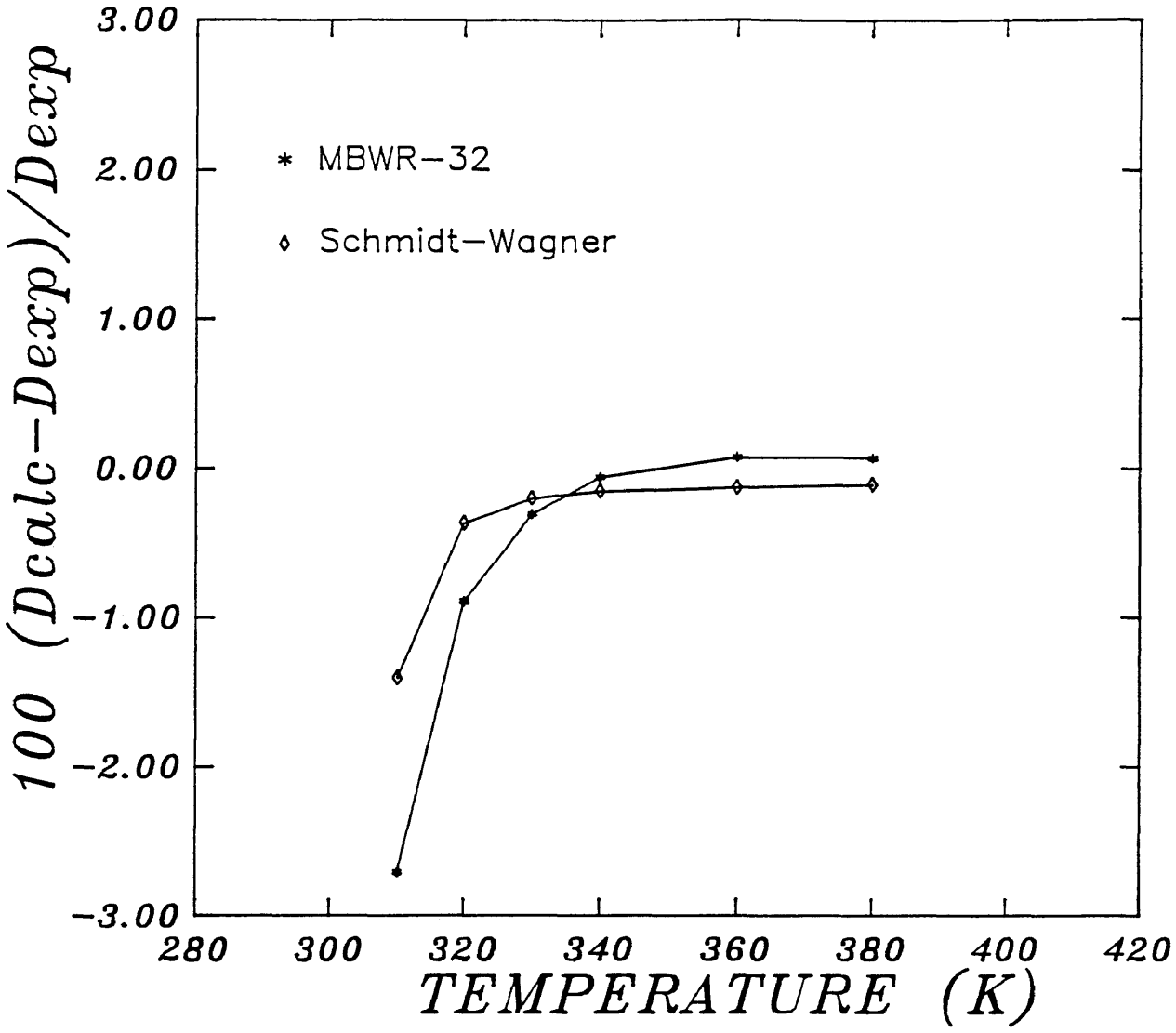

Figure 28. Deviations of calculated densities for 0.99 CO_2 + 0.01 C_2H_6 using the MBWR-32 and Schmidt-Wagner equations of state for the 12.136 mol/l isochore.

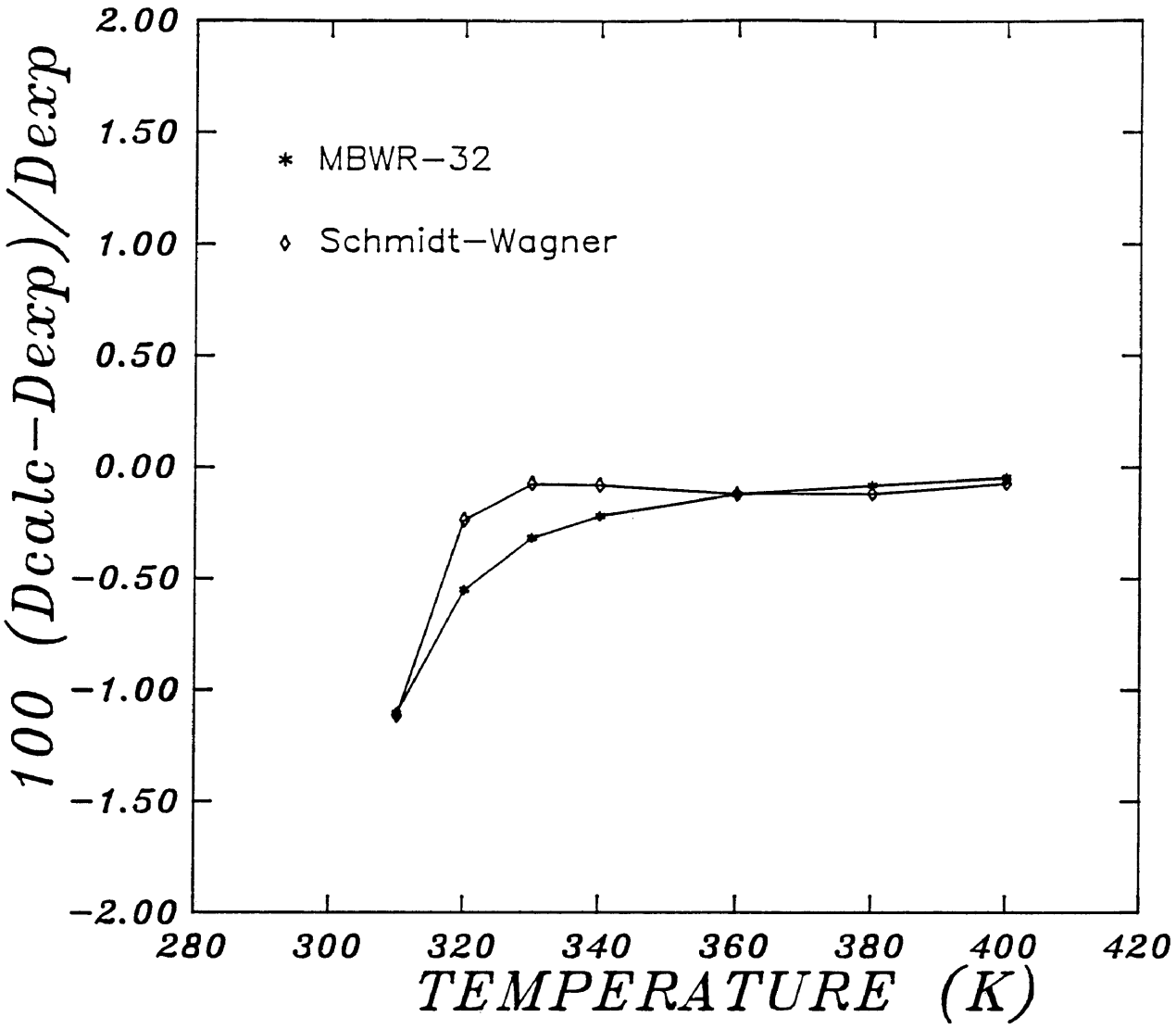

Figure 29. Deviations of calculated densities for 0.99 CO_2 + 0.01 C_2H_6 using the MBWR-32 and Schmidt-Wagner equations of state for the 10.131 mol/l isochore.

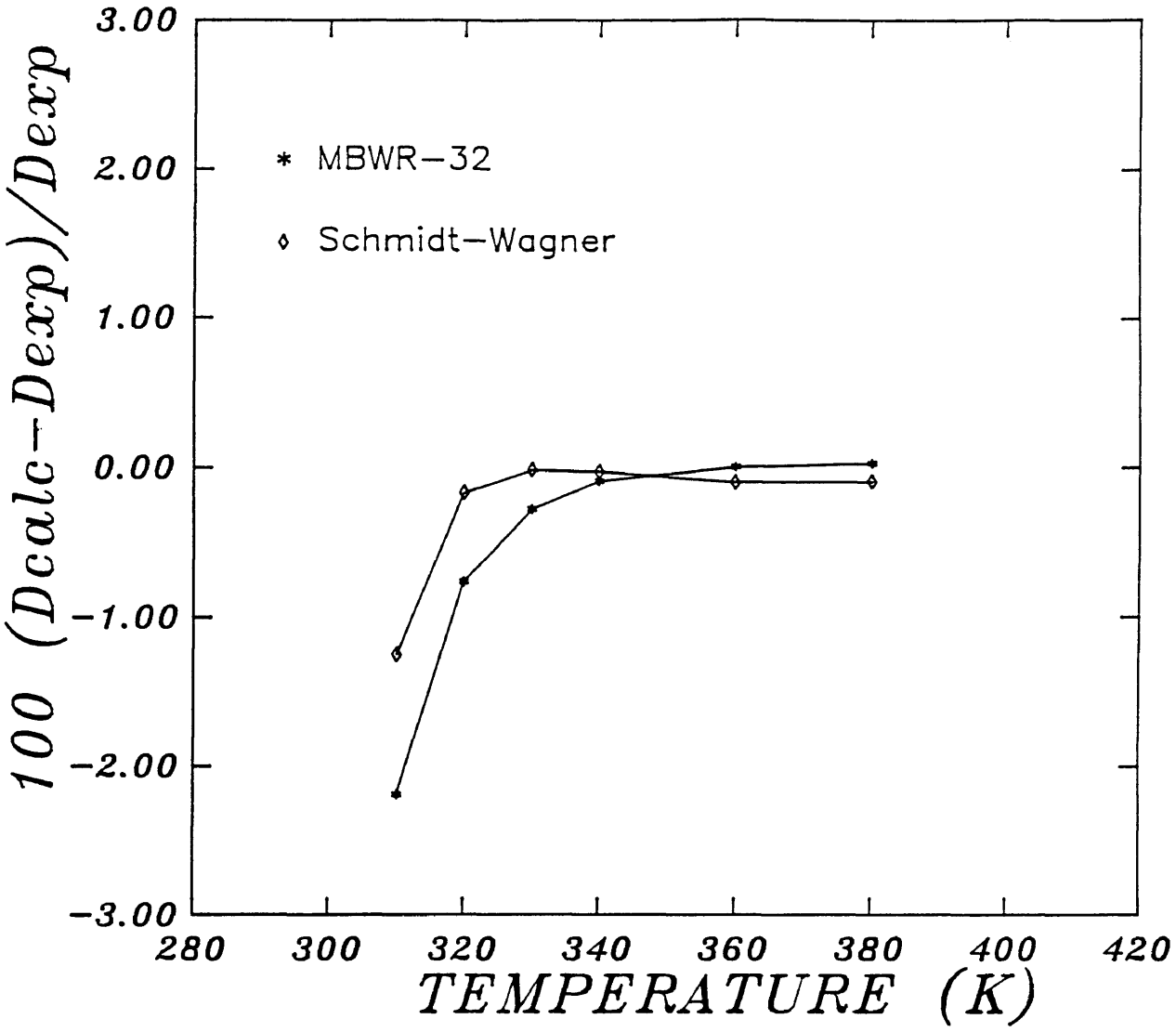

Figure 30. Deviations of calculated densities for 0.99 CO_2 + 0.01 C_2H_6 using the MBWR-32 and Schmidt-Wagner equations of state for the 11.202 mol/l isochore.

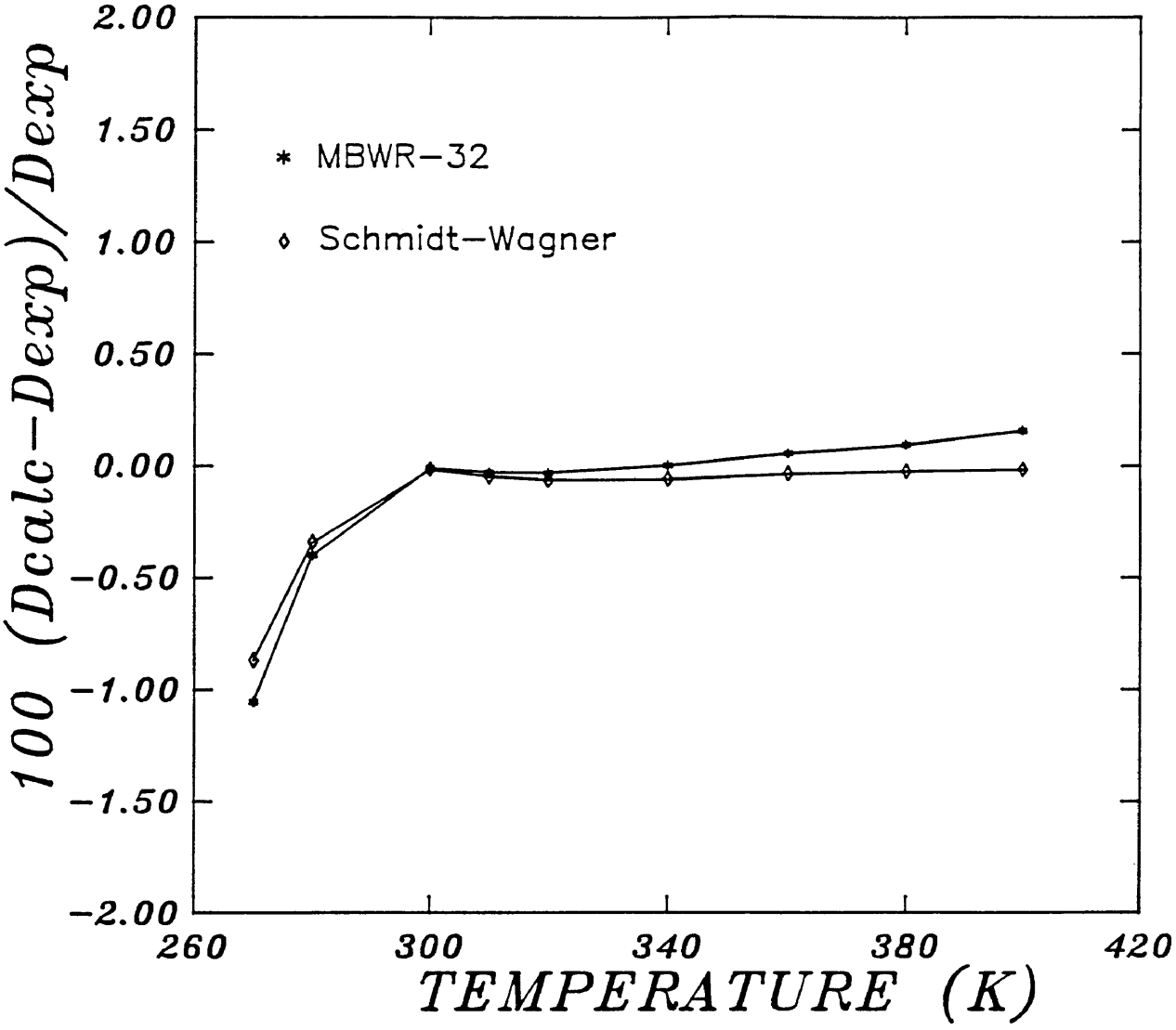

Figure 31. Deviations of calculated densities for 0.99 CO_2 + 0.01 C_2H_6 using the MBWR-32 and Schmidt-Wagner equations of state for the 2.009 mol/l isochore.

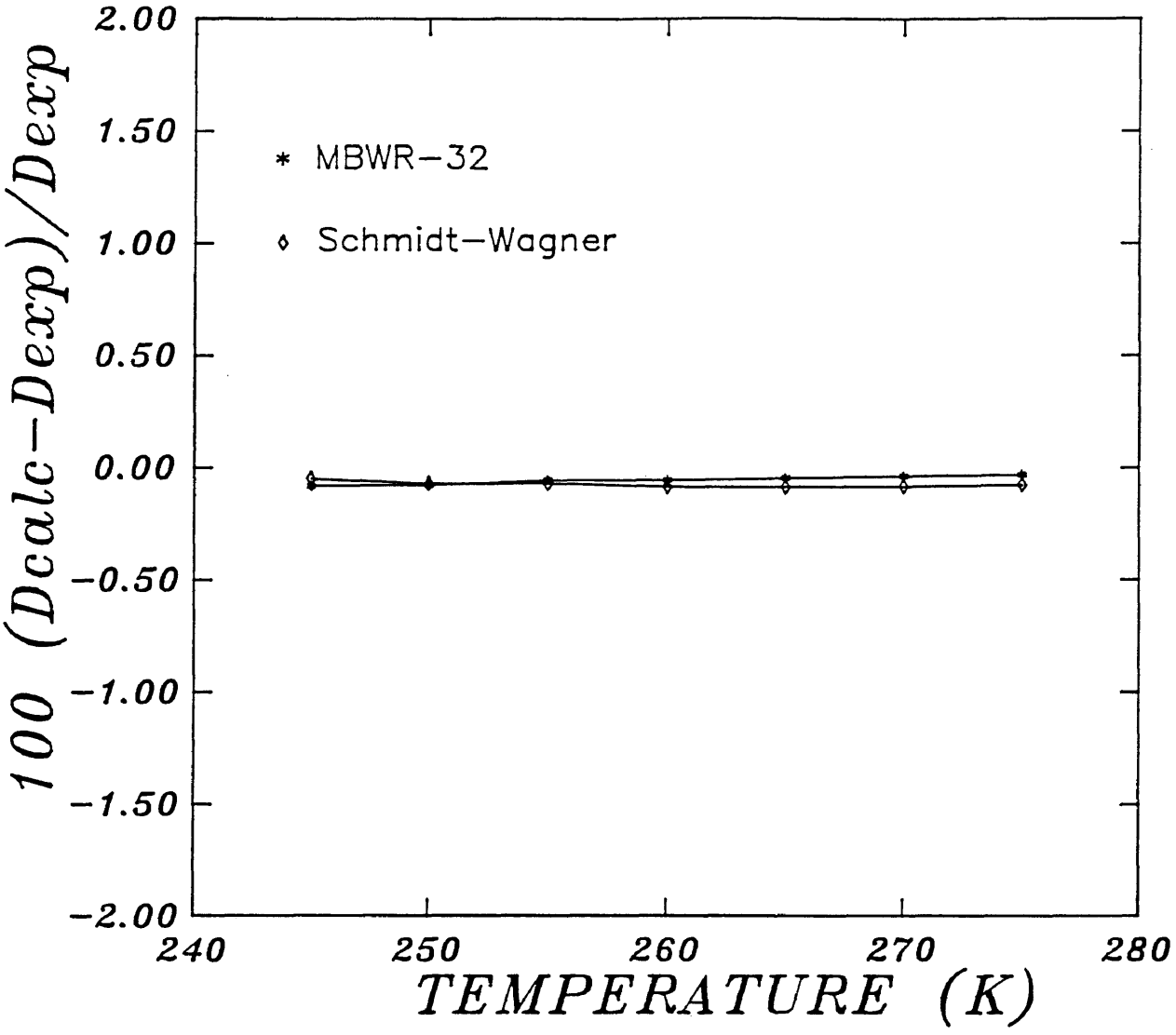

Figure 32 . Deviations of calculated densities for 0.99 CO_2 + 0.01 C_2H_6 using the MBWR-32 and Schmidt-Wagner equations of state for the 24.166 mol/l isochore.

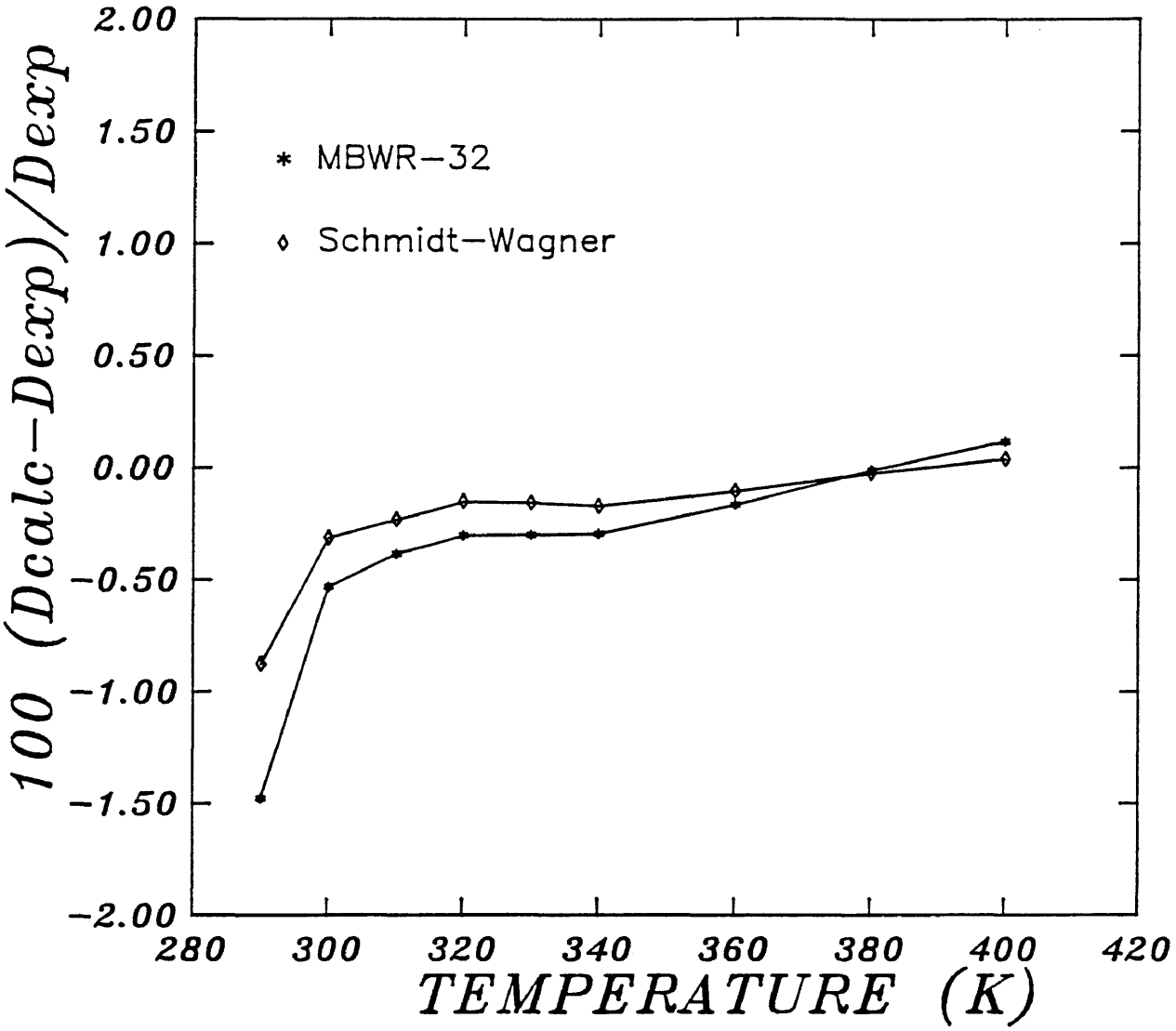

Figure 33. Deviations of calculated densities for 0.99 CO_2 + 0.01 C_2H_6 using the MBWR-32 and Schmidt-Wagner equations of state for the 4.003 mol/l isochore.

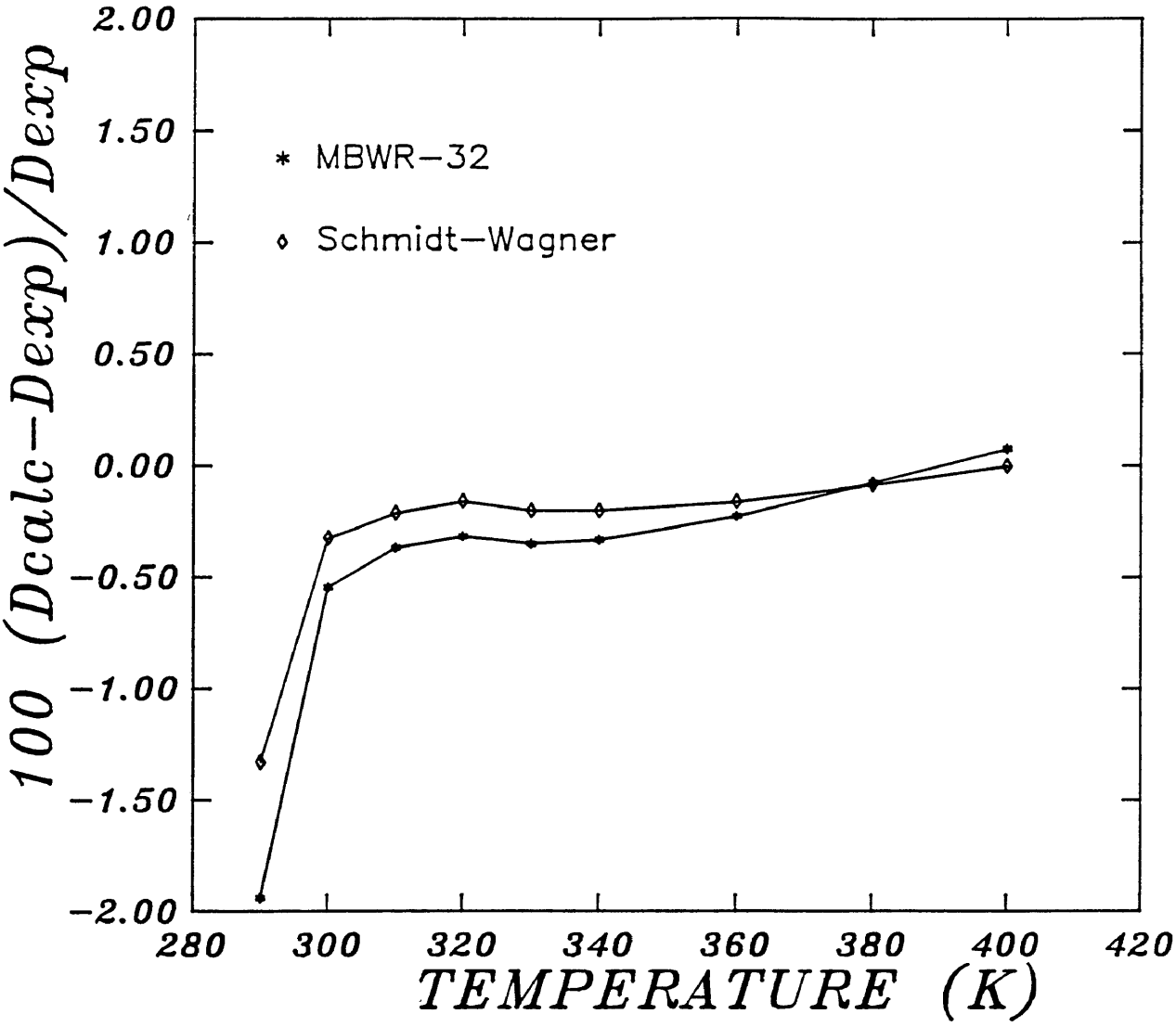

Figure 34. Deviations of calculated densities for 0.99 CO_2 + 0.01 C_2H_6 using the MBWR-32 and Schmidt-Wagner equations of state for the 3.962 mol/l isochore.

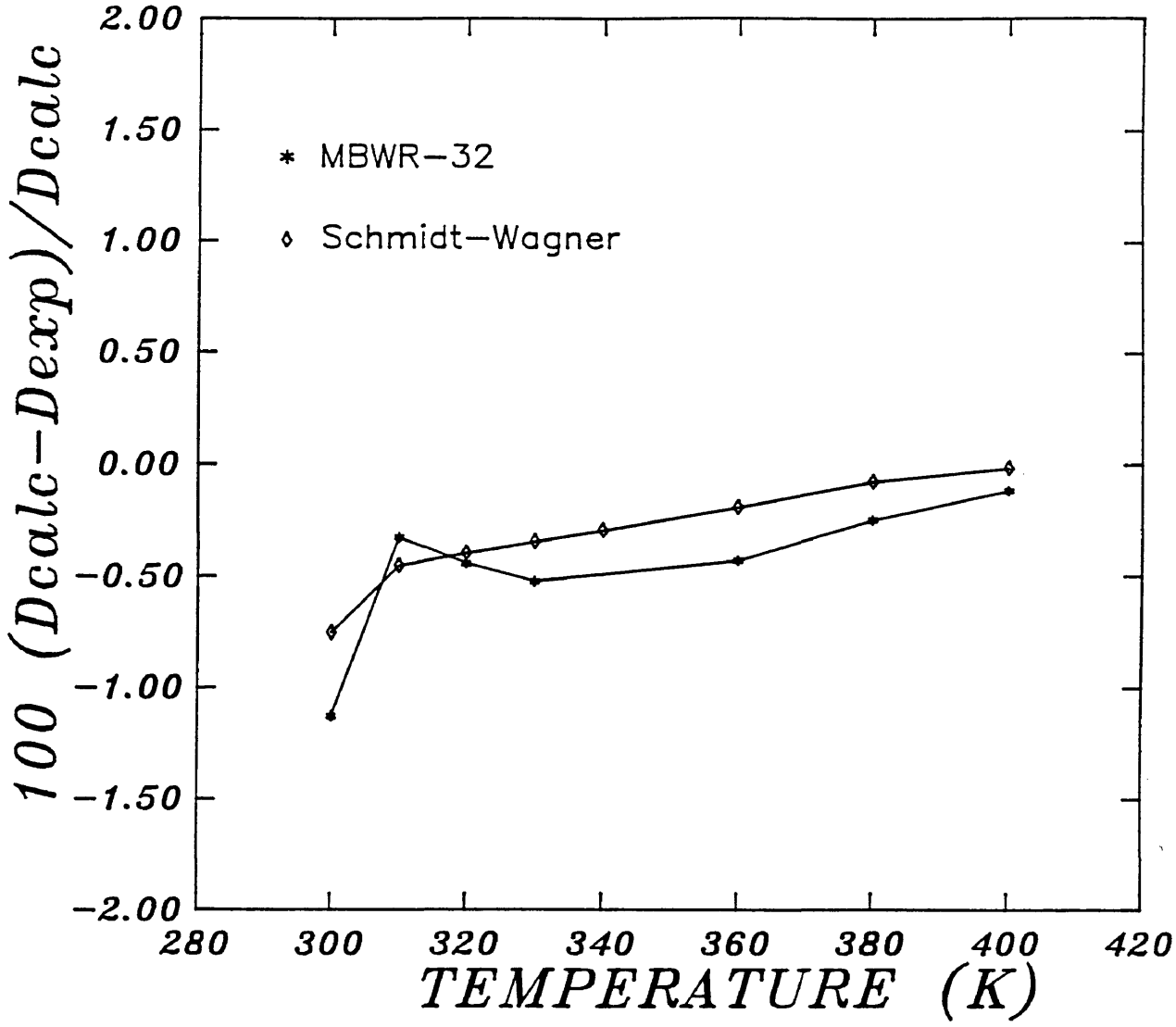

Figure 35. Deviations of calculated densities for 0.99 CO_2 + 0.01 C_2H_6 using the MBWR-32 and Schmidt-Wagner equations of state for the 6.035 mol/l isochore.

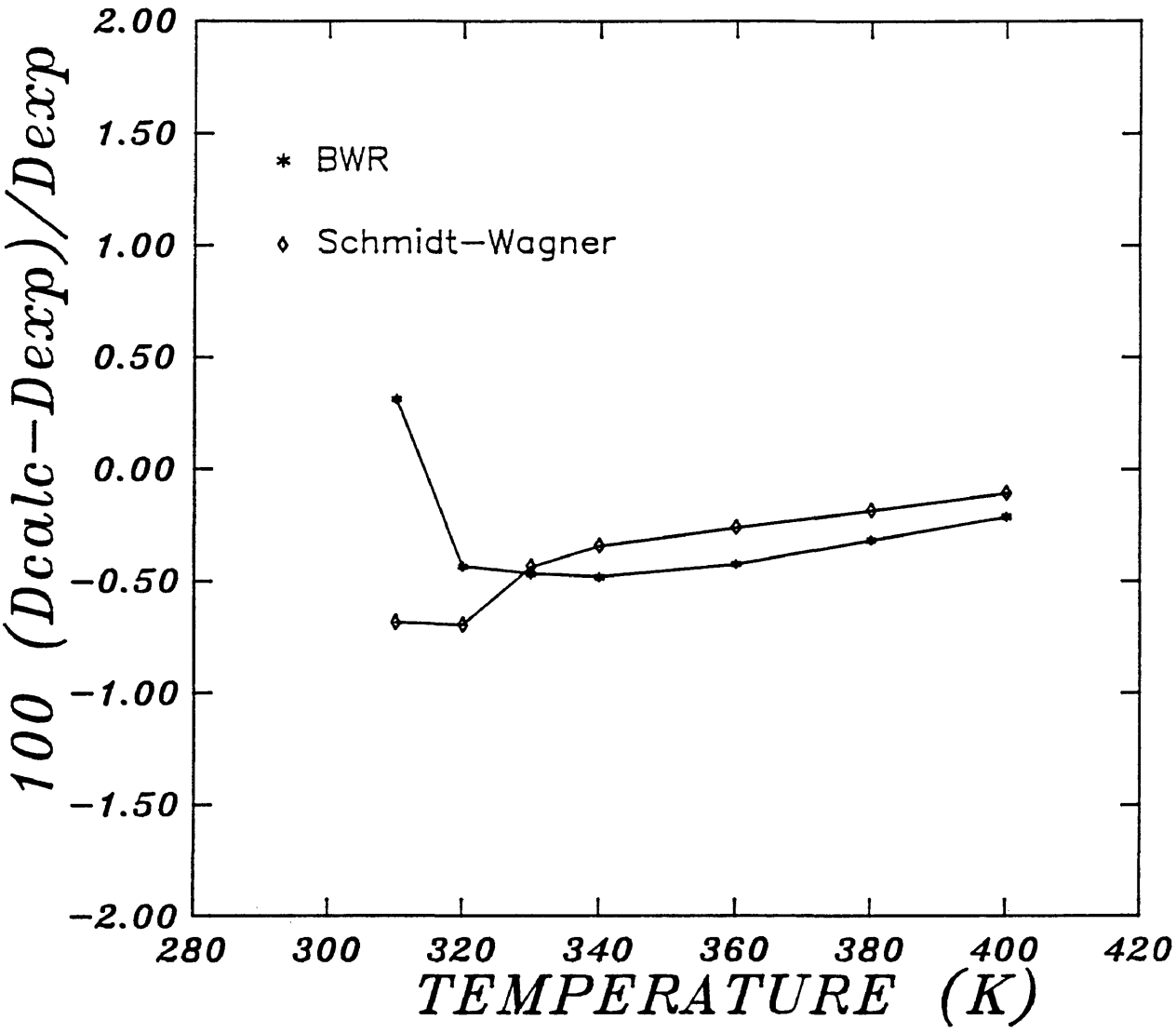

Figure 36. Deviations of calculated densities for 0.99 CO_2 + 0.01 C_2H_6 using the MBWR-32 and Schmidt-Wagner equations of state for the 8.136 mol/l isochore.

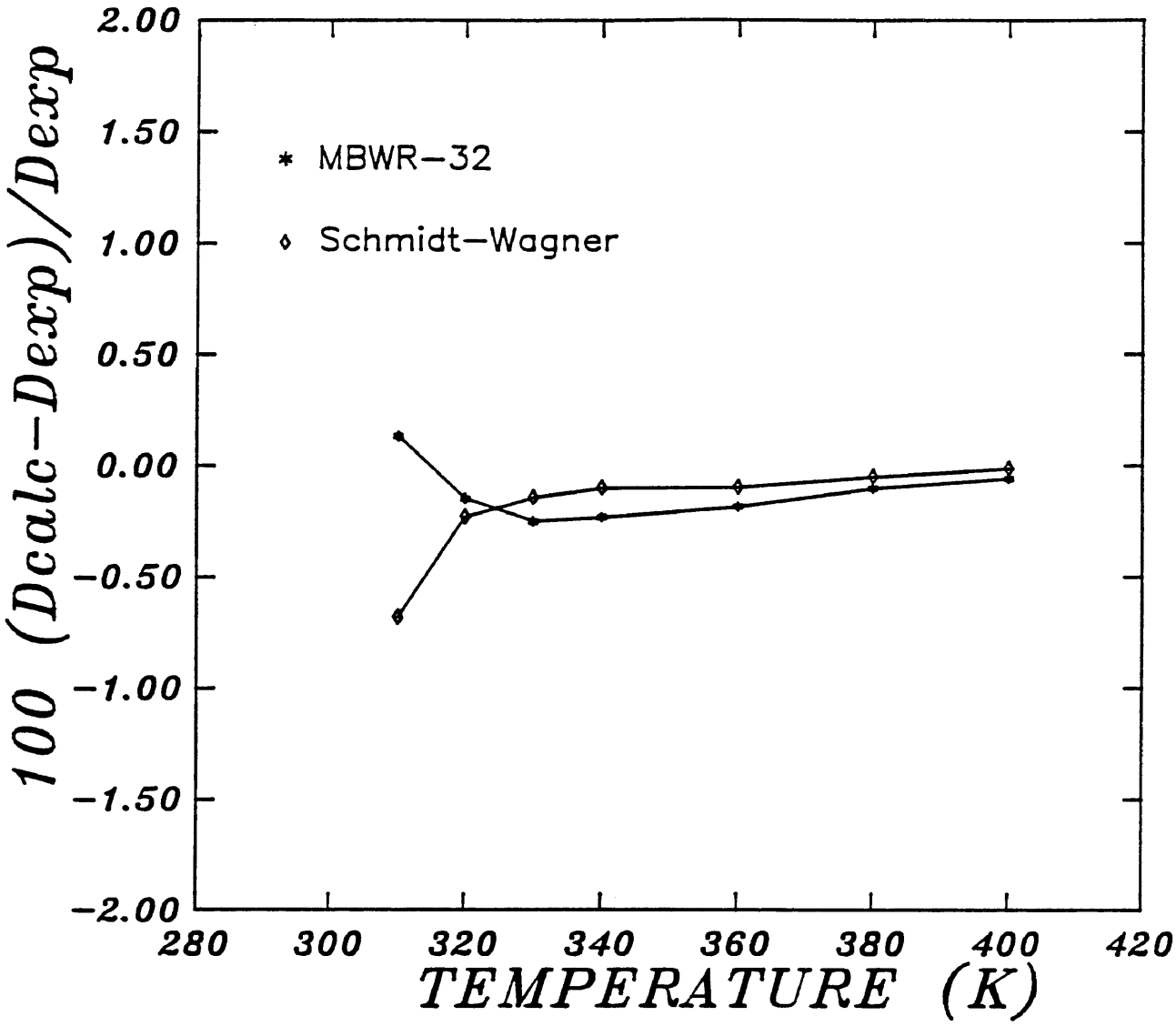

Figure 37. Deviations of calculated densities for 0.99 CO_2 + 0.01 C_2H_6 using the MBWR-32 and Schmidt-Wagner equations of state for the 9.096 mol/l isochore.

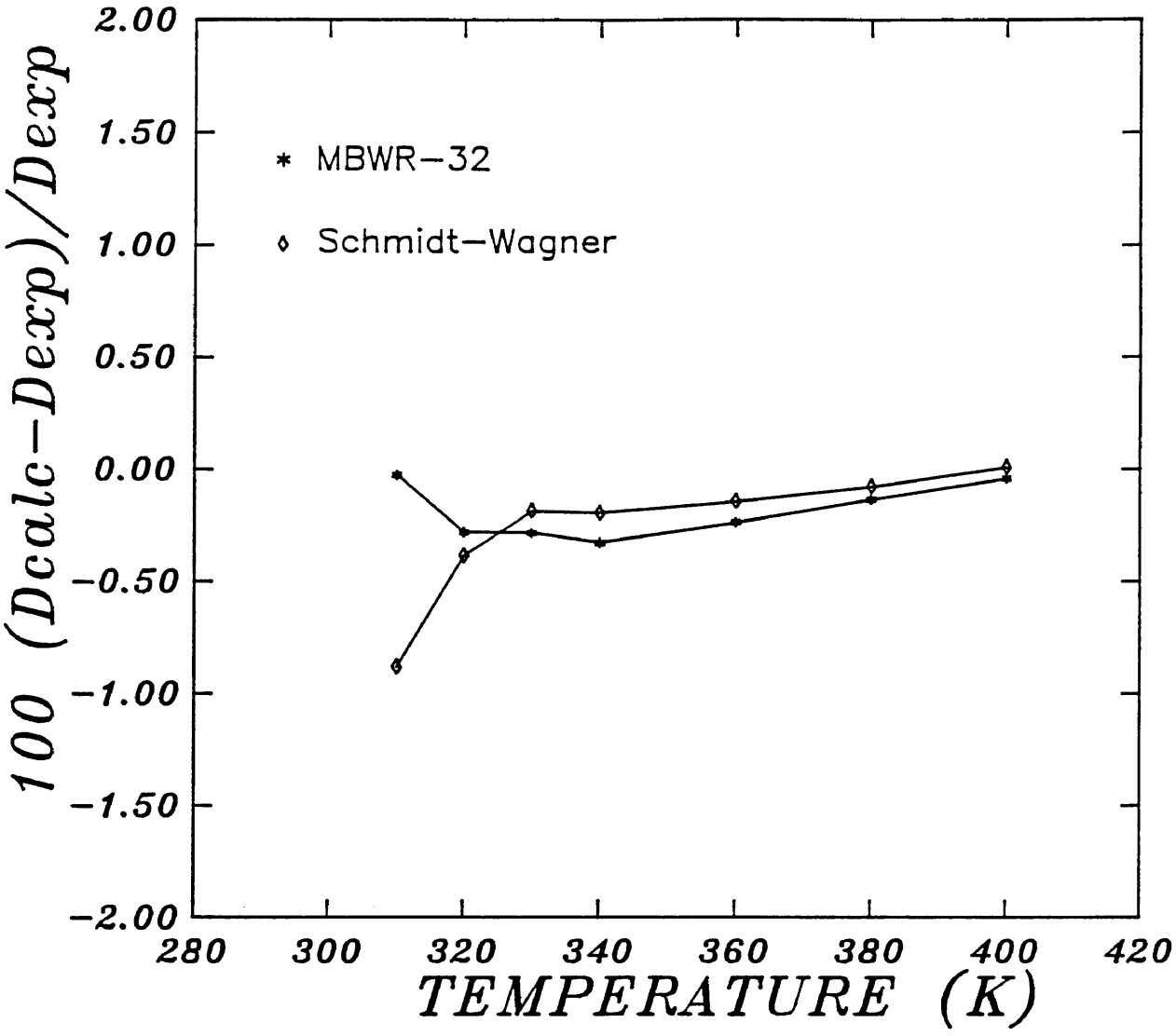

Figure 38. Deviations of calculated densities for 0.99 CO_2 + 0.01 C_2H_6 using the MBWR-32 and Schmidt-Wagner equations of state for the 9.030 mol/l isochore.

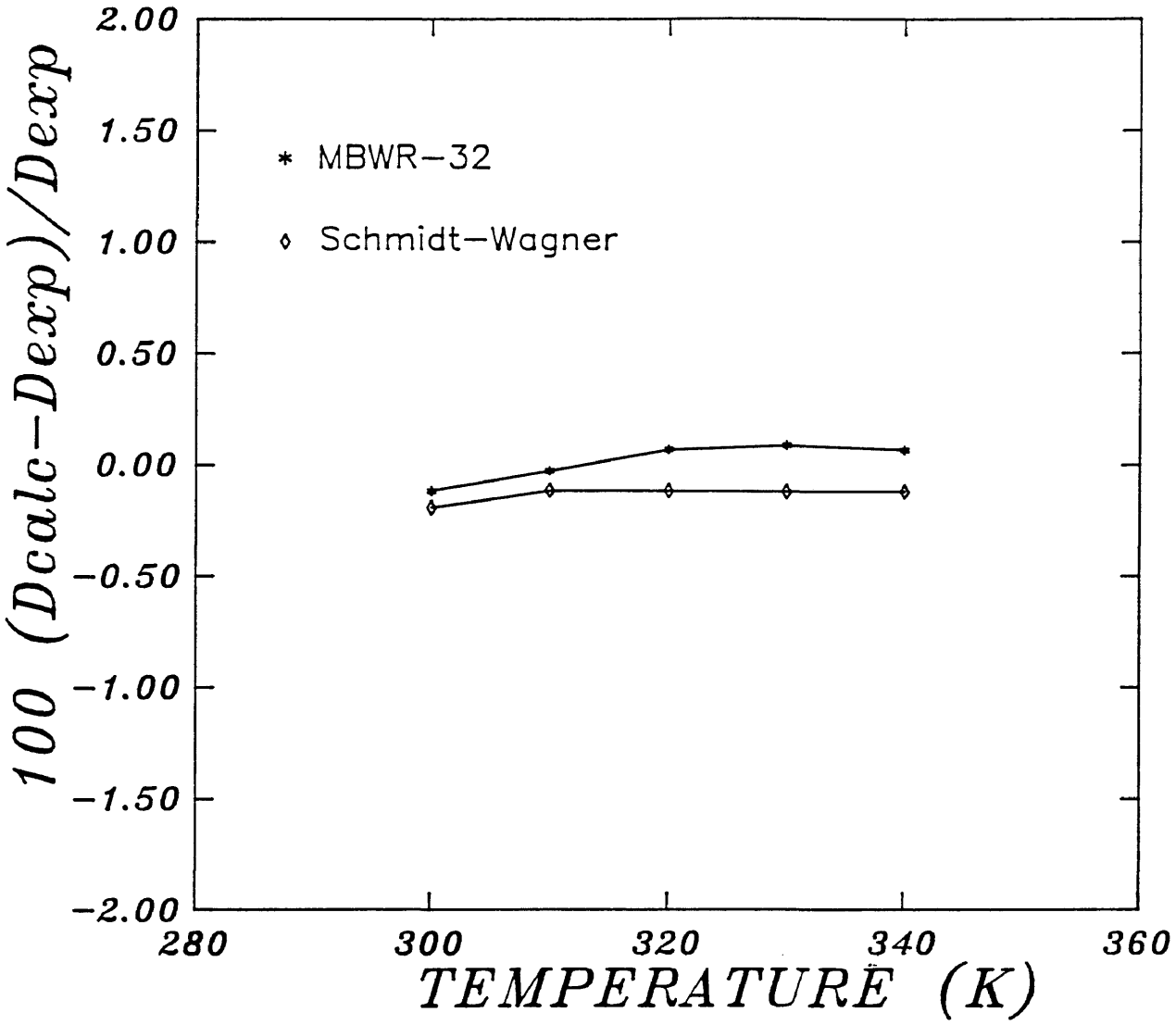

Figure 39. Deviations of calculated densities for 0.99 CO_2 + 0.01 C_2H_6 using the MBWR-32 and Schmidt-Wagner equations of state for the 16.090 mol/l isochore.

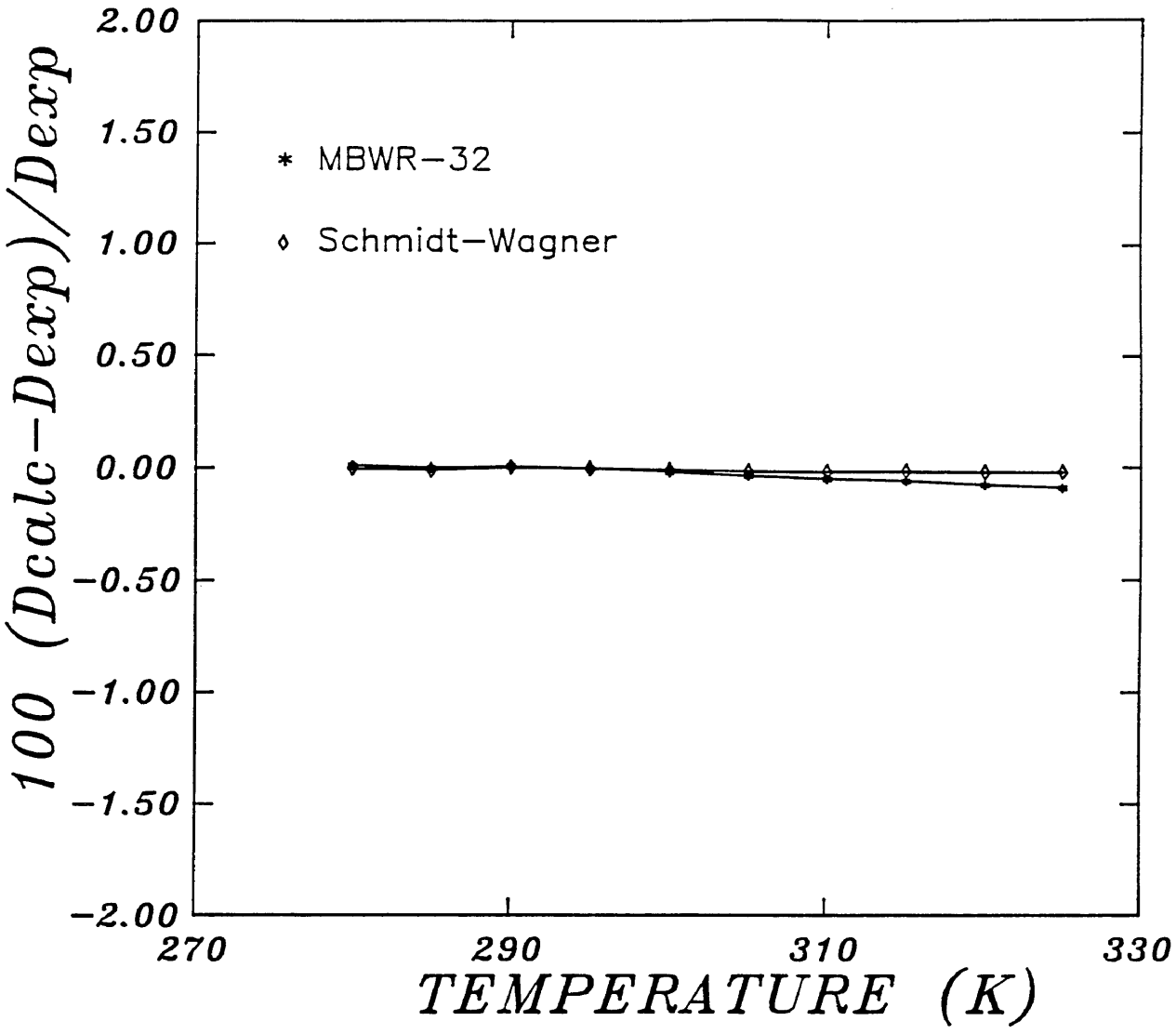

Figure 40. Deviations of calculated densities for 0.99 CO_2 + 0.01 C_2H_6 using the MBWR-32 and Schmidt-Wagner equations of state for the 20.295 mol/l isochore.

the remaining isochores react when the Schmidt-Wagner equation is compared to the MBWR-32 equation for density predictions.

CONCLUSIONS

The isochoric apparatus used in this investigation provides fast and accurate density measurements. It can be used for density measurements over wide ranges of temperature and pressure. The upper limit of temperature is 400 K while the upper limit of pressure is 35 MPa. The accuracy of the experimental data was 0.2 % for densities of 2 - 10 mol/dm^3 and 0.1% for densities of 11 - 24 mol/dm^3.

The original model performed quite well except in the near critical region. To try to reduce the errors in this area, the Schmidt-Wagner equation of state was incorporated into the model. When the Schmidt-Wagner EOS was used in the model, the errors in the near critical region were greatly reduced. But, when calculations were made away from the critical point, both the MBWR-32 and the Schmidt-Wagner equations of state performed well. The use of the Schmidt-Wagner equation in the near critical region is therefore essential in order to improve the model.

RECOMMENDATIONS

The most notable recomendation that can be made from this investigation is that more density data are needed for CO_2 rich mixtures. As the literature survey showed, there is very little density data available for these systems. In order to upgrade the theoretical model, more data of this type are needed. As far as the model is concerned, when the Schmidt-Wagner equation of state was implemented, propane remained the reference fluid. The next step would be to use carbon dioxide as the reference fluid for mixtures with high CO_2 content. The problem which may arise by using carbon dioxide as the reference fluid is its limited range applicability. Carbon dioxide is limited by a low temperature limit of 215 K while propane's low temperature limit is 85 K. One last aspect of the model: let the model choose the reference fluid and the reference fluid equation of state. It could be possible to create another subroutine which would choose these from the data which is input.

REFERENCES CITED

Arai, Y., Kaminishi, G., and Saito, S., "Experimental Determinenation of the P-V-T-X Relations for the Carbon Dioxide-Nitrogen and the Carbon Dioxide-Methane Systems.", J. Chem. Eng. Jap., 4 (2): 113-122 (1971).

Besserer, G.J., and Robinson, D.B., "Equilibrium-Phase Properties of i-Butane-Carbon Dioxide System.",J. Chem. Eng. Data , 18: 298-301 (1973).

Burnett, E.S., "Compressibility determinations without volume measurements". J. Appl. Mech. 3: 136-140 (1936).

Chang, R.F., Morrison, G., and Levet Sengers, J.M.H., J. Phys. Chem. 88: 3389-3391 (1984).

Ely, J.F., Magee, J.W., and Haynes, W.M., "Thermophyscial Properties for Special High CO_2 Content Mixtures", Unpublished NASA Report, GPA Research Report, RR-110 (1987).

Ely, J.F., "Application of the Extended Corresponding States Model to Hydrocarbon Mixture", (1985).

Ely, J.F., "Improved Mixing Rules for One-Fluid Conformal Solution Calculations.", ACS SYMPOSIUM SERIES No. 300, Equations of State:Theories and Applications, 331-350 (1986).

Elliot, D.G., Yao, J., Chen, R.J.J., Hong, J.H. and Kobayashi, R., Proc. 63rd Gas Processors Assn. Annual Conv., 1: 1-8 (1984).

Ferris, C.B., "Unusual Design Factors for Supercritical CO_2 Pipelines"., Energy Progress, 3 (3): 150-158 (1983).

Goodwin, R.D., "Appartatus for Determination of Pressure-Density-Temperature Relations and Specific Heats of Hydrogen to 350 Atmospheres at Temperatures Above 14 K. J. Research Nat. Bur. Stand. (U.S.), 65c: 231-243 (1961).

Gugnoni, R.J., Eldridge, J.W., Okay, V.C., and Lee, T.J., "Carbon Dioxide-Ethane Phase Equilibrium and Densities from Experimental Measurements and the B-W-R Equation.", AiChE Journal, 20 (2): 357-362 (1974).

Gupta, S., Ph.D Disseration, Clemson University, (1984).

Haynes, W.M., and McCarty, R.D., "Low Density Isochoric (p,V,T) Measurements on (Nitrogen + Methane)", J. Chem Thermodynamics, 15: 815-819 (1983).

Haynes, W.M., Bain, B.C. and Ely, J.F., J. Chem Thermodynam., (submitted for publication, 1988).

Hall, K.R., and Canfield, F.B., "A Least-Squares Method for Reduction of Burnett Data to Compressibility Factors and Virial Coefficients. Physica, 47 (1): 99-108 (1970).

Hall, K.R., and Eubank, P.T., "Burnett-isochoric Coupled Data with Application to Adsorbing Gases.", Physica, 61 (3): 346-354 (1972).

Hall, K.R., Eubank, P.T., Holste, J.C., Marsh, K.N., "Properties of CO_2-Rich Mixtures Literature Search and Pure CO_2 Data Phase I", GPA Research Report RR-86 (1985).

Hoheisel, C., Deiters, U., and Lucas, K., "The Extension of Pure Fluid Thermodynamic Properties to Supercritical Mixtures. A Comparision of Current Theories with Computer Data over a Large Region of States.", Mol. Phys., 49 (1): 159-170 (1983).

Kalra, H., Krishnan, T.R. and Robinson, D.B., "Equilibrium-Phase Properties of Carbon Dioxide-n-Butane and Nitrogen-Hydrogen Sulfide Systems at Subambient Temperatures.",J. Chem. Eng. Data , 21 (2): 222-225 (1976).

Kirkwood, J.G., Lewinson, V.A., and Adler, B.S., "Radial Distribution Function and the Equation of State of Fluids Composed of Molecules Interacting According to the Lennard-Jones Potential.", J. Chem. Phys., 20 929-938 (1952).

Kosov, N.D., and Brovanov, I.S., "The Compressibility of Binary Mixtures of Helium, Nitrogen and Argon with Carbon Dioxide from 59 x 10^5 to 590 x 10^5 Pa.Teploenergetika, 22 (11): 77-79 (1975).

Kratky, O., Leopold, H., and Stabinger, H., "Determination of the Partial Specific Volume of Proteins by the Mechanical Oscillator Technique", Methods in Enzymology, 27: 98-104 (1973).

Kuenen J.P., "Experiments on the Condensation and Critical Phenomena of Some Substances and Mixtures", Phil Mag., 51 (44): 174-179 (1897).

Kuenen J.P., and Robson, W.G., "Observations on Mixtures with Maximum or Minimum Vapor-Pressure.",Phil. Mag., 6 (4): 116-132 (1902).

Lau, W.W.R., "A Continuously Weighed Pycnometer Providing Densities for Carbon Dioxide + Ethane Mixtures Between 240 and 350 K at Pressures up to 35 MPa.", Ph.D. Disseration, Texas A & M University (1987).

Leach, J.W., "Molecular Structure Corrections for Application of the Theory of Corresponding States to Non-spherical Pure Fluids and Mixtures." Ph.D. Disseration, Rice University (1967).

Leland, T.W. and Mueller, W.H., "Applying the Theory of Corresponding States to Multicomponent Systems." Ind. Eng. Chem., 51: 597-600 (1959).

Leland, T.W., Rowlinson, J.S., and Sather, G.A., "Statistical Thermodynamics of Mixtures of Molecules of Different Sizes." Trans Farad. Soc., 64 (6): 1447-1460 (1968).

Magee, J.W., Personal Communications (1986).

Magee, J.W., and Ely, J.F., "Isochoric (p,v,T) Measurements on Carbon Dioxide and (0.98 CO_2 + 0.02 CH_4) from 225 to 400 K at Pressures to 35 MPa.", International J. Thermophysics, (Submitted to be published, 1988).

McCarty, R.D., "Experimental Thermodynamic, Vol II, - Experimental Thermodynamics of Non-Reacting Fluids", p 501, Butterworth and Co., London (1975).

McCarty, R.D. and Jacobsen, R.T., Natl. Bur. Stand. (U.S.) Technical Note, 1045 (1981).

McQuarrie, D.A., "Statistical Mechanics", Harper and Row, New York (1976).

Meissner, R.E., "Purifying CO_2 for Use in Enhanced Oil Recovery", World Oil, 189-198, (1980).

Mentzer, R.A., Greenkorn, R.A., and Chao, K.C., "Principles of Corresponding States and Vapor-Liquid Equilibriums of Molecular Fluids and Their Mixtures with Light Gases.", Ind. Eng. Chem. Process Des. Der., 20 (2): 240-252 (1981).

Michels, A. Blaise, B., and Wouters, H., "The isotherms of CO_2 in the neighborhood of the Critical Point and Round the Coexistence Line.", Proc. Roy. Soc., a160: 358-375 (1937).

Olds, R.H., Reamer, H.H., Sage, B.H., and Lacy, W.M., "Phase Equilibria in Hydrocarbon Systems: n-Butane-Carbon Dioxide System", Ind. Eng. Chem., 416 (3): 475-482 (1949).

Orr,Jr., F.M., and Tabor, J.J., "Use of Carbon Dioxide in Enhanced Oil Recovery", Science, 224 (4649): 563-569 (1984).

Picker, P., Tremblay E. and Jolicoeur C. "A high-precision digital readout flow densimeter for liquids". J. of Solution Chem. 3: 377-391 (1974).

Pope, G.A., "Calculation of Argon, Methane, and Ethane Virial Coefficients at Low Reduced Temperature Based on Data Obtained by Isochorically Coupled Burnett Experiments", Ph.D. Dissertation, Rice University, (1971).

Reamer, H.H, Sage, B.H., and Lacy, W.M., "Phase Equilibria in Hydrocarbon Systems: Volumetric and Phase Behavior of the Propane-Carbon Dioxide System", Ind. Eng. Chem., 43 (1): 2515-2525 (1951).

Reamer, H.H, Olds, R.H., Sage, B.H., and Lacy, W.M., "Phase Equilibria in Hydrocarbon Systems: Volumetric and Phase Behavior of the Ethane-Carbon Dioxide System", Ind. Eng. Chem., 37 (7): 688-691 (1945).

Reamer, H.H, Olds, R.H., Sage, B.H., and Lacy, W.M., "Phase Equilibria in Hydrocarbon Systems: Methane-Carbon Dioxide in the Gaseous Region", Ind. Eng. Chem., 36: 88-90 (1944).

Reed, T.M., and Gubbins, K.E., "Applied Statistical Mechanics", McGraw-Hill, New York (1973).

Reid, R.C. and Leland, T.W., "Pseudocritical Constants", AiChE Jour., 11 (2): 228-236 (1965).

Schmidt, R., and Wagner, W., "A New Form of the Equation of State for Pure Substances and its Application to Oxygen", Fluid Phase Equilibria 19: 175-200 (1985).

Shing, K.S., and Gubbins, K.E., "The Chemical Potential in Dense Fluids and Fluid Mixtures Via Computer Simulation.", Mol. Phys., 46 (5): 1109-1128 (1982).

Stewart, R.B., and Jacobsen, R.T., "Determination of Equations of state for Nitrogen and Oxygen.", Cryogenics, 13 (9): 526-534 (1973).

Stewart, R.B., Center for Applied Thermodynamic Studies Report (1981).

Straty, G.C., "(p,V,T) of Compressed Fluid Ethene.", J. Chem. Thermodynam., 12: 709-716 (1980)

Straty, G.C., and Diller, D.E., "(p,V,T) of Saturated and Compressed Fluid Nitrogen." J. Chem. Thermodynam., 12: 927-936 (1980).

Straty, G.C., and Prydz, R., "Florine Compatible Apparatus for Accurate PVT Measurements.", The Review of Scientific Instruments, 41 (8): 1223-1227 (1970).

Stripling, T.E., "Carbon Dioxide Pipelines", PLT Engineering Inc., Houston, Texas (1980).

Swink, M.N., "Design of Sheep Mountain CO_2 Pipeline", Interpipe, (1982).

Tekac, V., Cibulka, I., and Holub, R., "PVT Properties of Liquids and Liquid Mixtures: A Review of the Experimental Methods and the Literature Data", Fluid Phase Equilibria, 19: 33-149 (1985).

Wielopolski, P., and Warowny, W., "A Fast Least-Squares Method for Reduction of Burnett Data to Compressibility Factors and Virial Coefficients. Physica, 91A (1-2): 66-72 (1978).

Zudkevitch, D., Czerwienski, G.J. and Wang, Y.Z., Proc. 64th Gas Processors Assn. Annual Conv., 266: 266-281 (1985).

APPENDIX A

MIXING RULES

Mixing Rules

The compositional and density dependence of the terms A - F which appeared in eqs. (38) and (39) are given by:

$$A = \frac{1}{\eta_x}(SUM)\{(1/g_{ij})(a + b\,\delta_{ij})(\tfrac{\pi}{6}\rho\sigma_k^3 - \eta_m)\}$$

$$B = \frac{1}{\eta_x}(SUM)\{(1/g_{ij})c\delta_{ij}(\tfrac{\pi}{6}\rho\sigma_k^2 - \chi_m)\}$$

$$C = \frac{1}{\eta_x}(SUM)\{\frac{-\eta_x}{g_o}(d + e)\}$$

$$D = \frac{2}{\eta_x} \sum x_i \eta_{ik} R_{ik}$$

$$E = \frac{2}{\varepsilon_x \eta_x} \sum x_i \varepsilon_{ik} \eta_{ik} R_{ik}$$

$$F = \frac{1}{\varepsilon_x \eta_x} \sum \sum x_i x_j \; ij \; ij R_{ij} \left| \frac{n}{R_{ij}} \left(\frac{\partial R_{ij}}{\partial n_k} \right) \right|$$

$$\left| \frac{n}{R_{ij}} \left(\frac{\partial R_{ij}}{\partial n_k} \right) \right| = G + H - I$$

$$G = (1/g_{ij})\{(a + b\delta_{ij})(\tfrac{\pi}{6}\rho\sigma_k^3 - \eta_m)\}$$

$$H = (1/g_{ij})c\delta_{ij}(\tfrac{\pi}{6}\rho\sigma_k^2 - \chi_m)$$

$$I = \frac{\eta_x}{g_o}(d + e)\left| \frac{n}{\eta_x} \left(\frac{\partial \eta_x}{\partial n_k} \right) \right|$$

where

$$a = \frac{1}{(1 - \eta_m)^2} \quad , \quad b = \frac{3\chi_m}{(1 - \eta_m)^3}$$

$$c = \frac{3}{2(1 - \eta_m)^2} \qquad d = \frac{1}{2(1 - \eta_x)^3} \quad , \quad e = \frac{2(1 + \eta_x/2)}{(1 - \eta_x)^3}$$

and

$$g_{ij} = \frac{1}{(1 - \eta_m)} + \frac{3\chi_m}{2(1 - \eta_m)^2} \delta_{ij}$$

$$g_o = (1 + \eta_x/2)/(1 - \eta_x)^2$$

$$\eta_m = \frac{\pi}{6}\rho \sum x_i \sigma_i^3$$

$$\chi_m = \frac{\pi}{6}\rho \sum x_i \sigma_i^2$$

$$\eta_x = \frac{\pi}{6}\rho\sigma_x^3 N_o$$

$$\delta_{ij} = (2\sigma_i\sigma_j)/(\sigma_i + \sigma_j)$$

$$\text{SUM} = \sum \sum x_i x_j \eta_{ij} R_{ij}$$